Parton Distributions and the Relation to LHC and Higgs Physics

Robert Thorne

February 15th, 2012

University College London

Thanks to Alan Martin, James Stirling and Graeme Watt

Strong force makes it difficult to perform analytic calculations of scattering processes involving hadronic particles.

The weakening of $\alpha_S(\mu^2)$ at higher scales $\rightarrow$ the **Factorization Theorem**.

Hadron scattering with an electron factorizes.

Q^2 – Scale of scattering

$x = \frac{Q^2}{2m\nu}$ – Momentum fraction of Parton (ν=energy transfer)

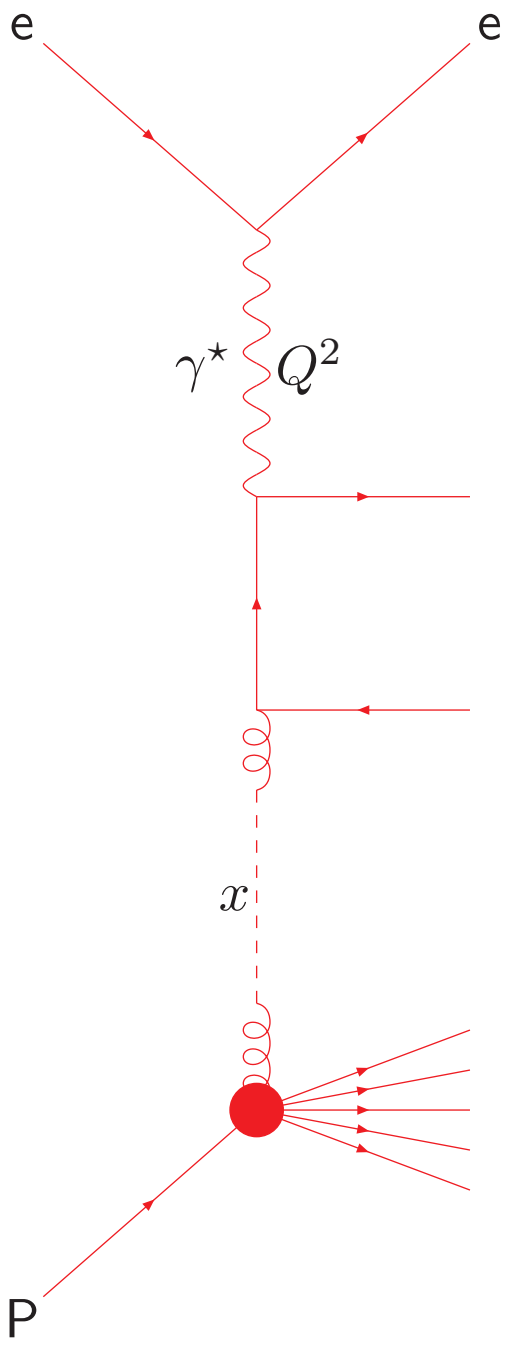

perturbative
calculable
coefficient function
$C_i^P(x, \alpha_s(Q^2))$

nonperturbative
incalculable
parton distribution
$f_i(x, Q^2, \alpha_s(Q^2))$

The coefficient functions $C_i^P(x, \alpha_s(Q^2))$ are process dependent (new physics) but are calculable as a power-series in $\alpha_s(Q^2)$.

$$C_i^P(x, \alpha_s(Q^2)) = \sum_k C_i^{P,k}(x) \alpha_s^k(Q^2).$$

Since the parton distributions $f_i(x, Q^2, \alpha_s(Q^2))$ are process-independent, i.e. **universal**, and evolution with scale is calculable, once they have been measured at one experiment, one can predict many other scattering processes.

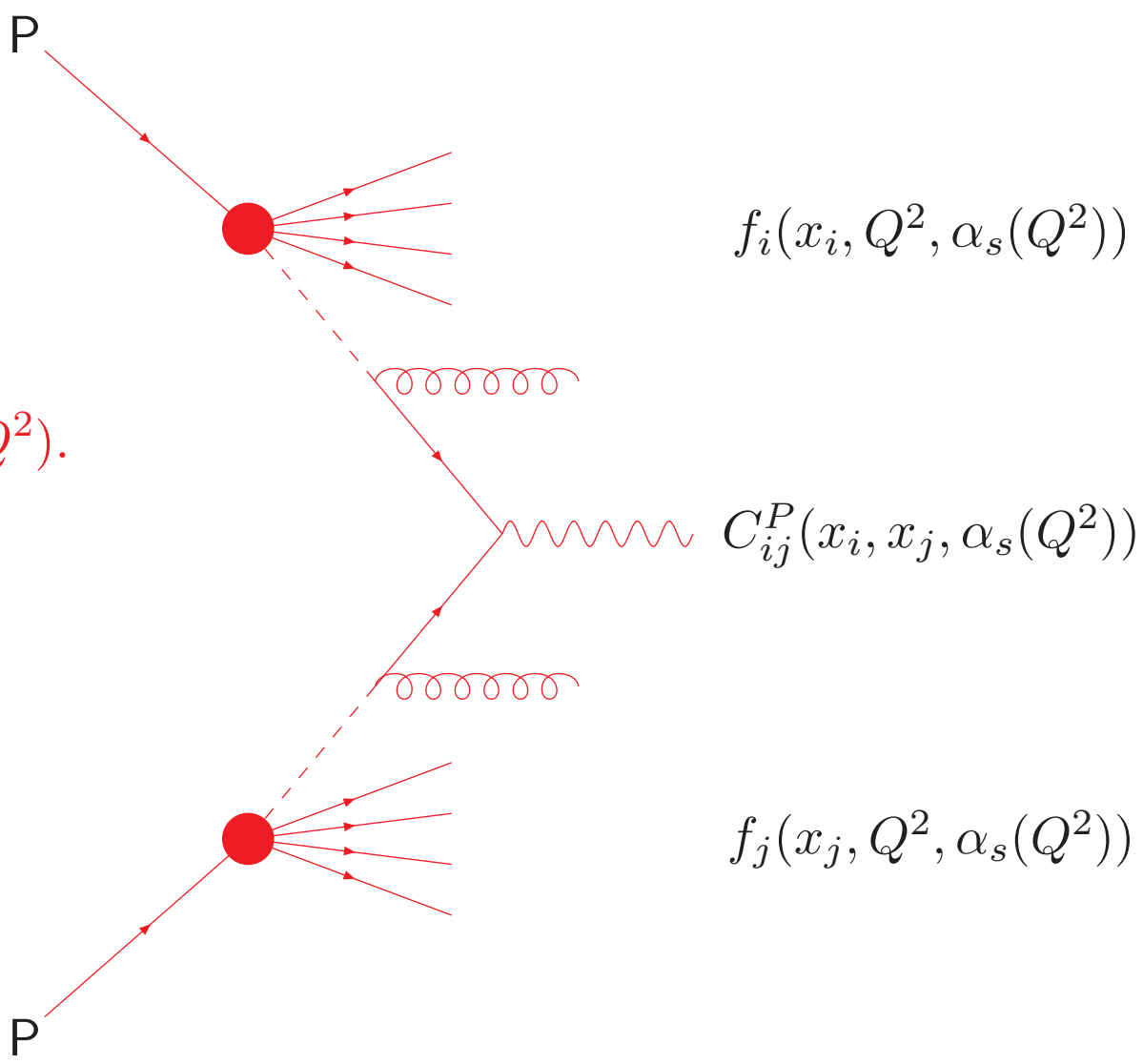

Obtaining PDF sets – General procedure.

Start parton evolution at low scale $Q_0^2 \sim 1\mathrm{GeV}^2$. In principle 11 different partons to consider.

$$u, \bar{u}, \quad d, \bar{d}, \quad s, \bar{s}, \quad c, \bar{c}, \quad b, \bar{b}, \quad g$$

$m_c, m_b \gg \Lambda_{\mathrm{QCD}}$ so heavy parton distributions determined perturbatively. Leaves 7 independent combinations, or 6 if we assume $s = \bar{s}$ (just started not to).

$$u_V = u - \bar{u}, \quad d_V = d - \bar{d}, \quad \mathrm{sea} = 2 * (\bar{u} + \bar{d} + \bar{s}), \quad s + \bar{s} \quad \bar{d} - \bar{u}, \quad g.$$

Input partons parameterised as, e.g. MSTW,

$$x f(x, Q_0^2) = (1 - x)^{\eta}(1 + \epsilon x^{0.5} + \gamma x) x^{\delta}.$$

Evolve partons upwards using LO, NLO (or increasingly NNLO) DGLAP equations.

$$\frac{df_i(x, Q^2, \alpha_s(Q^2))}{d \ln Q^2} = \sum_j P_{ij}(x, \alpha_s(Q^2)) \otimes f_j(x, Q^2, \alpha_s(Q^2))$$

Fit data for scales above $2-5\mathrm{GeV}^2$. Need many different types for full determination.

- Lepton-proton collider HERA – (DIS) $\rightarrow$ small-x quarks (best below $x \sim 0.05$). Also gluons from evolution (same x), and now $F_L(x, Q^2)$. Also, jets $\rightarrow$ moderate-x gluon.Charged current data some limited info on flavour separation. Heavy flavour structure functions – gluon and charm, bottom distributions and masses.

- Fixed target DIS – higher x – leptons (BCDMS, NMC, ...) $\rightarrow$ up quark (proton) or down quark (deuterium) and neutrinos (CHORUS, NuTeV, CCFR) $\rightarrow$ valence or singlet combinations.

- Di-muon production in neutrino DIS – strange quarks and neutrino-antineutrino comparison $\rightarrow$ asymmetry . Only for $x > 0.01$.

- Drell-Yan production of dileptons – quark-antiquark annihilation (E605, E866) – high-x sea quarks. Deuterium target – $\bar{u}/\bar{d}$ asymmetry.

- High-p_T jets at colliders (Tevatron) – high-x gluon distribution – $x > 0.01$.

- W and Z production at colliders (Tevatron/LHC) – different quark contributions to DIS.

This procedure is generally successful and is part of a large-scale, ongoing project. Results in partons of the form shown.

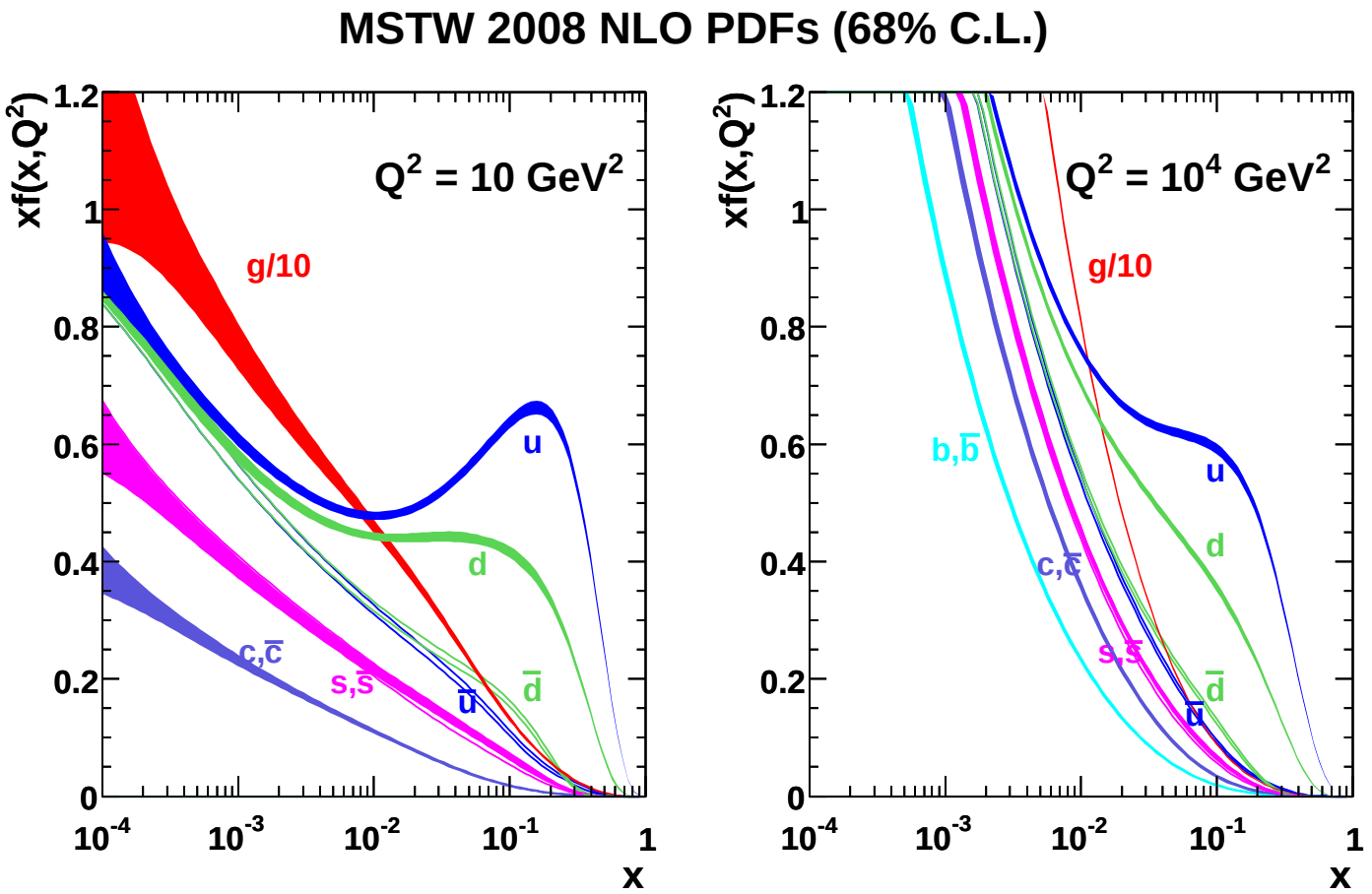

Various choices of PDF – MSTW, CTEQ, NNPDF, AB(K)M, HERA, Jimenez-Delgado *et al etc.*. All LHC cross-sections rely on our understanding of these partons.

Leads to very accurate and precise predictions.

Comparison of MSTW prediction for Z rapidity distribution with data.

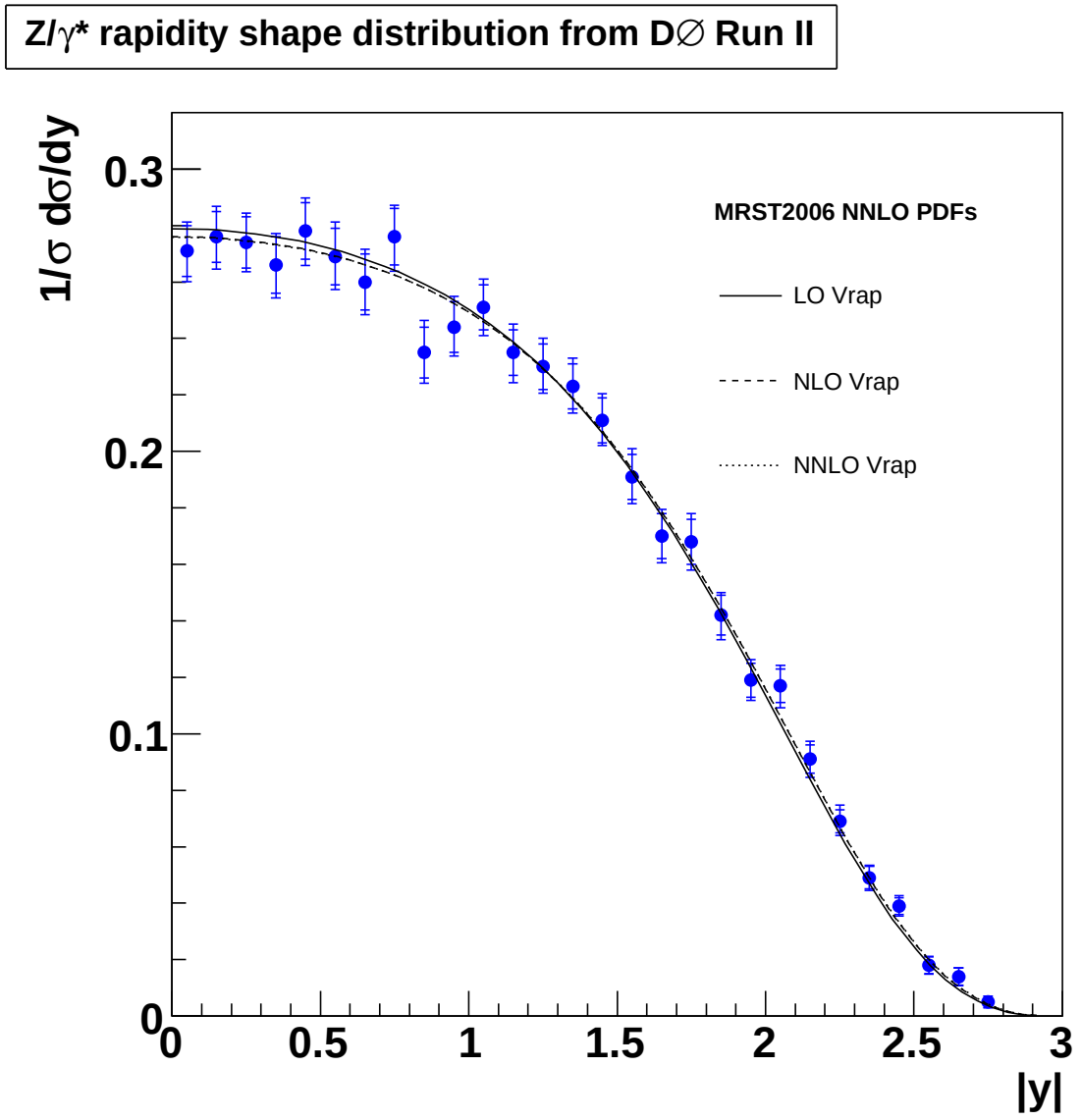

Interplay of LHC and pdfs/QCD

Make predictions for all processes, both SM and BSM, as accurately as possible given current experimental input and theoretical accuracy.

Check against well-understood processes, e.g. central rapidity W, Z production (luminosity monitor), lowish-E_T jets, ...

Compare with predictions with more uncertainty and lower confidence, e.g. high-E_T jets, high rapidity bosons or heavy quarks .....

Improve uncertainty on parton distributions by improved constraints, and check understanding of theoretical uncertainties, and determine where NNLO, electroweak corrections, resummations $etc.$ needed.

Make improved predictions for both background and signals with improved partons and surrounding theory.

Spot new physics from deviations in these predictions. As a nice by-product improve our understanding of the strong sector of the Standard Model considerably.

Remainder of talk describes this process in more detail.

LHC **Physics**

The kinematic range for particle production at the LHC is shown.

$$x_{1,2} = x_0 \exp(\pm y), \quad x_0 = \frac{M}{\sqrt{s}}.$$

Smallish $x \sim 0.001 - 0.01$ parton distributions therefore vital for understanding the standard production processes at the LHC.

However, even smaller (and higher) x required when one moves away from zero rapidity, e.g. when calculating total cross-sections.

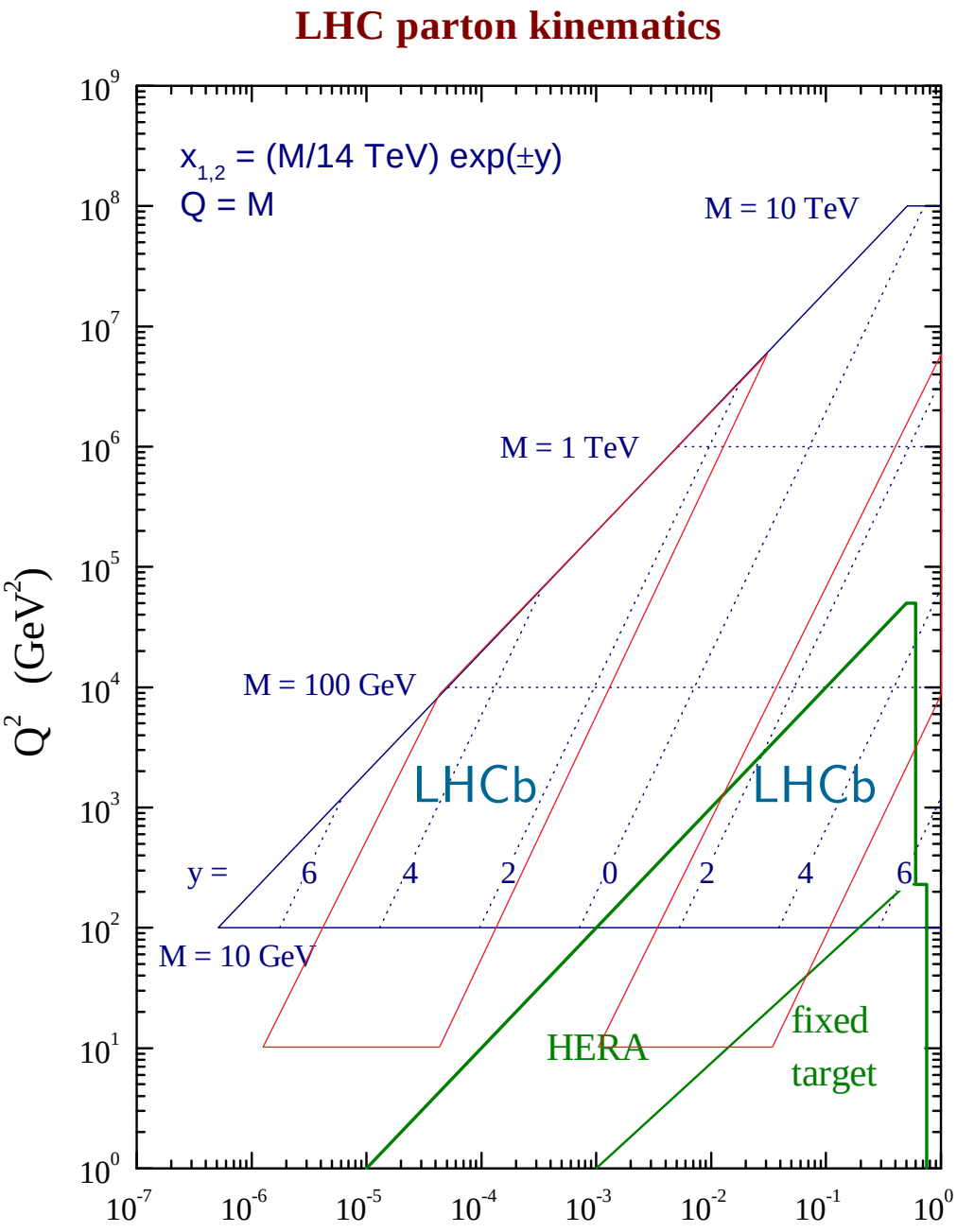

Uncertainty on $\sigma(Z)$ and $\sigma(W^+)$ grows at high rapidity. Converges – both dominated by $u(x_1)\bar{u}(x_2)$ at very high y.

Uncertainty on $\sigma(W^-)$ grows more quickly at very high y.

Uncertainty on $\sigma(\gamma^\star)$ is greatest as y increases.

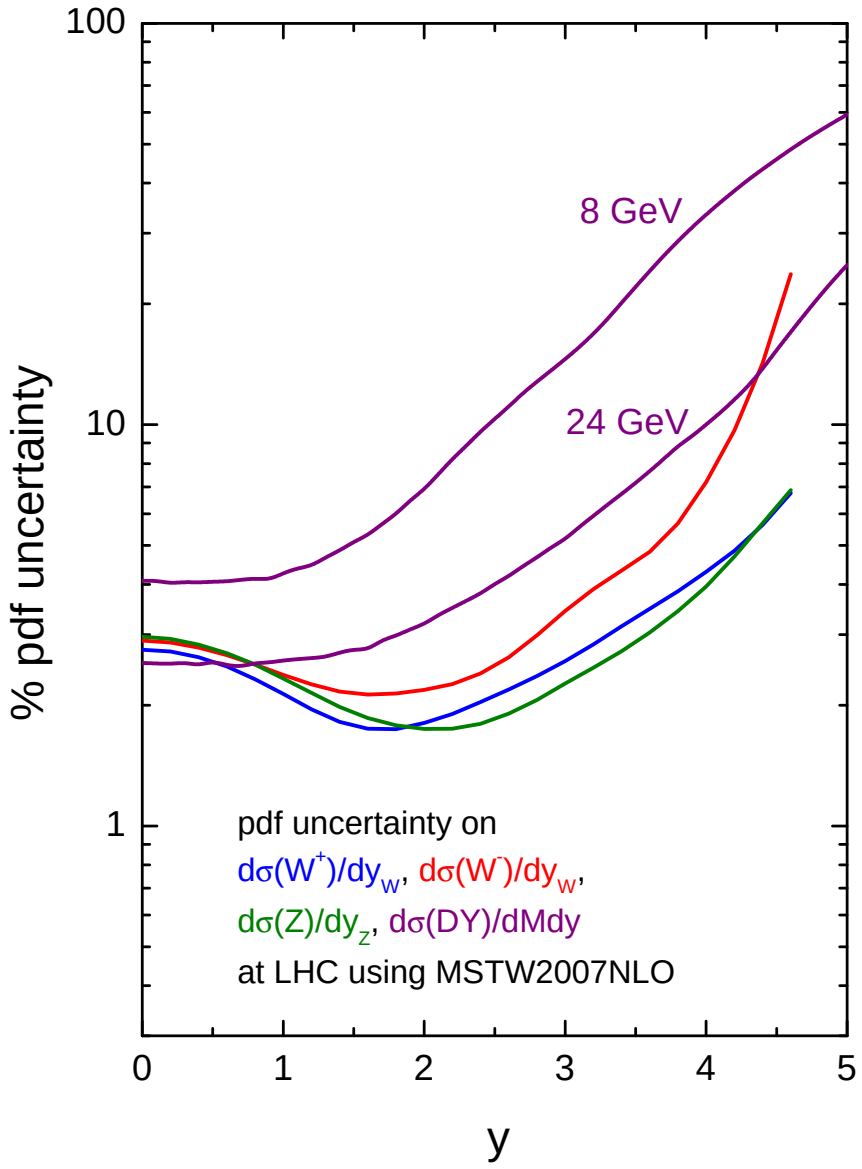

Predictions (Watt) for W and Z cross-sections for LHC with common NLO QCD and vector boson width effects, and common branching ratios, and at $7\mathrm{TeV}$.

Good agreement at NLO for variety of PDFs.

In fact comparing all groups get significant discrepancies between them even for this benchmark process.

Can understand some of the systematic differences.

Total W, Z total cross-sections best-case scenario – rapidities show more variation.

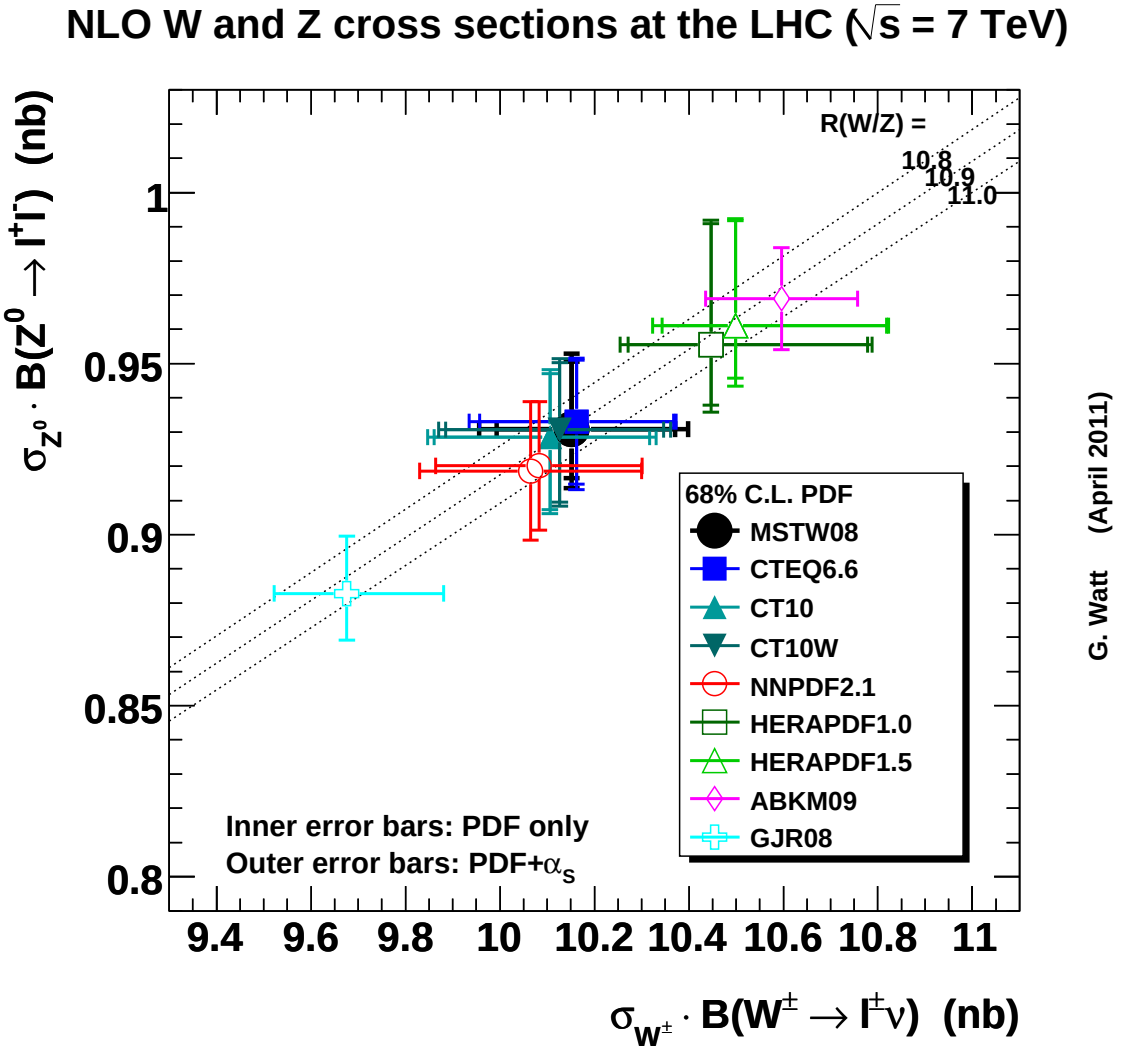

More discrepancy.

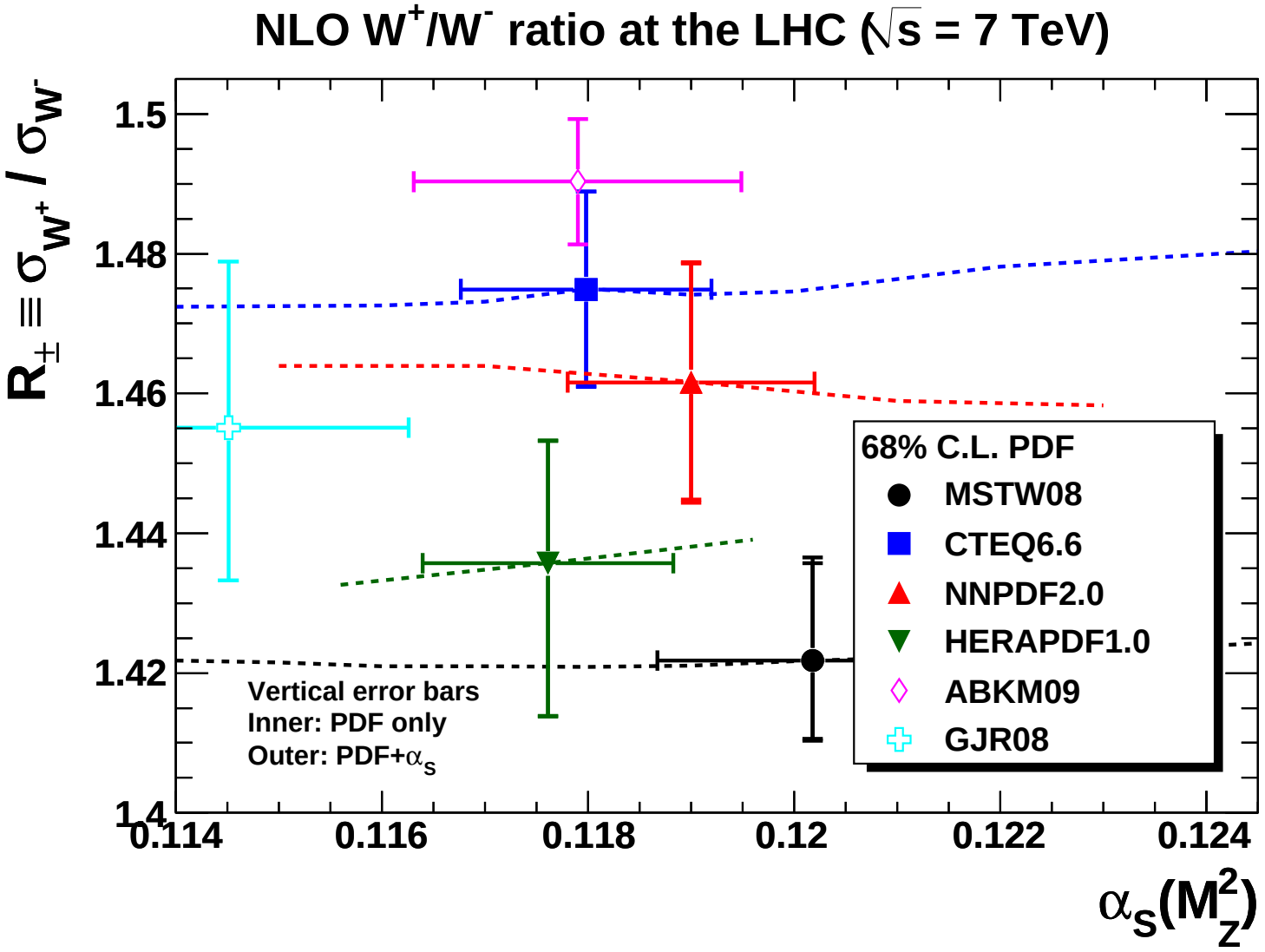

More variation also in W^+/W^- ratio. Shows variations in flavour and quark-antiquark decompositions.

Variations in Higgs Cross-Section Predictions – NLO

Much more dependent on gluon distributions.

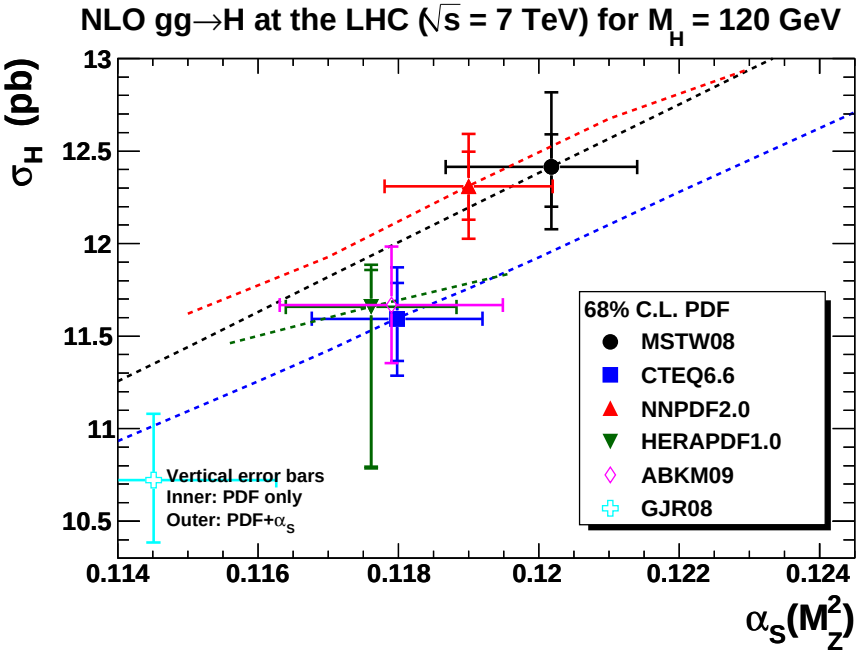

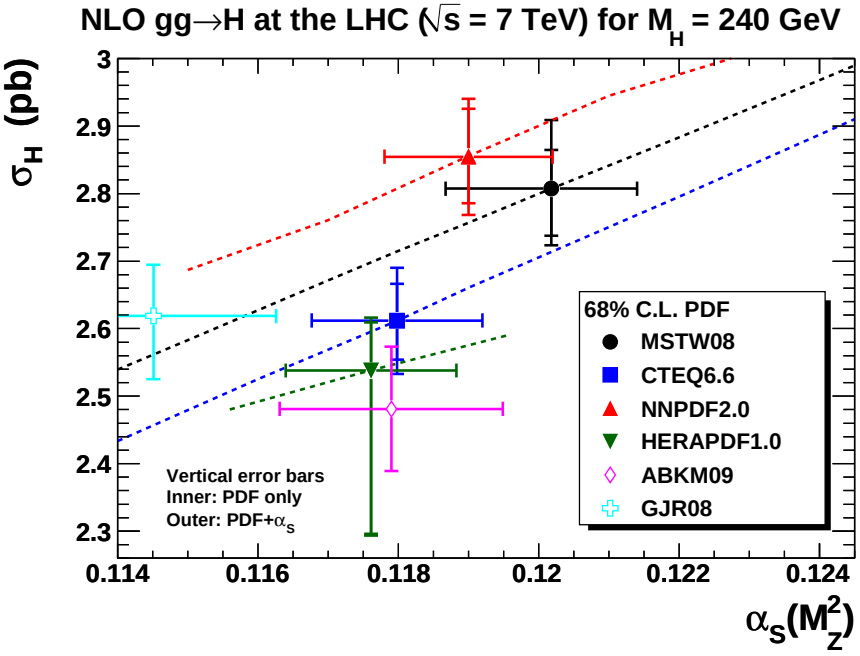

Dotted lines show how central PDF predictions vary with $\alpha_S(M_Z^2)$. (Again plots by G Watt.)

Sources of Variations/Uncertainty

It is vital to consider theoretical/assumption-dependent uncertainties:

- Methods of determining "best fit" and uncertainties.
- Underlying assumptions in procedure, e.g. parameterisations and data used.
- Treatment of heavy flavours.
- PDF and α_S correlations.

Responsible for differences between groups for extraction of fixed-order PDFs.

Variety of PDFs

MSTW make available PDFs in a very wide variety of forms.

- At , LO, NLO and NNLO, with some minor approximations at NNLO.
- Also a variety of extensions such as different α_S values, heavy quark masses, different flavour numbers. Latter covered tomorrow.
- Older MRST versions of modified LO* and LO** PDFs and of PDFs including QED evolution.

Fit data for scales above $2\mathrm{GeV}^2$. (most) DIS data for $W^2 > 15\mathrm{GeV}^2$. Will mention effect of cuts later.

Don't yet include combined HERA cross-section data. Have checked effects of this. In some cases predictions change by a little over 1σ, in many cases less.

Major problems with high-luminosity D0 lepton asymmetry in some binnings. Same for other groups.

Comparison of gluon from fit using combined HERA data to MSTW2008 NNLO versions with $1-\sigma$, uncertainty shown.

Slight difference in details of normalisation treatment compared to previous versions, still preliminary. First times showed uncertainty.

Value of $\alpha_S(M_Z^2)$ moves slightly, $0.1171 \rightarrow 0.1178$.

Changes always within $1-\sigma$, and really less due to correlations with α_S.

Uncertainty slightly smaller, especially at very small x.

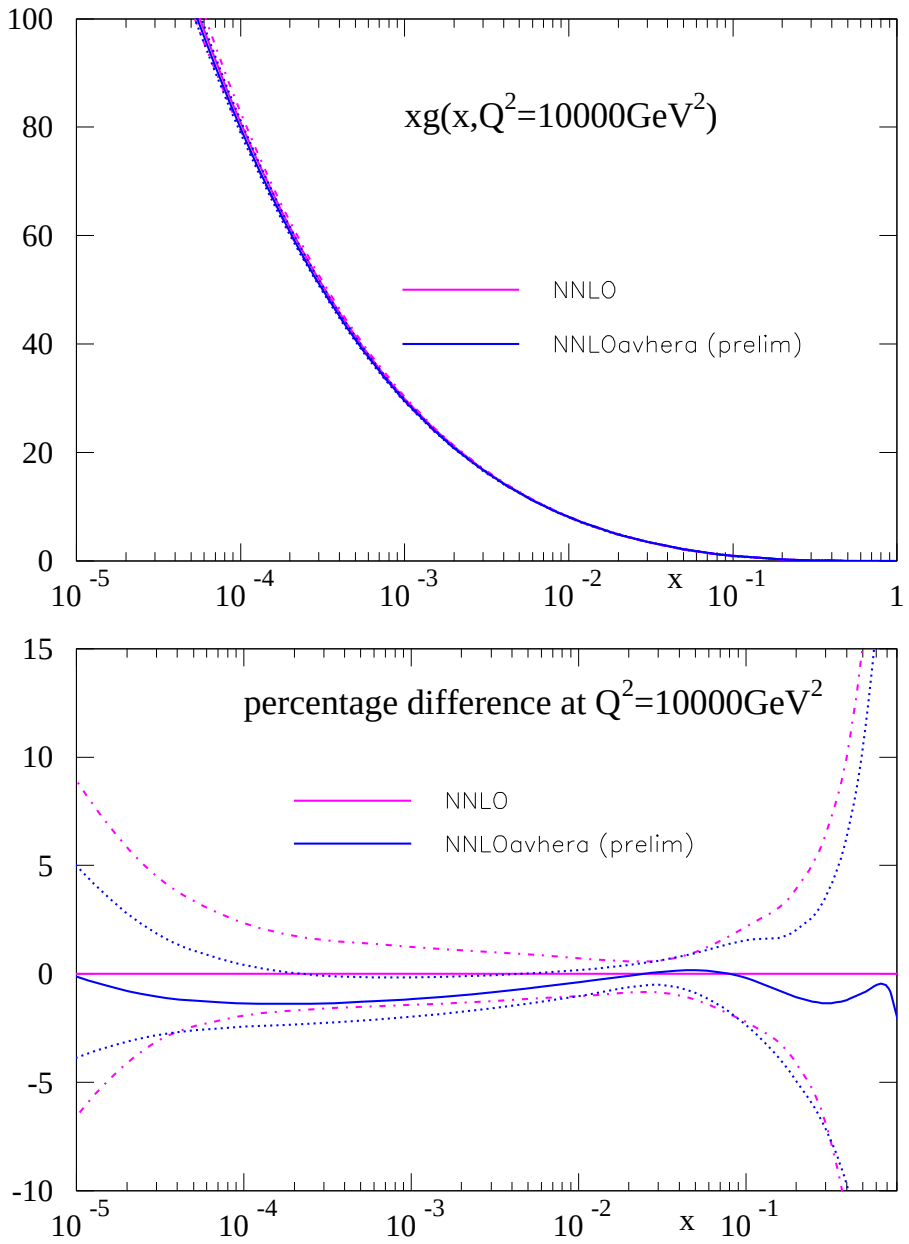

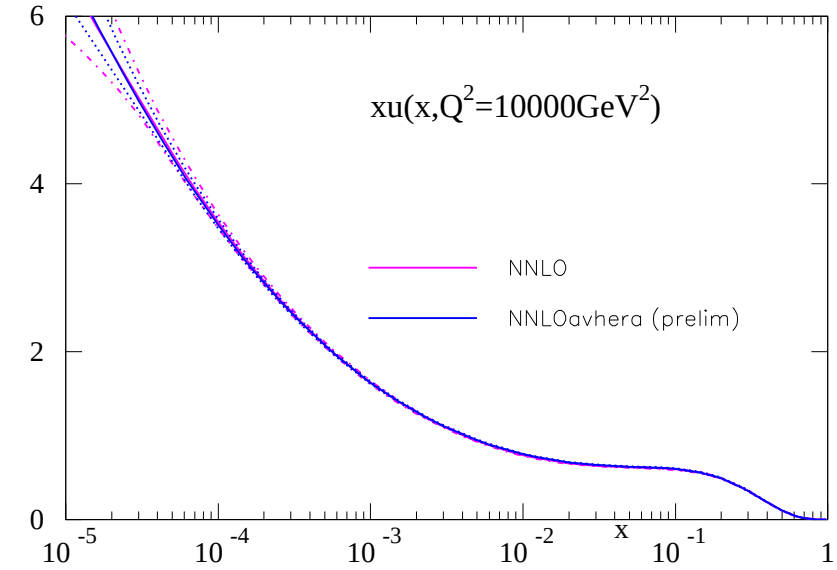

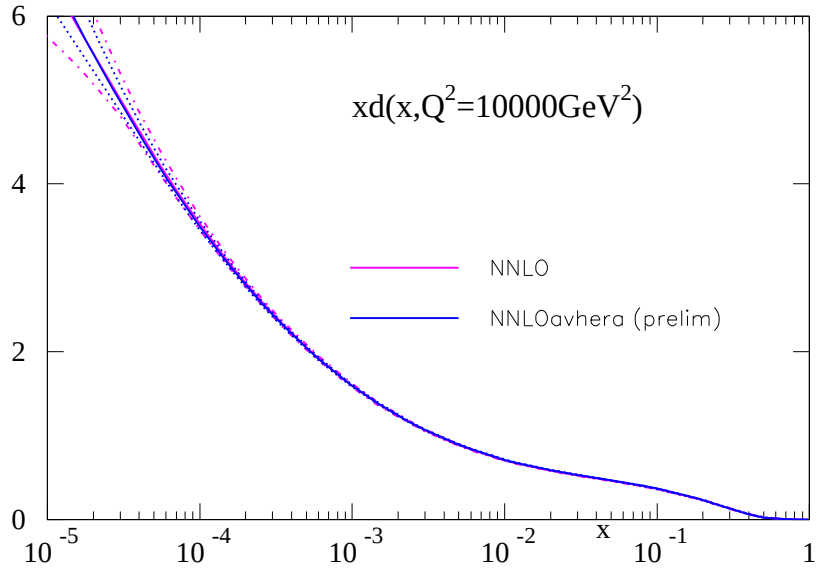

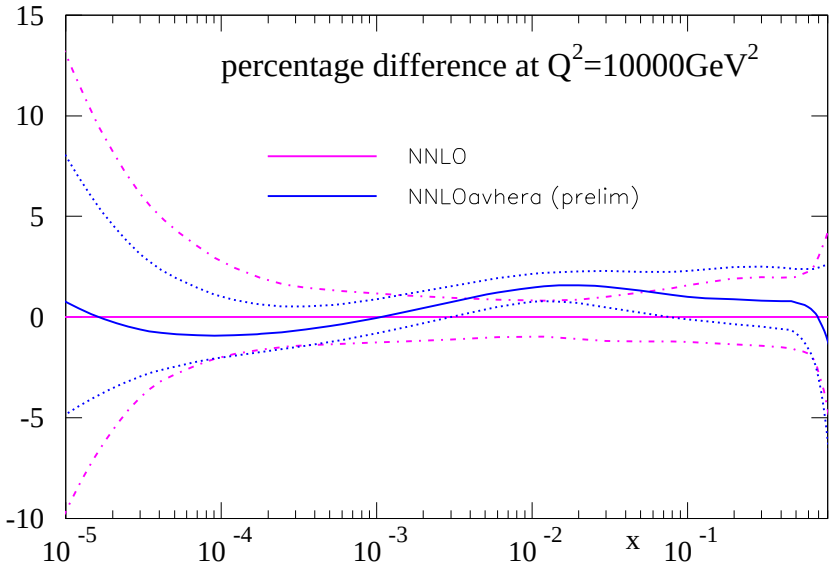

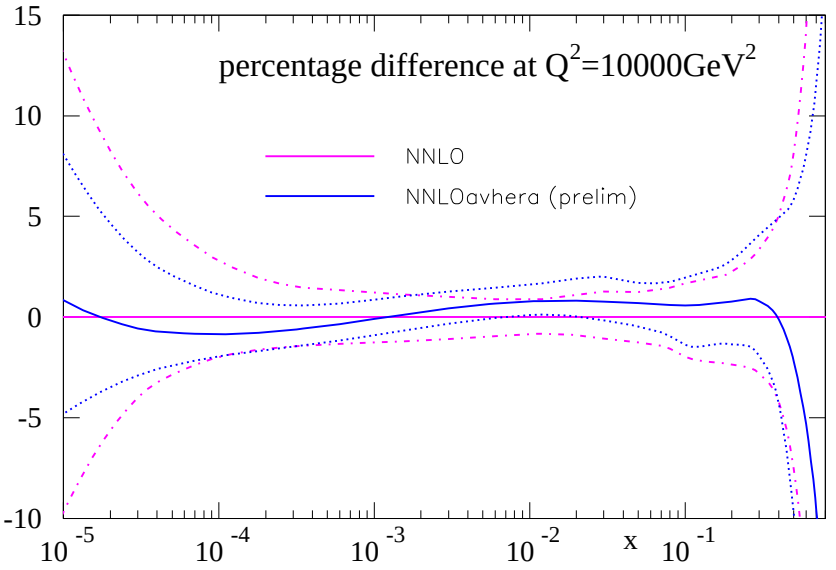

Most dramatic change for up quark at about $x = 0.01$.

Impact on Cross Sections.

The values of the predicted cross-sections at NNLO for Z and a 120 GeV Higgs boson at the Tevatron and the LHC (latter for 14 TeV centre of mass energy).

PDF set	$B_{l^+l^-}\cdot\sigma_Z$(nb)TeV	σ_H(pb)TeV	$B_{l^+l^-}\cdot\sigma_Z$(nb)LHC	σ_H(pb)LHC
MSTW08	0.2507	0.9549	2.051	50.51
Comb HERA	$+2.1\%$	$+1.2\%$	$+0.9\%$	$+0.7\%$

For new global fits 2% effect on Z (and W) cross sections at Tevatron, but small change at LHC. Similar to, or less than $1-\sigma$ uncertainty in former case.

Maximum of $\sim 1\%$ for Higgs. Small effect.

Parton Fits and Uncertainties. Two main approaches.

Parton parameterization and Hessian (Error Matrix) approach first used by H1 and ZEUS, and extended by CTEQ.

$$\chi^2 - \chi^2_{min} \equiv \Delta\chi^2 = \sum_{i,j} H_{ij}(a_i - a_i^{(0)})(a_j - a_j^{(0)})$$

The Hessian matrix H is related to the covariance matrix of the parameters by

$$C_{ij}(a) = \Delta\chi^2 (H^{-1})_{ij}.$$

We can then use the standard formula for linear error propagation.

$$(\Delta F)^2 = \Delta\chi^2 \sum_{i,j} \frac{\partial F}{\partial a_i} (H)^{-1}_{ij} \frac{\partial F}{\partial a_j},$$

This is now the most common approach.

Can find and rescale eigenvectors of H leading to diagonal form

$$\Delta\chi^2 = \sum_i z_i^2$$

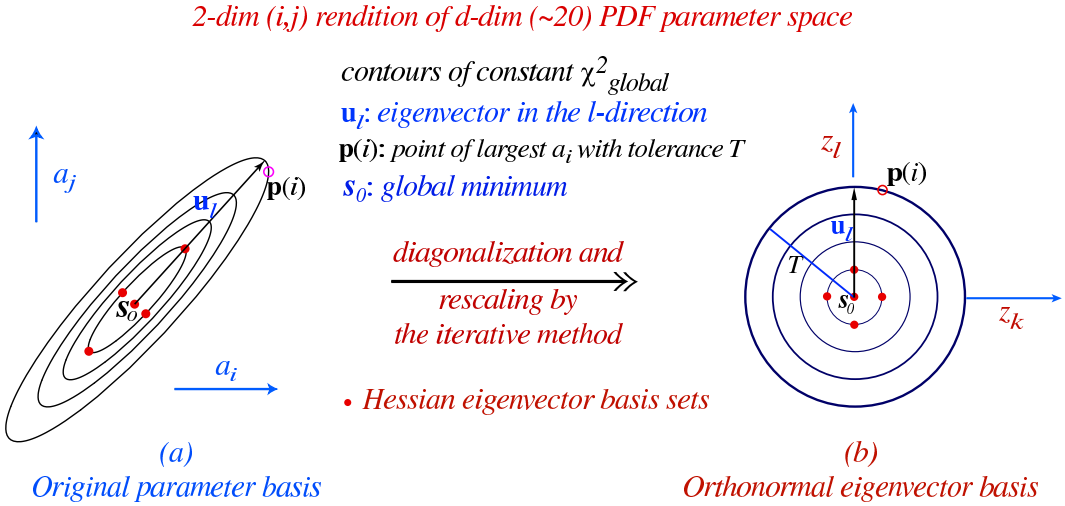

Implemented by CTEQ, then MRST/MSTW, HERAPDF. Uncertainty on physical quantity then given by

$$(\Delta F)^2 = \sum_i \left(F(S_i^{(+)}) - F(S_i^{(-)})\right)^2,$$

where $S_i^{(+)}$ and $S_i^{(-)}$ are PDF sets displaced along eigenvector direction.

Must choose "correct" $\Delta\chi^2$ given complication of errors in full fit and sometimes conflicting data sets.

Determination of best fit and uncertainties

All but NNPDF minimise χ^2 and expand about best fit.

- MSTW08 – 20 eigenvectors. Due to incompatibility of different sets and (perhaps to some extent) parameterisation inflexibility (little direct evidence for this) have inflated $\Delta\chi^2$ of $5 - 20$ for eigenvectors.
- CT10 – 26 eigenvectors. Inflated $\Delta\chi^2$ of ~ 50 for 1 sigma for eigenvectors.
- HERAPDF2.0 – 10 eigenvectors. Use "$\Delta\chi^2 = 1$". Additional model and parameterisation uncertainties.
- ABKM09 – 21 parton parameters. Use $\Delta\chi^2 = 1$. Also α_S, m_c, m_b.
- GJR08 – 20 parton parameters (8 fixed for uncertainty) and α_S. Use $\Delta\chi^2 \approx 20$. Impose strong theory constraint on input form of PDFs.

Perhaps surprisingly all get rather similar uncertainties for PDFs cross-sections, though don't all mean the same.

Neural Network group (Ball *et al.*) limit parameterization dependence. Leads to alternative approach to "best fit" and uncertainties.

First part of approach, no longer perturb about best fit. Construct a set of Monte Carlo replicas $F_{i,p}^{art,k}$ of the original data set $F_{i,p}^{exp,(k)}$.

- REPLICAS FLUCTUATE ABOUT CENTRAL DATA:

$$F_{i,p}^{(art)(k)} = S_{p,N}^{(k)} F_{i,p}^{\exp} \left(1 + r_p^{(k)} \sigma_p^{\rm stat} + \sum_{j=1}^{N_{\rm sys}} r_{p,j}^{(k)} \sigma_{p,j}^{\rm sys}\right)$$

Where $r_p^{(k)}$ are random numbers following Gaussian distribution, and $S_{p,N}^{(k)}$ is the analogous normalization shift of the of the replica depending on $1 + r_{p,n}^{(k)} \sigma_p^{norm}$. Hence, include information about measurements and errors in distribution of $F_{i,p}^{art,(k)}$.

Fit to the data replicas obtaining PDF replicas $q_i^{(net)(k)}$ (follows Giele *et al.*)

Mean μ_O and deviation σ_O of observable O then given by

$$\mu_O = \frac{1}{N_{rep}} \sum_1^{N_{rep}} O[q_i^{(net)(k)}], \quad \sigma_O^2 = \frac{1}{N_{rep}} \sum_1^{N_{rep}} (O[q_i^{(net)(k)}] - \mu_O)^2.$$

Eliminates parameterisation dependence by using a neural net which undergoes a series of (mutations via genetic algorithm) to find the best fit. In effect is a much larger sets of parameters – ~ 37 per distribution.

Parameterisations - for the gluon at small x different parameterisations lead to very different uncertainty for small x gluon.

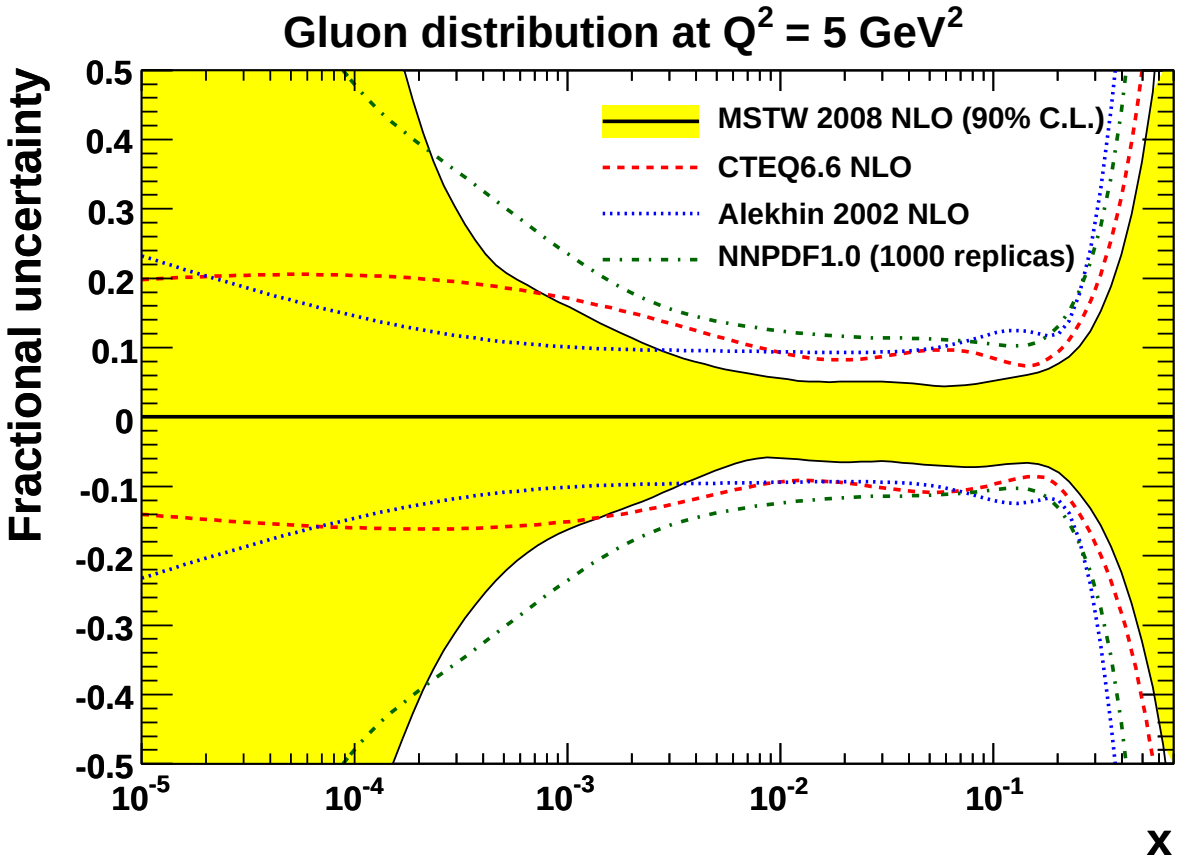

Most assume single power x^λ at input $\rightarrow$ limited uncertainty. If input at low Q^2 λ positive and small-x input gluon *fine-tuned* to ~ 0. Artificially small uncertainty.

If $g(x) \propto x^{\lambda \pm \Delta\lambda}$ then $\Delta g(x) = \Delta\lambda \ln(1/x) * g(x)$.

MRST/MSTW and NNPDF more flexible (can be negative) $\rightarrow$ rapid expansion of uncertainty where data runs out. CT10 more flexible than previous versions.

Generally high-x PDFs parameterised so will behave like $(1-x)^{\eta}$ as $x \to 1$. More flexibility in CTEQ.

Very hard high-x gluon distribution (more-so even than NNPDF uncertainties).

However, is gluon, which is radiated from quarks, harder than the up valence distribution for $x \to 1$?

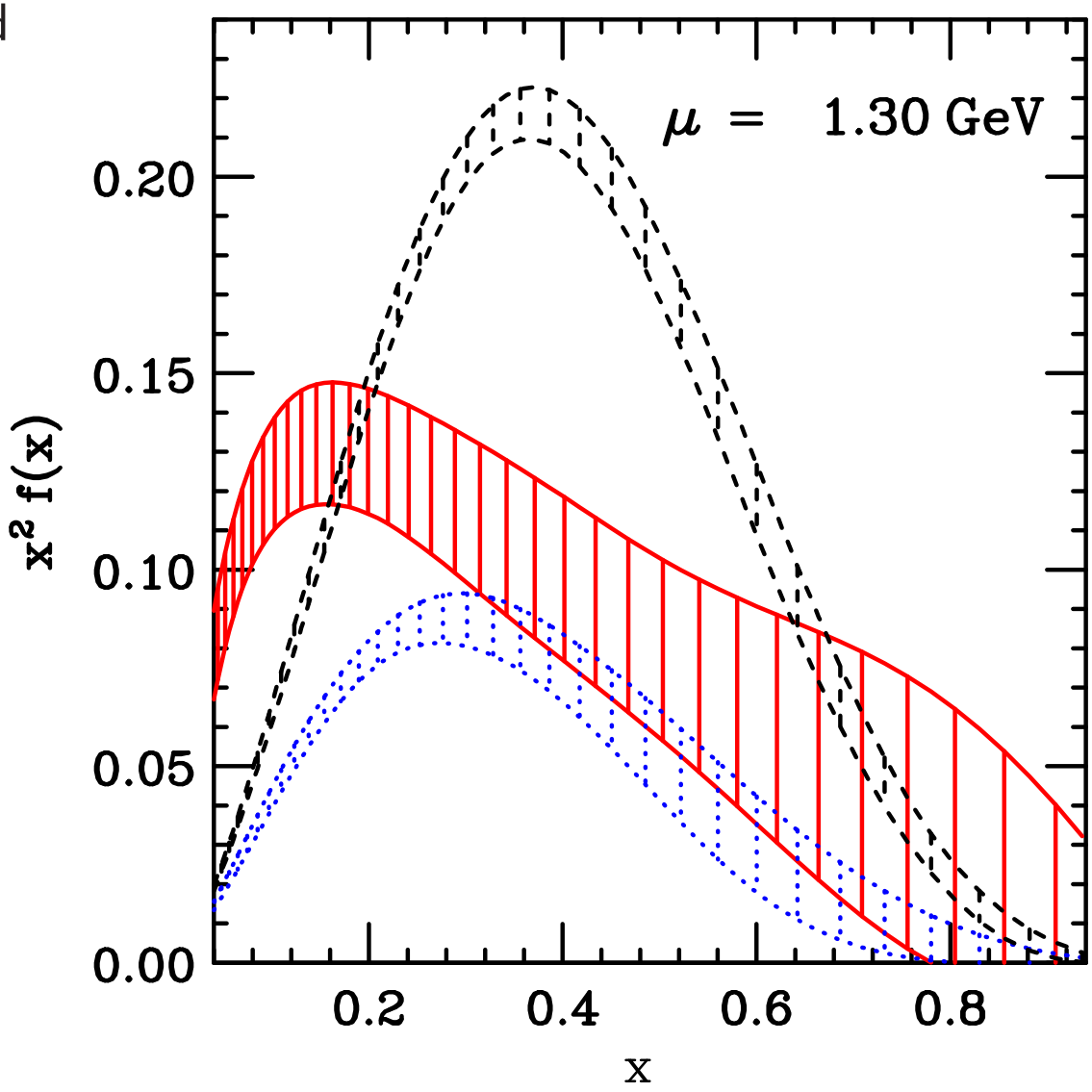

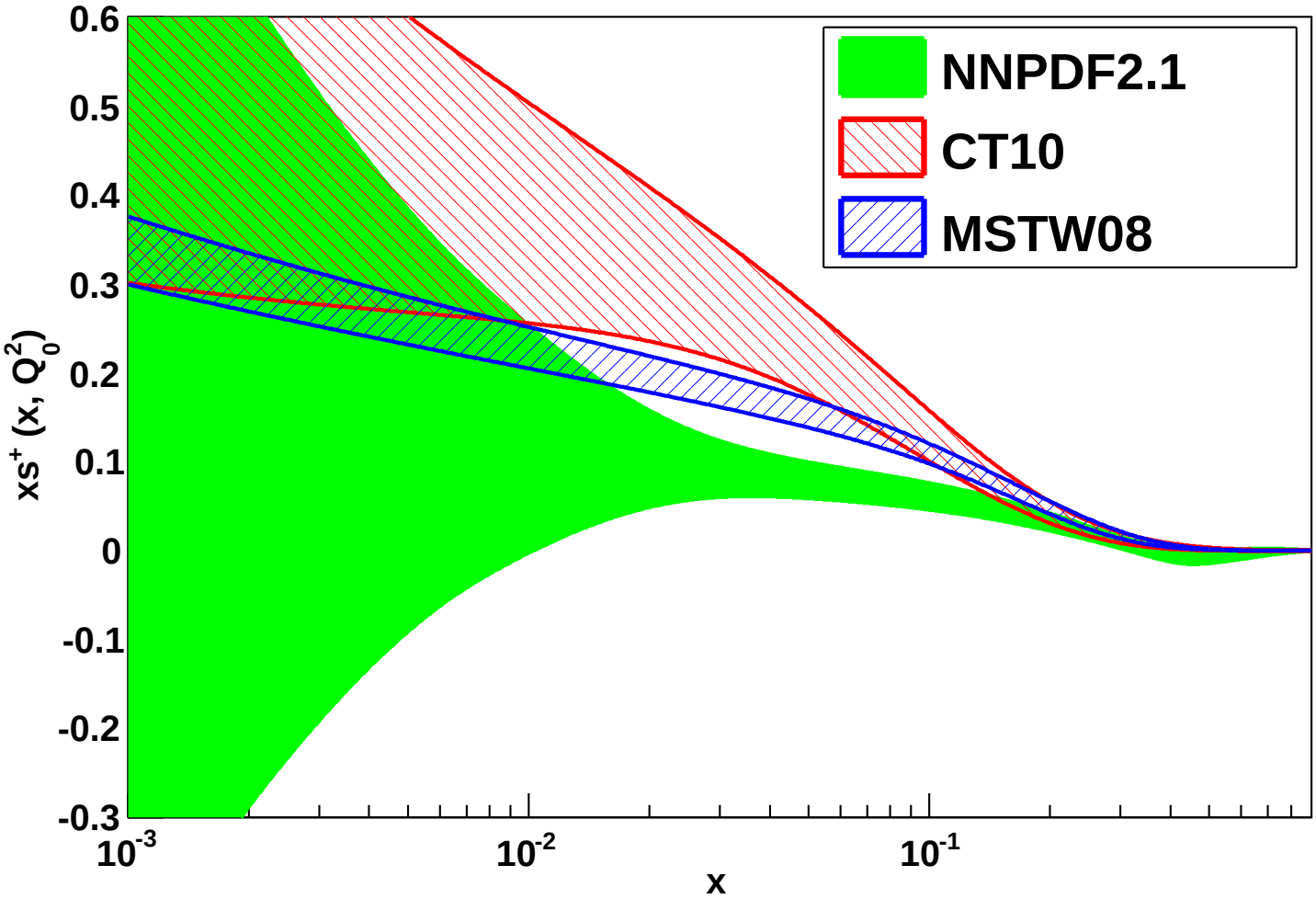

MSTW has theory assumption on strange at small x, CT10 less strong and NNPDF fully flexible.

Variation near $x = 0.05$ where data exists likely due to heavy flavour definitions/nuclear corrections.

Heavy Quarks – Essential to treat these correctly. Two distinct regimes:

Near threshold $Q^2 \sim m_H^2$ massive quarks not partons. Created in final state. Described using **Fixed Flavour Number Scheme** (FFNS).

$$F(x,Q^2) = C_k^{FF}(Q^2/m_H^2) \otimes f_k^{n_f}(Q^2)$$

Does not sum $\ln^n(Q^2/m_H^2)$ terms, and not calculated for many processes beyond LO. Used by AB(K)M and (G)JR. Sometimes final state details in this scheme only.

Alternative, at high scales $Q^2 \gg m_H^2$ heavy quarks like massless partons. Behave like up, down, strange. Sum $\ln(Q^2/m_H^2)$ terms via evolution. **Zero Mass Variable Flavour Number Scheme** (ZM-VFNS). Normal assumption in calculations. Ignores $\mathcal{O}(m_H^2/Q^2)$ corrections. No longer used.

$$F(x,Q^2) = C_j^{ZMVF} \otimes f_j^{n_f+1}(Q^2).$$

Advocate a **General Mass Variable Flavour Number Scheme** (GM-VFNS) interpolating between the two well-defined limits of $Q^2 \leq m_H^2$ and $Q^2 \gg m_H^2$. Used by MRST/MSTW and more recently (as default) by CTEQ, and now also by HERAPDF and NNPDF.

Various definitions possible. Versions used by MSTW (RT) and CTEQ (ACOT) have converged somewhat.

Various significant differences still exist as illustrated by comparison to most recent H1 data on bottom production.

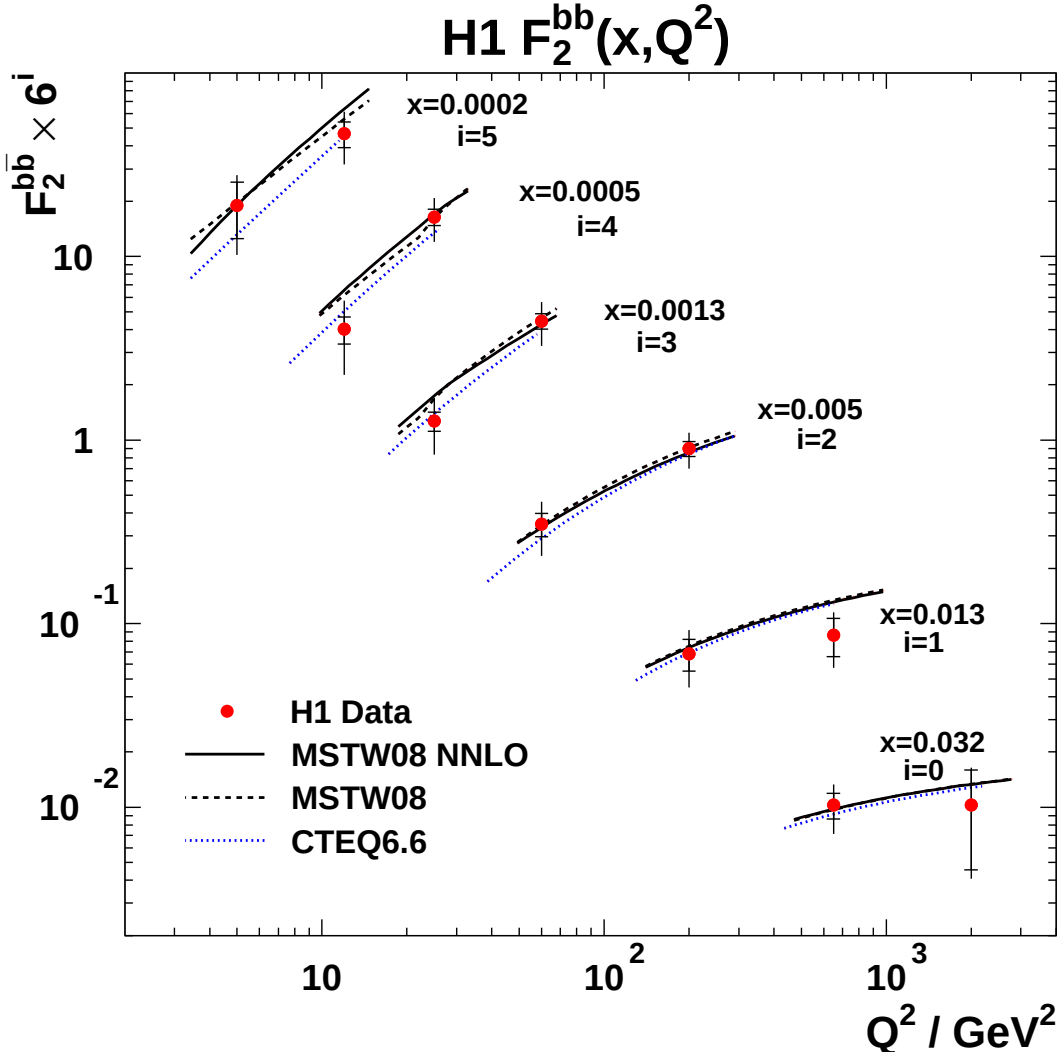

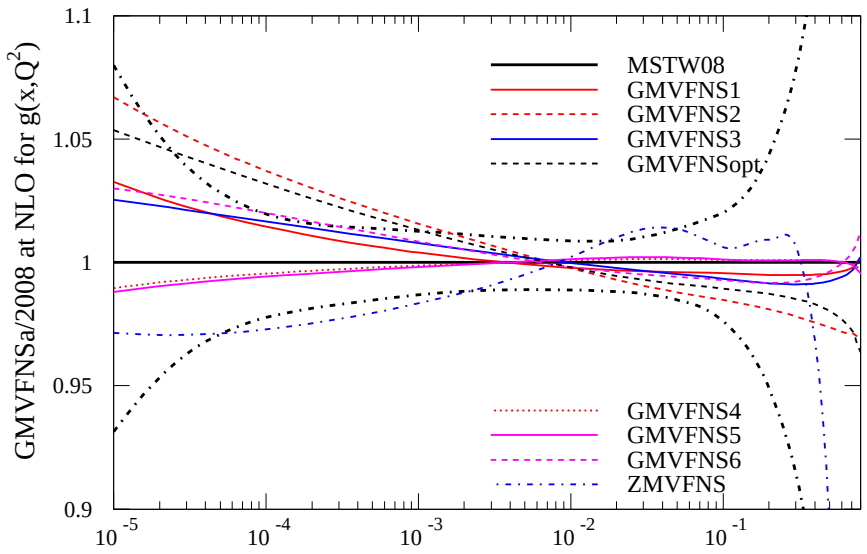

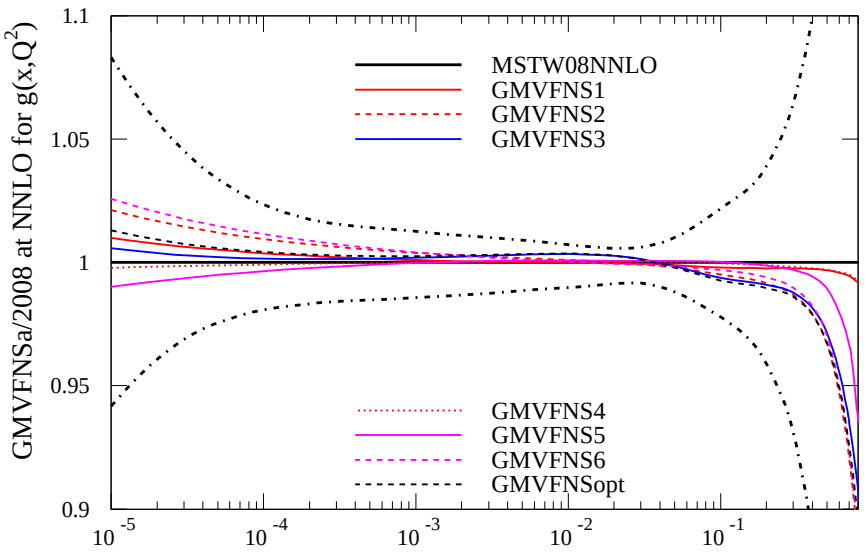

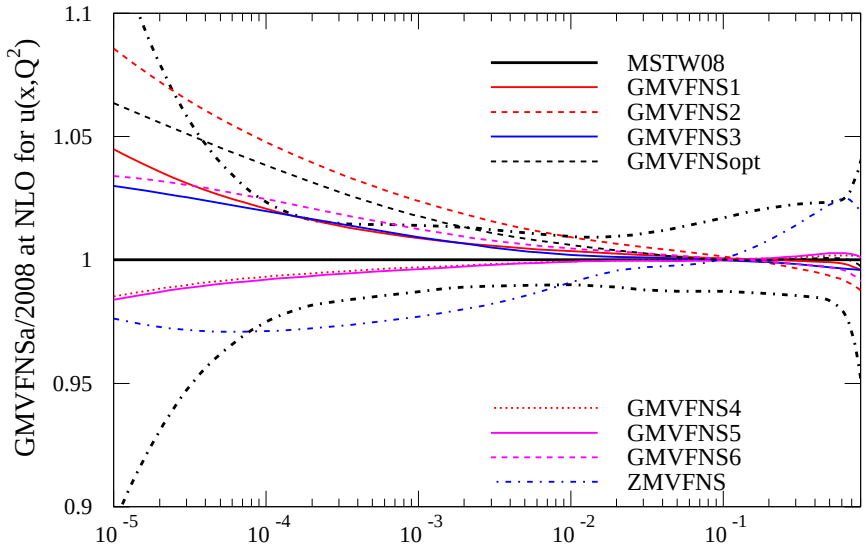

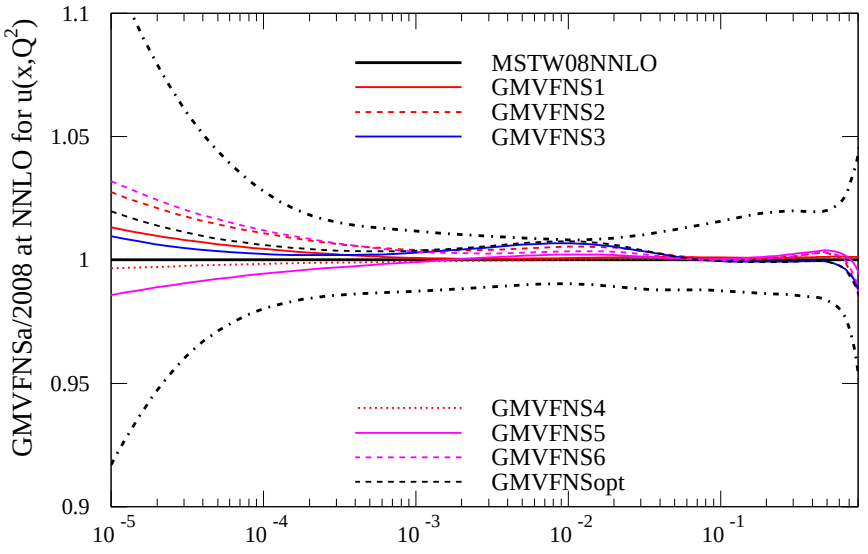

Variations in partons extracted from global fit due to different choices of GM-VFNS at NLO and at NNLO.

PDF correlation with α_S.

Can also look at PDF changes and uncertainties at different $\alpha_S(M_Z^2)$. Fully included (difficult to disentangle) in ABKM, (G)JR), but often only for one fixed $\alpha_S(M_Z^2)$.

MSTW produce sets for limits of α_S uncertainty – PDF uncertainties reduced since quality of fit already worse than best fit.

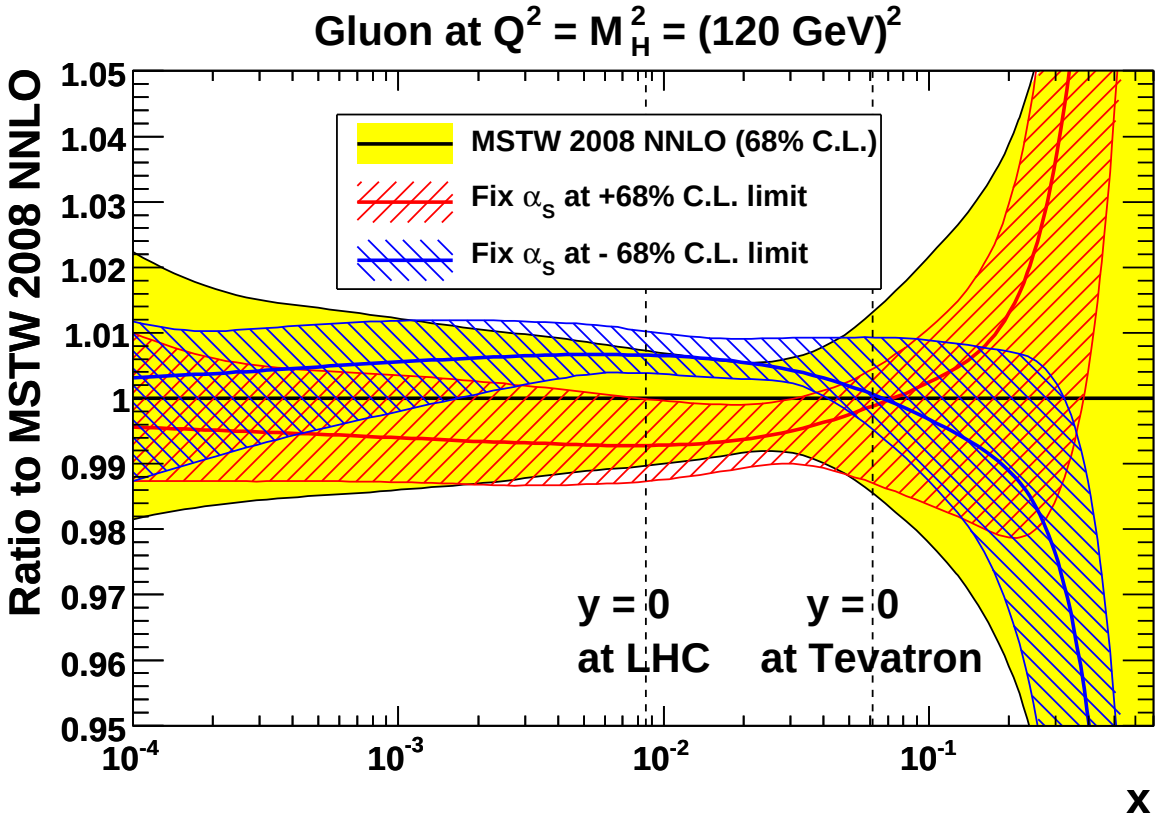

Expected gluon–$\alpha_S(M_Z^2)$ small–x anti-correlation $\rightarrow$ high-x correlation from sum rule.

NNLO predictions for Higgs ($120\mathrm{GeV}$) production for different allowed $\alpha_S(M_Z^2)$ values and their uncertainties.

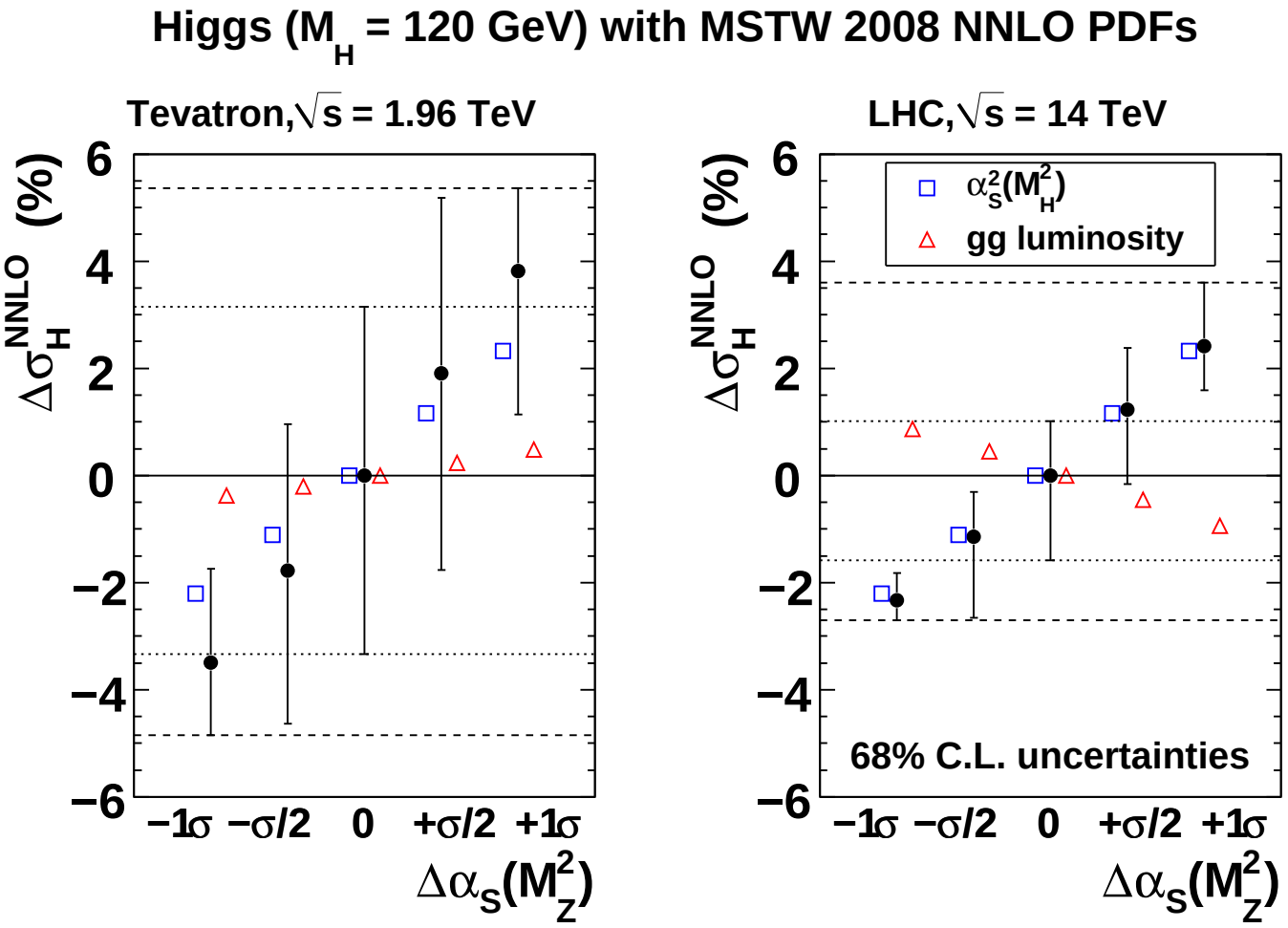

Increases by a factor of $2-3$ (up more than down) at LHC. Direct $\alpha_S(M_Z^2)$ dependence mitigated somewhat by anti-correlated small-x gluon (asymmetry feature of *minor* problems in fit to HERA data). At Tevatron intrinsic gluon uncertainty dominates.

Other sources of Uncertainty.

Also other sources which (mainly) lead to inaccuracies common to all fixed-order extractions.

- Standard higher orders NNLO. Many sets available here, soon all of them.
- QED and Weak (comparable to NNLO ?) ($\alpha_s^3 \sim \alpha$). Sometime enhancements.
- Nuclear/deuterium corrections to structure functions.
- Resummations, e.g. small x $(\alpha_s^n \ln^{n-1}(1/x))$, or large x $(\alpha_s^n \ln^{2n-1}(1-x))$.
- low Q^2 (higher twist), saturation.

Deuterium corrections.

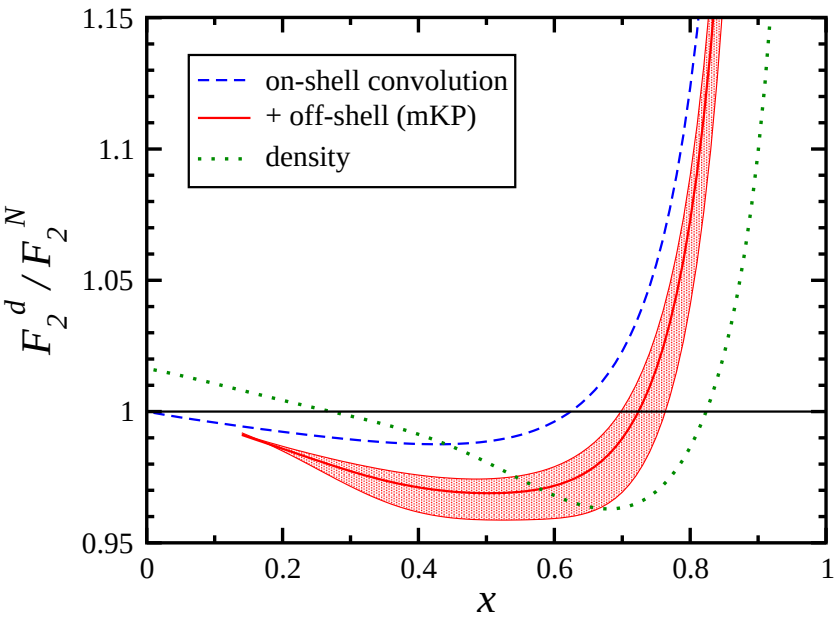

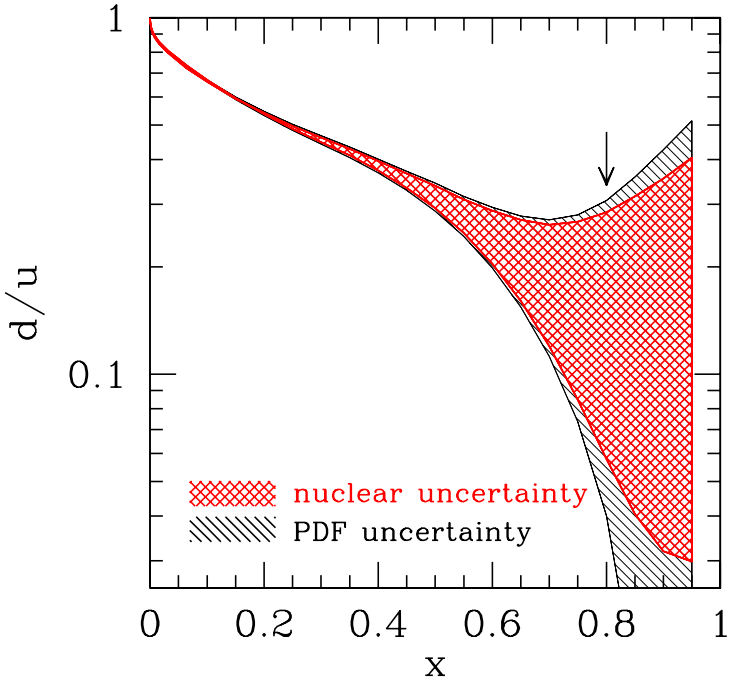

Variation in W^+/W^- ratio probably partially related to the issue of deuterium corrections.

Recent study (Accardi *et al*) suggests these may be large.

Uncertainty in correction as large as PDF uncertainty, but size of corrections can be larger.

MSTW found improvement in fit to both global data set and lepton asymmetry with deuterium corrections, but < 1 for all but very high x.

Also find significant improvement with rather more plausible deuterium corrections.

Ongoing study for MSTW.

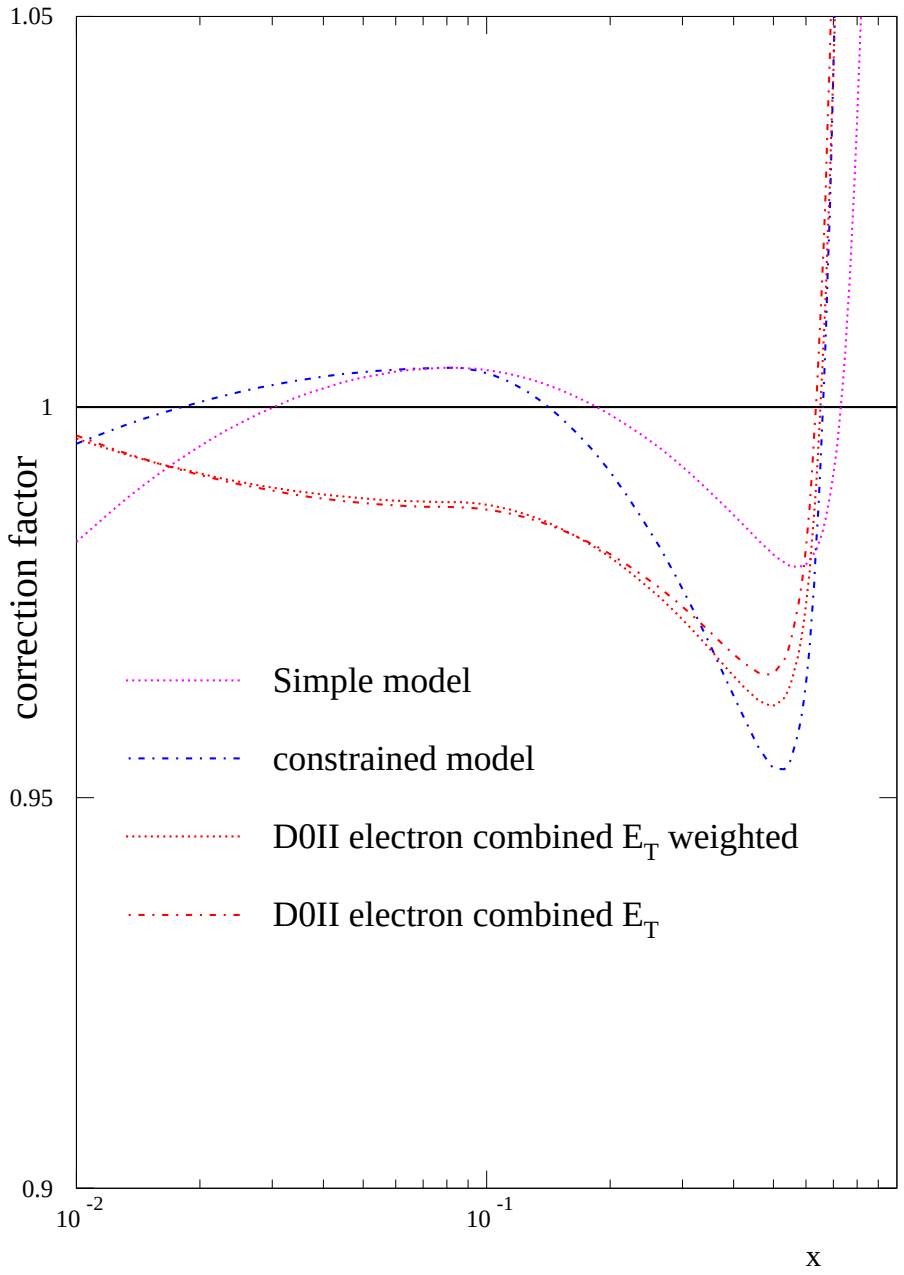

PDFs at NNLO

NNLO splitting functions (Moch, Vermaseren and Vogt) allow essentially full NNLO determination of partons now being performed, though heavy flavour not fully worked out in the fixed-flavour number scheme (FFNS) and jet cross-sections are only approximate. Improves consistency of fit very slightly, and reduces α_S.

Surely this is best, i.e. most accurate.

Yes, but ..... only know some hard cross-sections at NNLO.

Processes with two strongly interacting particles largely completed

DIS coefficient functions and sum rules

$pp(\bar{p}) \to \gamma^\star, W, Z$ (including rapidity dist.), H, A^0, WH, ZH.

But for many other final states NNLO not known. NLO still more appropriate.

How do NNLO PDFs compare to NLO?

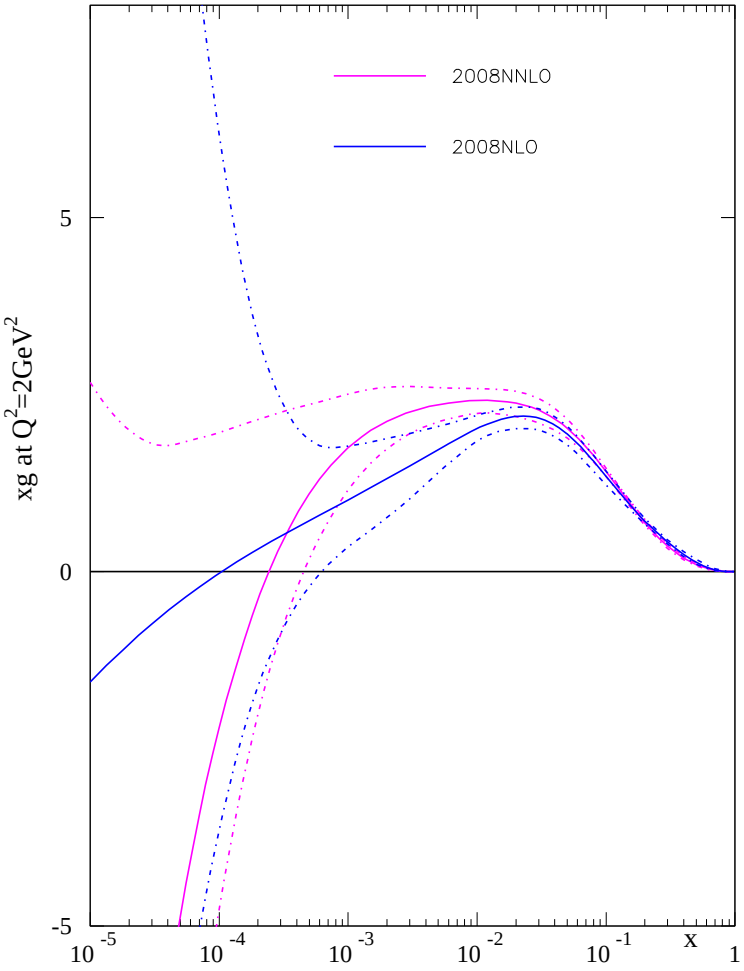

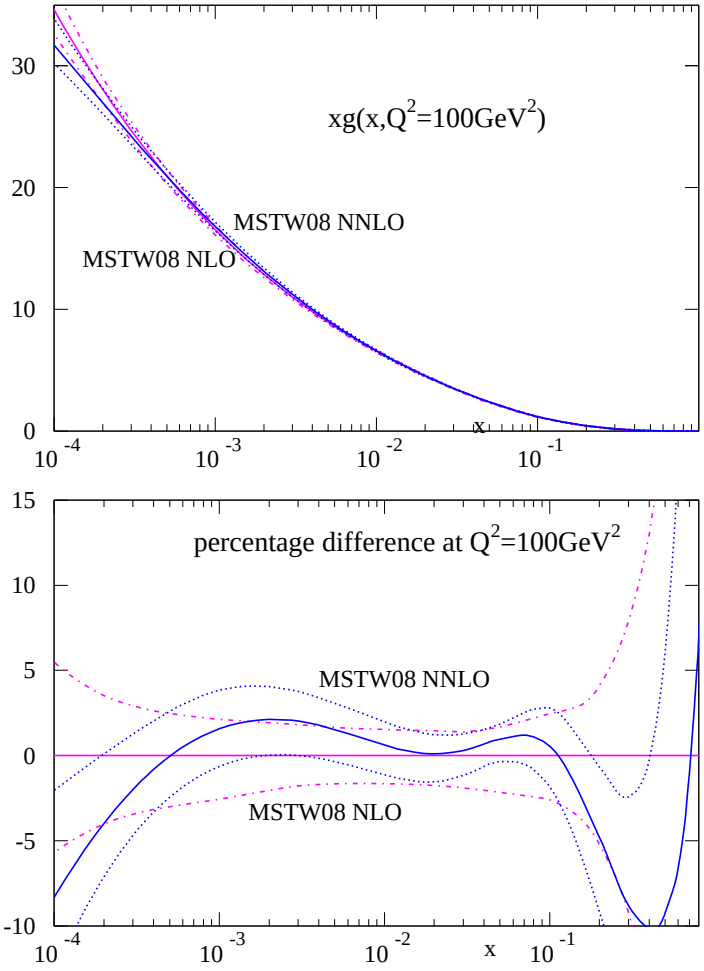

Gluons different at NLO and NNLO at low Q^2. Largely washed out by evolution, but only because of different α_S.

Sometimes vital to use NNLO PDFs if calculating at NNLO.

Systematic difference between PDF defined at NLO and at NNLO.

Due to large (negative) gluon coefficient function at not too small x.

Systematic difference between PDF defined at NLO and at NNLO.

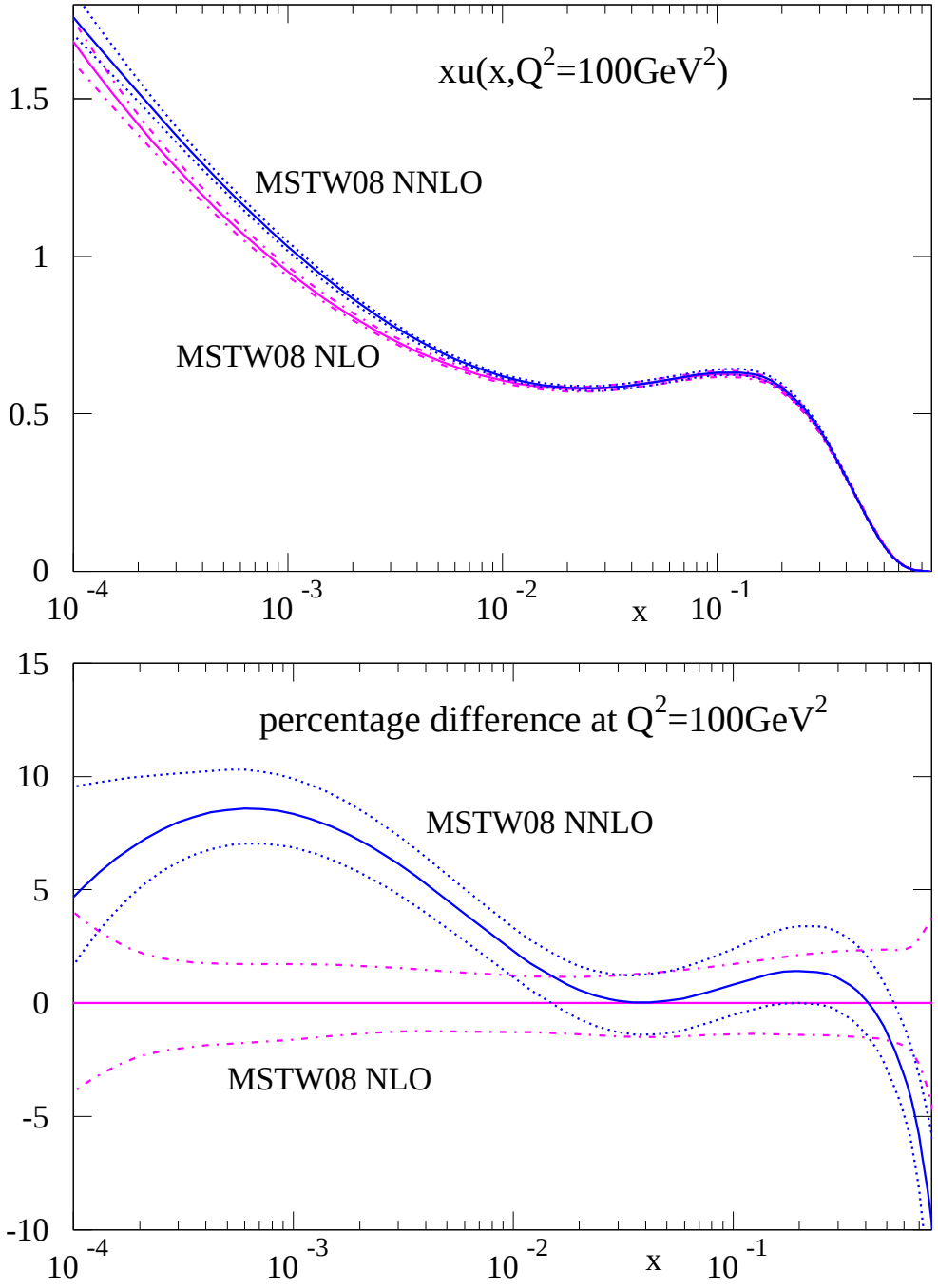

Considerations of differences and of NNLO

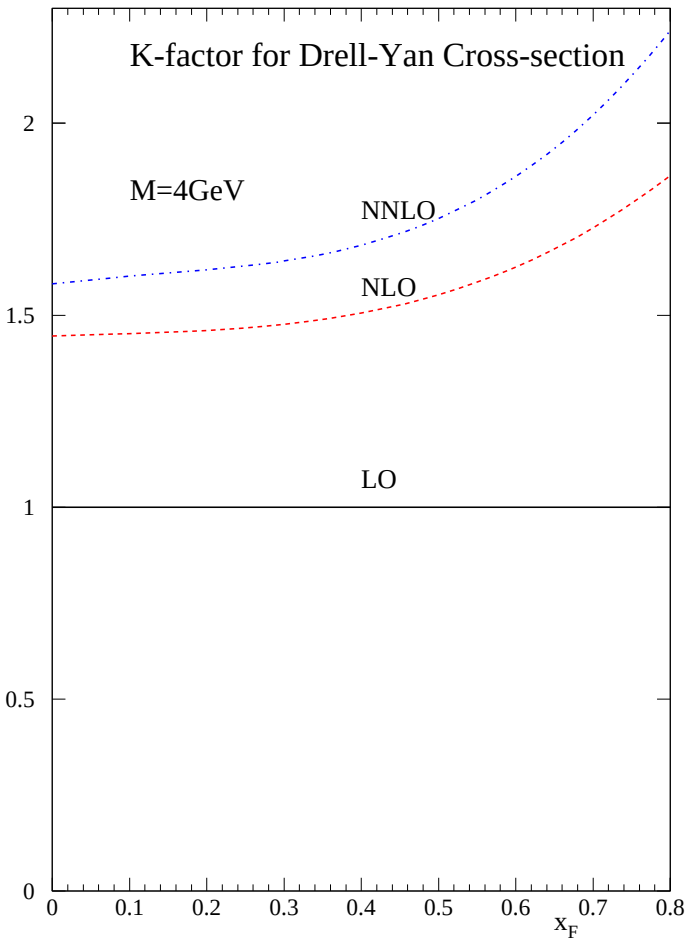

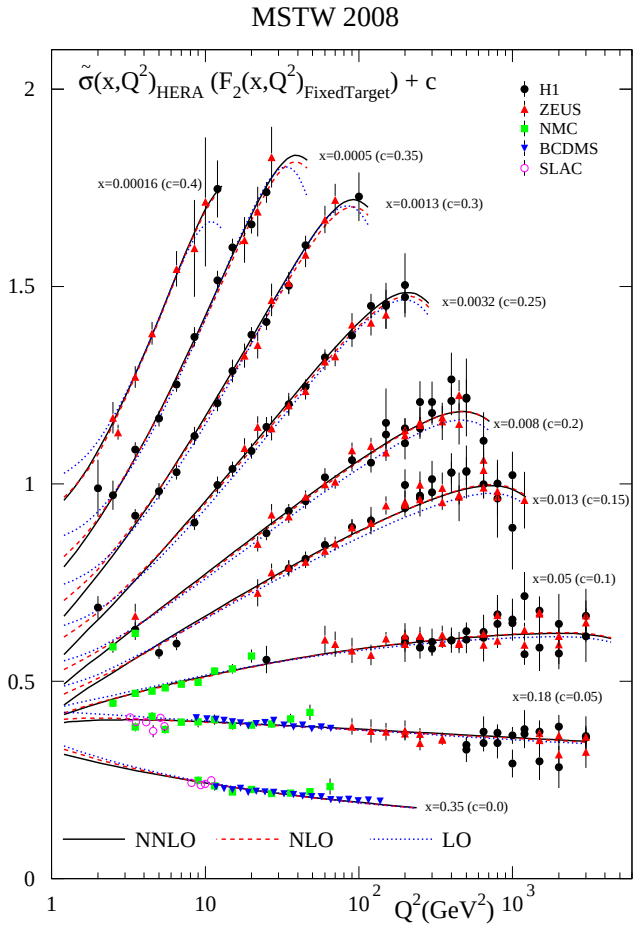

In general NNLO corrections either positive for cross sections, e.g. Drell Yan, or for evolution in structure functions.

Automatically leads to lower $\alpha_S(M_Z^2)$ at NNLO than at NLO, i.e. 0.1171 rather than 0.1202. Difference between two quite stable.

Converging on general agreement that the NNLO values of α_S are $0.0002 - 0.0003$ smaller than the NLO values of α_S?

MSTW08 – $\alpha_S(M_Z^2) = 0.1202 \to 0.1171$.

ABKM09 – $\alpha_S(M_Z^2) = 0.1179 \to 0.1135$.

GJR/JR – $\alpha_S(M_Z^2) = 0.1145 \to 0.1124$.

NNPDF2.1 – $\alpha_S(M_Z^2) = 0.1191 \to 0.1174$.

CT10.1 – $\alpha_S(M_Z^2) = 0.1196 \to 0.1180$(both prelim – PDF4LHC, DESY July).

HERAPDF1.6 – $\alpha_S(M_Z^2) = 0.1202$ at NLO and general preference for ~ 0.1176 at NNLO.

Central values differ far more than NLO $\to$ NNLO trend.

NLO → NNLO **PDF differences**

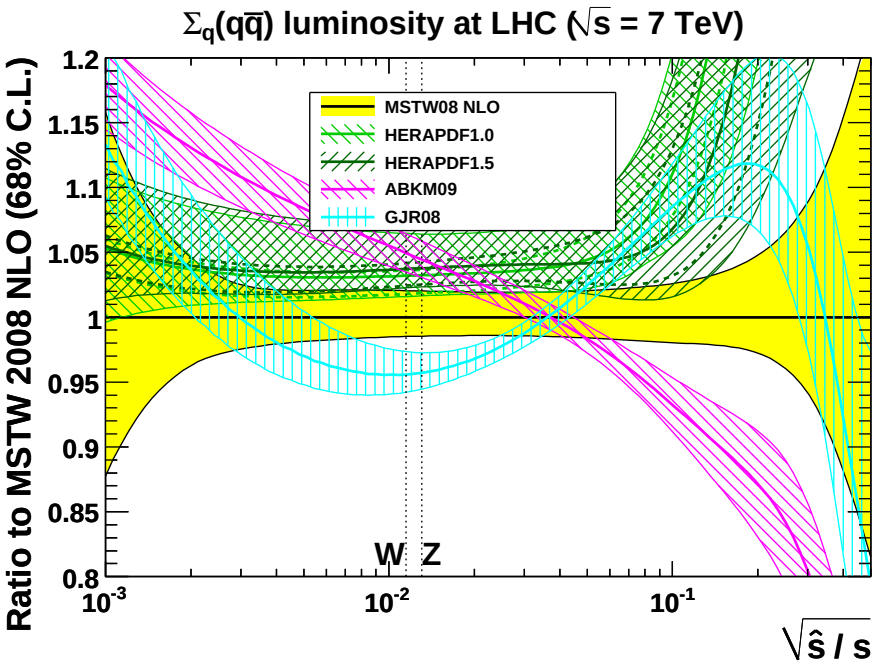

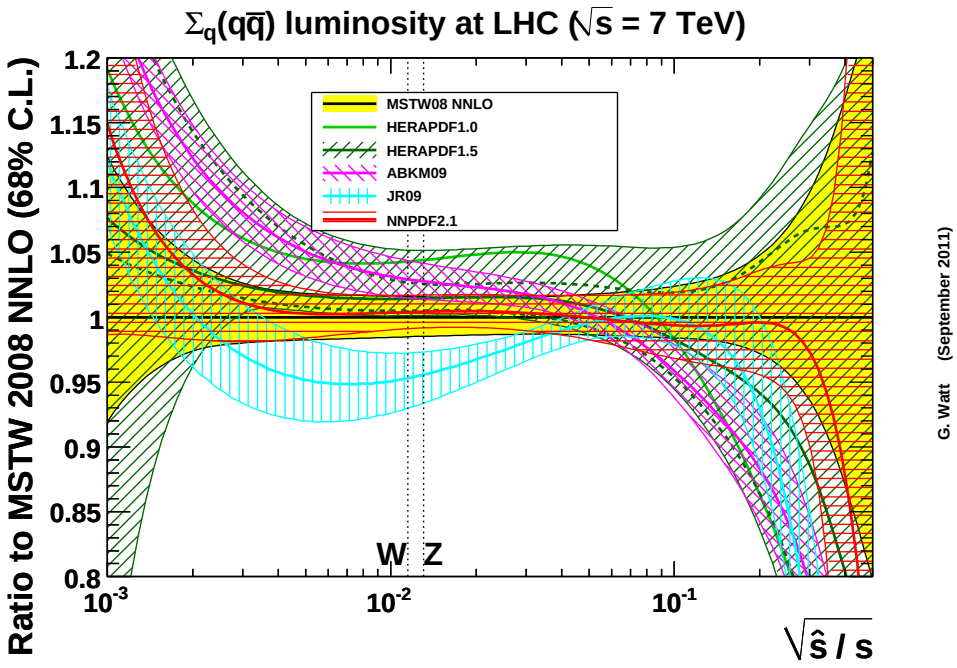

Luminosity differences for quarks largely the same at NNLO as at NLO, except for HERAPDF1.5 at large x.

Differences between different sets not likely to be due to theory choices which would diminish at higher orders, or approx. at NNLO which would change relative NLO and NNLO differences.

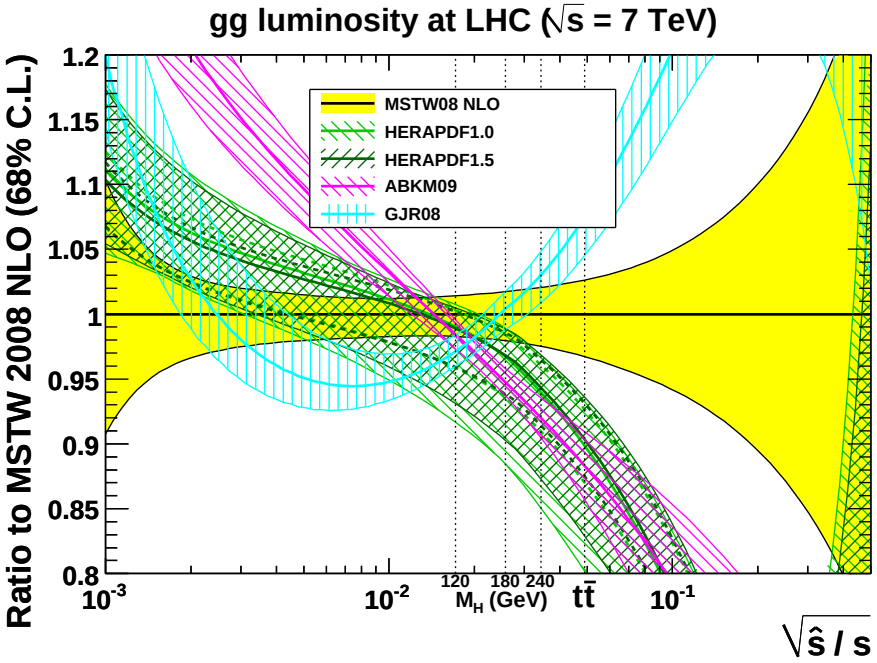

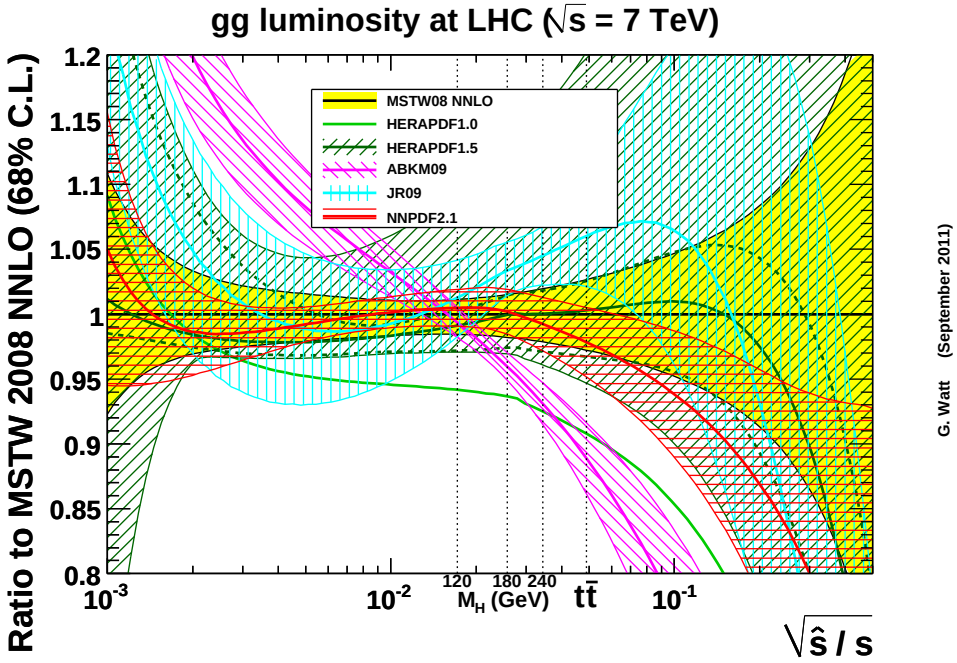

Luminosity differences for the gluon also largely the same at NNLO as at NLO, except for HERAPDF1.5 again.

Investigation to stability under changes in cuts.

Raise $W^2_{\rm cut}$ to $20{\rm GeV}^2$, but no real changes.

Also raise $Q^2_{\rm cut}$ to $5{\rm GeV}^2$ and then $10{\rm GeV}^2$.

At NLO some movement just outside default error bands at general x.

Find $\alpha_S(M_Z^2) = 0.1202 \rightarrow 0.1193 \rightarrow 0.1175$, though for $Q^2 = 10{\rm GeV}^2$ cut error has roughly doubled to about 0.0025.

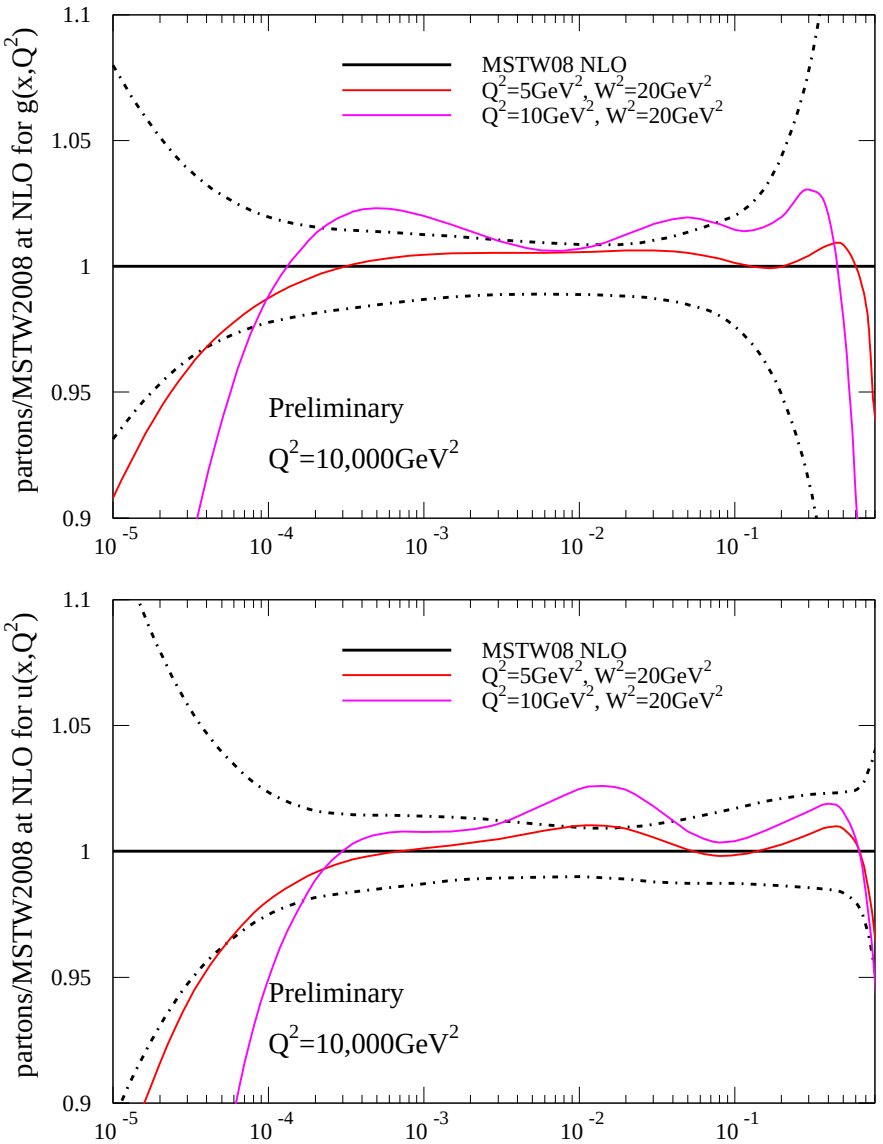

At NNLO most movement outside default error bands at low x, where constraint vanishes as Q^2 cut raises.

For $Q^2_{\rm cut} = 10{\rm GeV}^2$ no points below $x = 0.0001$, and little lever arm for evolution constraint for a bit higher.

Find $\alpha_S(M_Z^2) = 0.1171 \rightarrow 0.1171 \rightarrow 0.1164$, i.e. no change of significance.

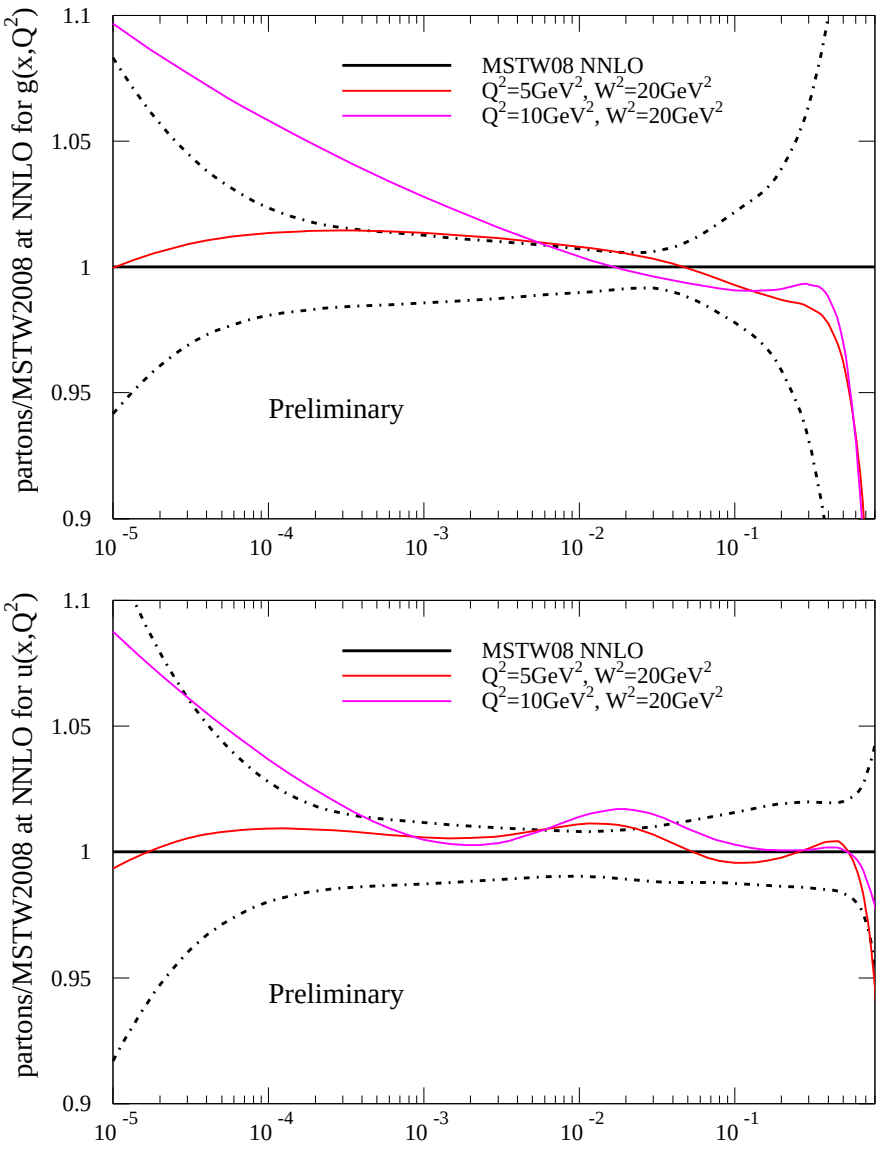

The % change in the cross sections after cuts ($M_H = 165\text{GeV}$).

Q^2_{cut}	NLO 5GeV^2	10GeV^2	NNLO 5GeV^2	10GeV^2
W Tev	0.0	-2.4	-0.7	-0.4
Z Tev	0.0	-0.8	-0.4	0.0
W LHC (7TeV)	-0.2	-0.1	-0.2	-0.2
Z LHC (7TeV)	-0.2	-0.3	-0.4	-0.5
W LHC (14TeV)	-0.6	-1.1	0.3	0.8
Z LHC (14TeV)	-0.6	-1.5	0.2	0.4
Higgs TeV	-1.1	-1.5	-1.2	-3.2
Higgs LHC (7TeV)	-0.8	-2.5	0.4	-1.8
Higgs LHC (14TeV)	-0.9	-1.9	1.0	-0.8

More variation at NLO than at NNLO, i.e. 7 changes of $> 1\%$ compared to 4.

However, both small, and changes with change in Q^2_{cut} slow. Does not suggest significant higher twist or problem with default cuts.

Small-x Theory

At each order in α_S each splitting function and coefficient function obtains an extra power of $\ln(1/x)$ (some accidental zeros in P_{gg}), i.e. $P_{ij}(x, \alpha_s(Q^2)), C_i^P(x, \alpha_s(Q^2)) \sim \alpha_s^m(Q^2) \ln^{m-1}(1/x)$.

Summed using BFKL equation (and a lot of work – Altarelli-Ball-Forte, Ciafaloni-Colferai-Salam-Stasto and White-RT)

Comparison to H1 prelim data on $F_L(x, Q^2)$ at low Q^2, only within White-RT approach, suggests resummations may be important.

Could possibly give a few percent effect on Higgs cross sections.

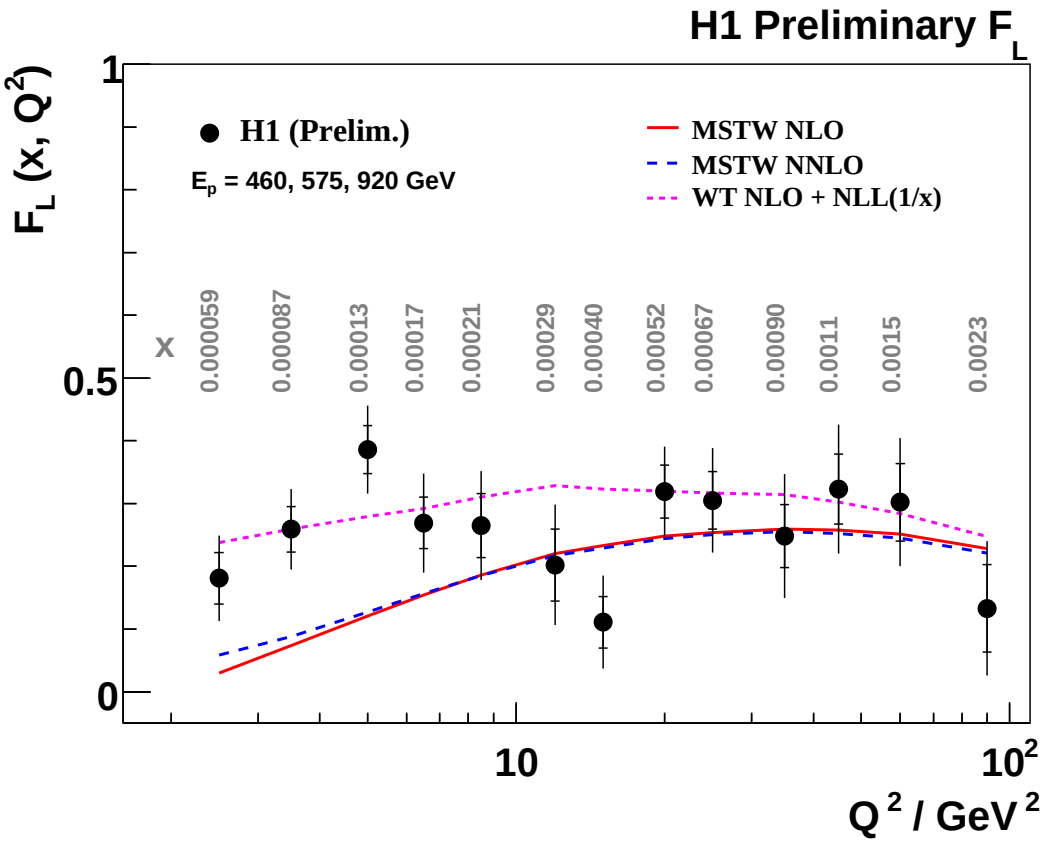

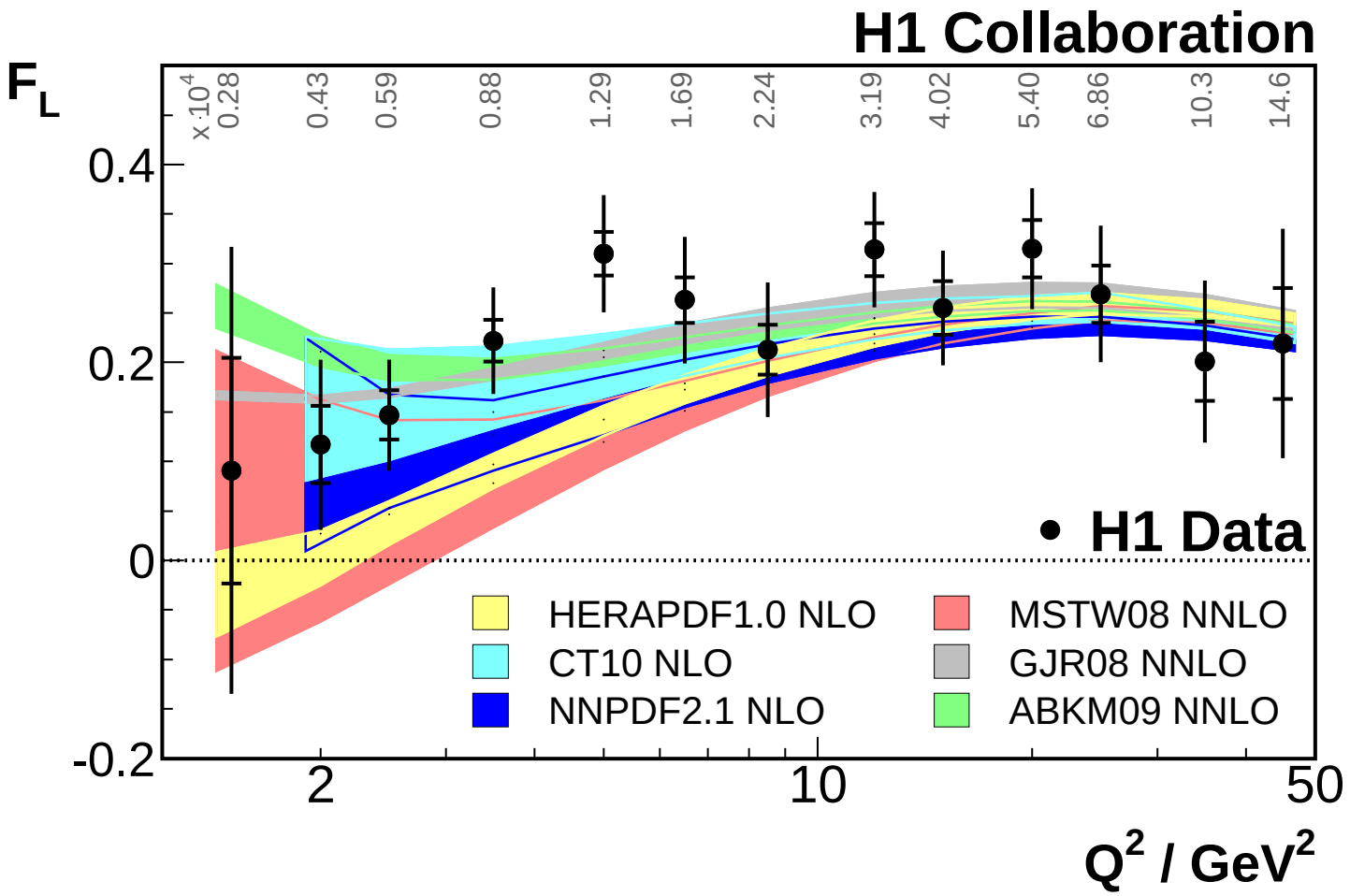

However, quite a large PDF uncertainty (in general) and even larger spread, at fixed order.

Fits to Jet Data and relation to NNLO

NNLO approx. jet corrections.

Shape of corrections as function of p_T at NLO and also at approx. NNLO in inclusive case.

NNLO uses threshold (Kidonakis and Owens) approx. for Tevatron jets.

NNLO approximation not large and aids stability – always worst at high-p_T i.e. high-x. Includes large $\ln(p_T/\mu)$ terms predicted by renormalisation group.

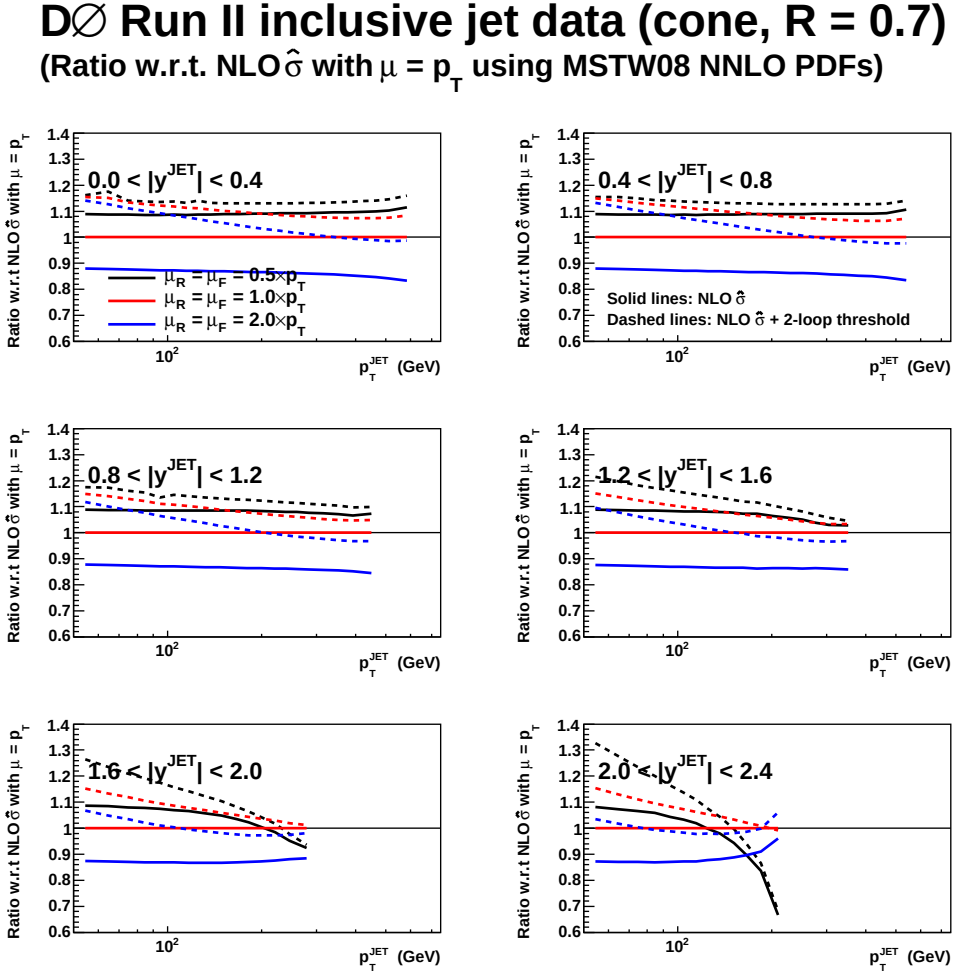

de Florian and Vogelsang result for inclusive jet K-factor for $d\sigma/dp_T$ at order α_S^{2+n} compared to NLO.

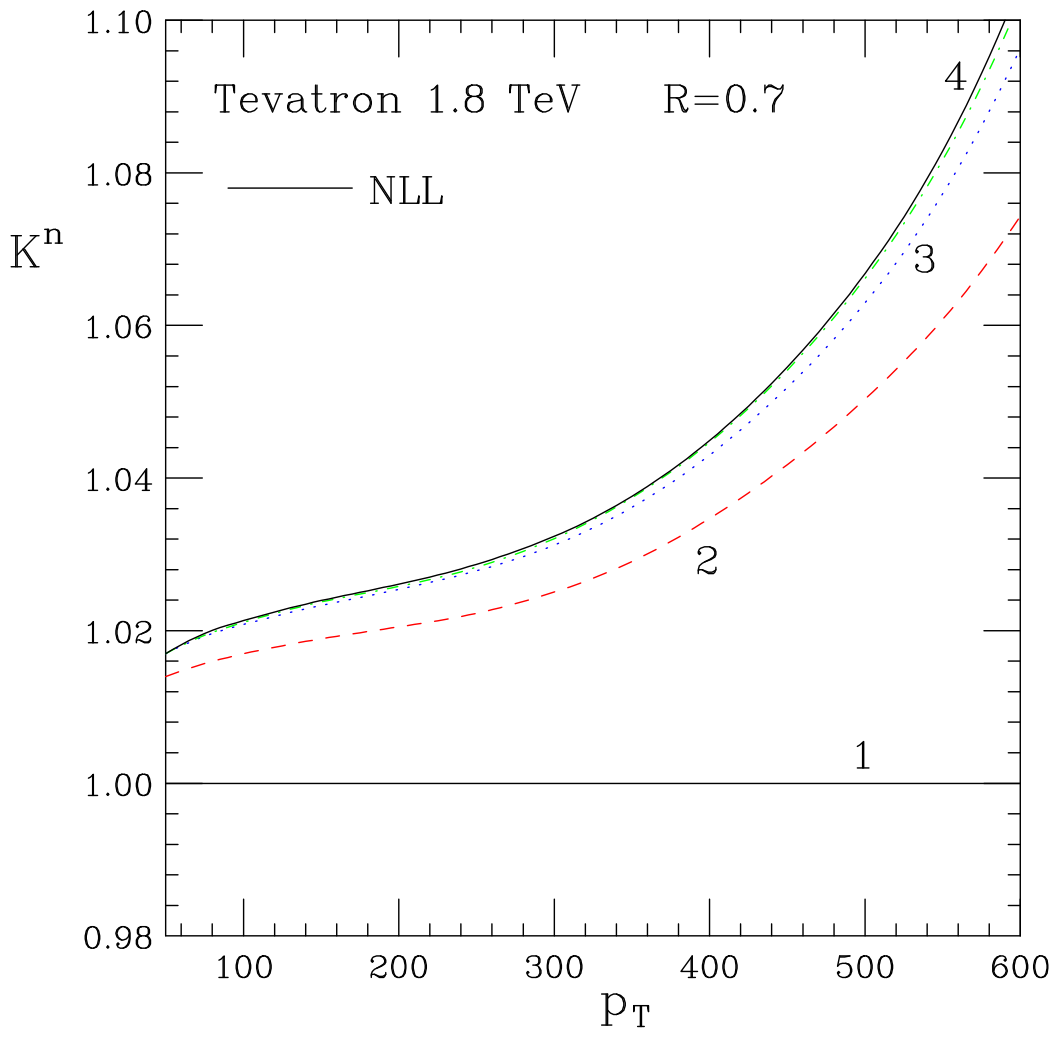

Impact on Higgs at Tevatron.

Plots (Watt) show the gluon luminosities at the Tevatron NLO and NNLO

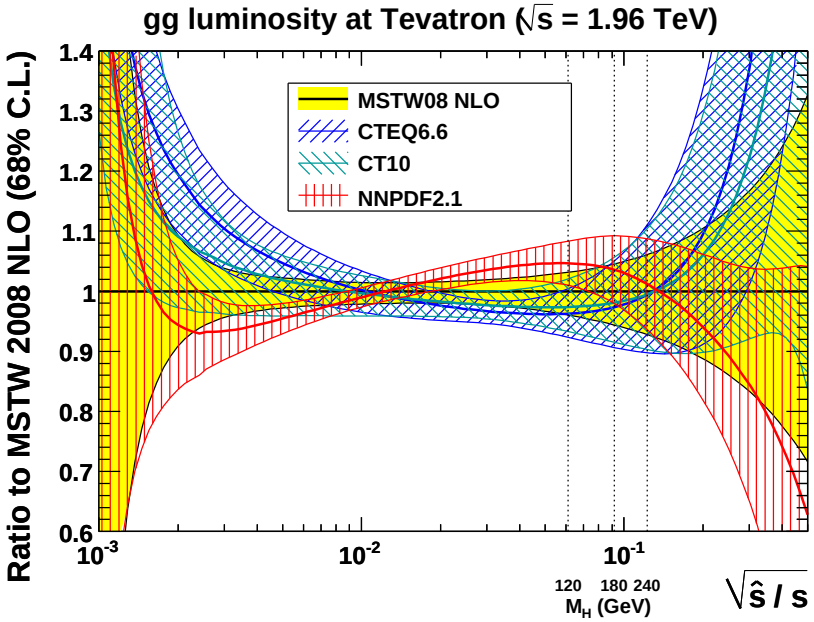

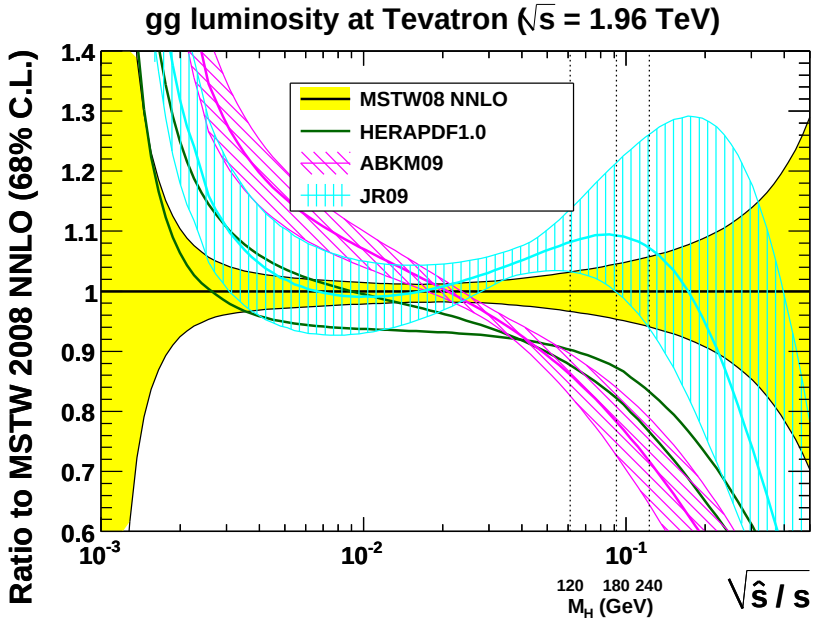

Similar to the LHC, but deviations with high-x PDF origin persist to lower $\hat{s}$.

Differences in $\alpha_S(M_Z^2)$ generally increase effect of discrepancy.

Higgs production via gluon fusion at the Tevatron and LHC at NLO and NNLO.

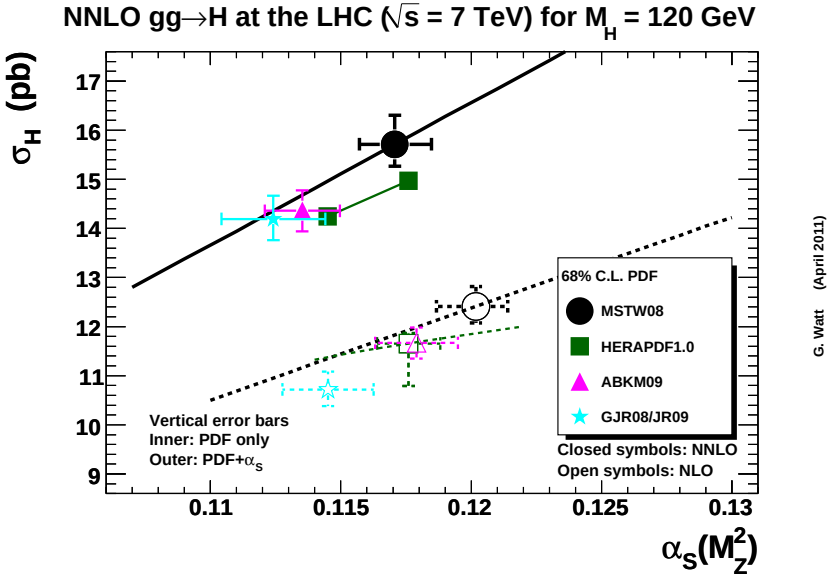

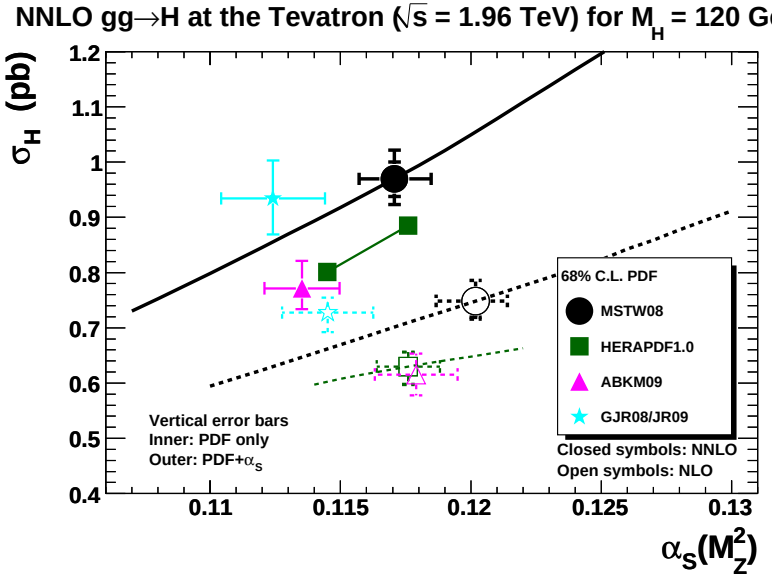

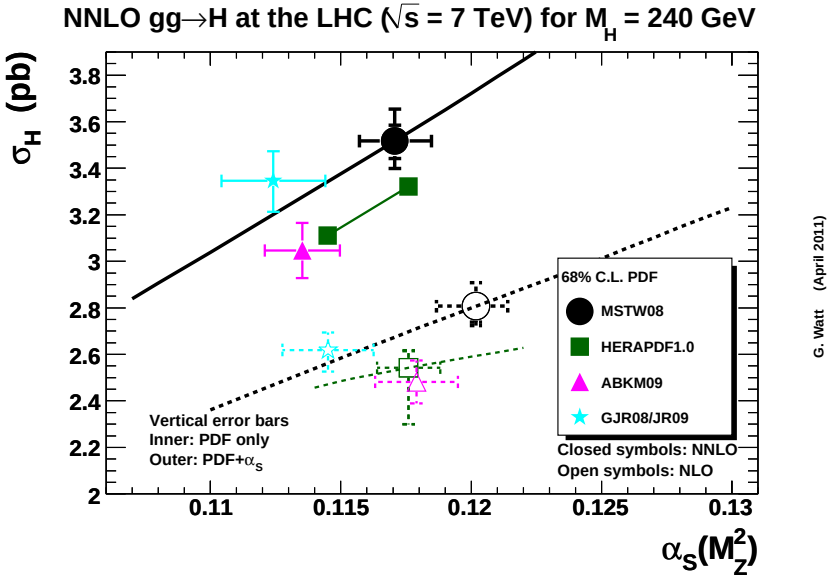

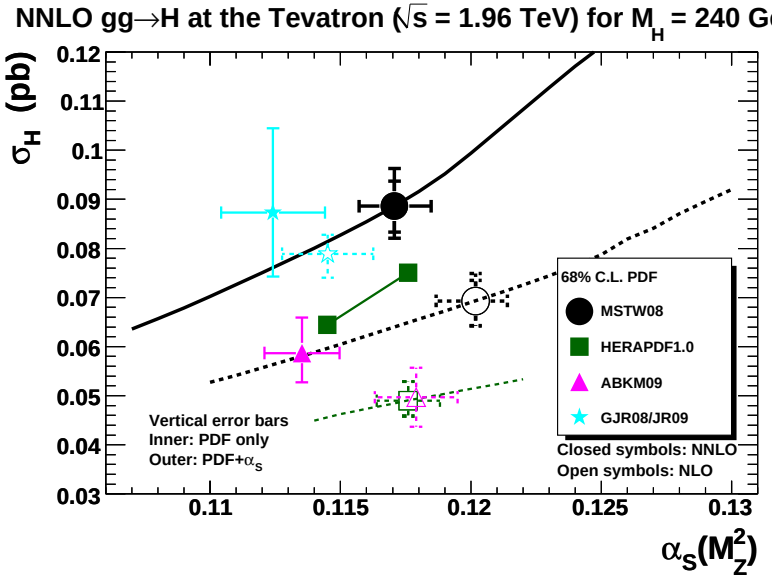

Larger deviation at the Tevatron. NNLO pattern very similar to NLO.

High-x gluon, at least to some extent, constrained by comparison to Tevatron jet data.

However, important point, CDF Z-rapidity data, or cross sections, sets Tevatron normalisation in a fit.

Only allows a few percent variation in normalisation.

Different PDF predictions for W and Z cross sections at the Tevatron compared to data.

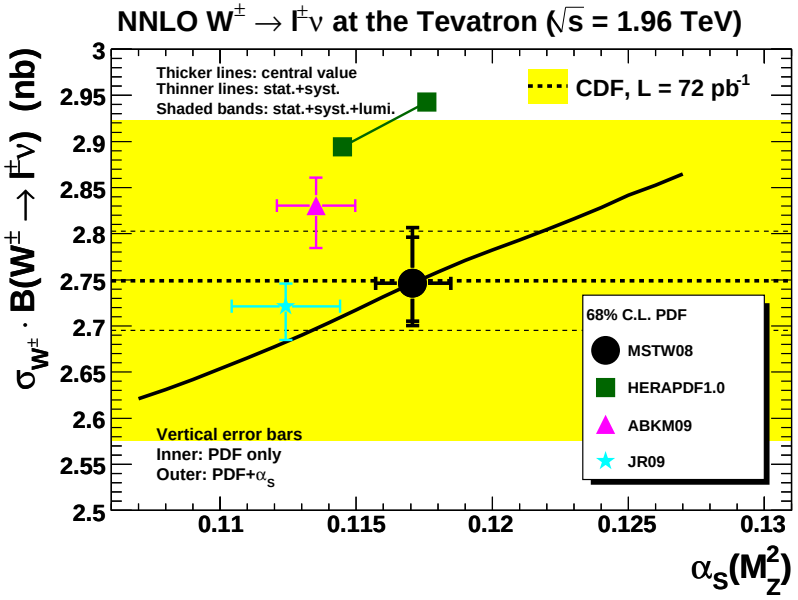

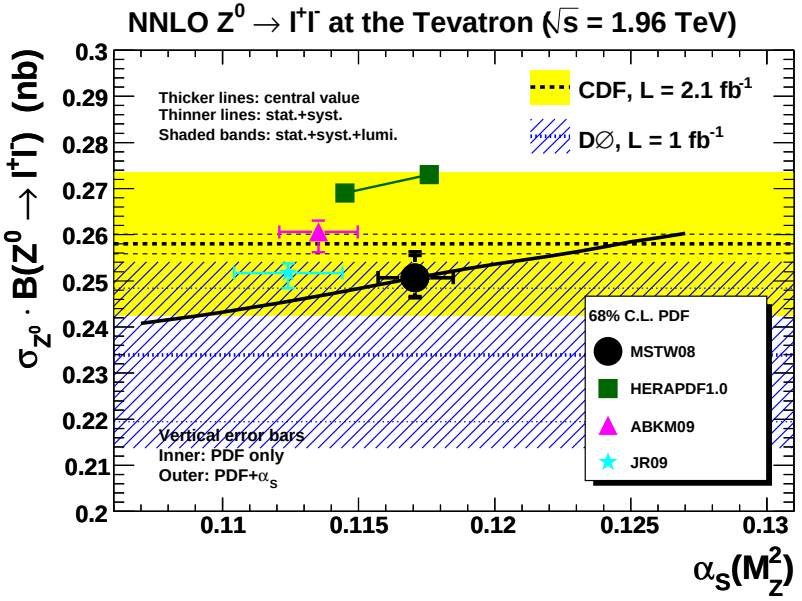

Everyone ok or a bit high. Normalisation no room to move down.

NLO PDF (with NLO $\hat{\sigma}$)	$\mu = p_T/2$	$\mu = p_T$	$\mu = 2p_T$
MSTW08	**0.75** (0.30)	**0.68** (0.28)	0.91 (0.84)
CTEQ6.6	1.25 (0.14)	1.66 (0.20)	2.38 (0.84)
CT10	1.03 (0.13)	1.20 (0.19)	1.81 (0.84)
NNPDF2.1	**0.74** (0.29)	**0.82** (0.25)	1.23 (0.69)
HERAPDF1.0	2.43 (0.39)	3.26 (0.66)	4.03 (1.67)
HERAPDF1.5	2.26 (0.40)	3.05 (0.66)	3.80 (1.66)
ABKM09	1.62 (0.52)	2.21 (0.85)	3.26 (2.10)
GJR08	1.36 (0.23)	0.94 (0.13)	**0.79** (0.36)

NNLO PDF (with NLO+2-loop $\hat{\sigma}$)	$\mu = p_T/2$	$\mu = p_T$	$\mu = 2p_T$
MSTW08	1.39 (0.42)	**0.69** (0.44)	0.97 (0.48)
HERAPDF1.0, $\alpha_S(M_Z^2) = 0.1145$	2.64 (0.36)	2.15 (0.36)	2.20 (0.46)
HERAPDF1.0, $\alpha_S(M_Z^2) = 0.1176$	2.24 (0.35)	1.17 (0.32)	1.23 (0.31)
ABKM09	2.55 (0.82)	2.76 (0.89)	3.41 (1.17)
JR09	**0.75** (0.37)	1.26 (0.41)	2.21 (0.49)

Table 1: Values of $\chi^2/N_{\text{pts.}}$ for the CDF Run II inclusive jet data using the k_T jet algorithm with $N_{\text{pts.}} = 76$ and $N_{\text{corr.}} = 17$, for different PDF sets and different scale choices At most a 1-σ shift in normalisation is allowed.

NLO PDF (with NLO $\hat{\sigma}$)	$\mu = p_T/2$	$\mu = p_T$	$\mu = 2p_T$
MSTW08	0.75 (+0.32)	0.68 (−0.88)	0.63 (*−2.69*)
CTEQ6.6	1.03 (*−2.47*)	1.04 (**−3.49**)	0.99 (**−4.75**)
CT10	0.99 (*−1.64*)	0.92 (*−2.69*)	0.86 (**−4.10**)
NNPDF2.1	0.74 (−0.33)	0.79 (*−1.60*)	0.80 (**−3.12**)
HERAPDF1.0	1.52 (**−4.07**)	1.57 (**−5.21**)	1.43 (**−6.22**)
HERAPDF1.5	1.48 (**−3.85**)	1.52 (**−5.00**)	1.39 (**−6.03**)
ABKM09	1.03 (**−3.49**)	1.01 (**−4.53**)	1.05 (**−5.80**)
GJR08	1.14 (*+2.47*)	0.93 (*+1.25*)	0.79 (−0.50)

NNLO PDF (with NLO+2-loop $\hat{\sigma}$)	$\mu = p_T/2$	$\mu = p_T$	$\mu = 2p_T$
MSTW08	1.39 (+0.35)	0.69 (−0.45)	0.97 (*−1.30*)
HERAPDF1.0, $\alpha_S(M_Z^2) = 0.1145$	2.37 (*−2.65*)	1.48 (**−3.64**)	1.29 (**−4.12**)
HERAPDF1.0, $\alpha_S(M_Z^2) = 0.1176$	2.24 (−0.48)	1.13 (*−1.60*)	1.09 (*−2.23*)
ABKM09	1.53 (**−4.27**)	1.23 (**−5.05**)	1.44 (**−5.65**)
JR09	0.75 (+0.13)	1.26 (−0.61)	2.20 (*−1.22*)

Table 2: Values of $\chi^2/N_{\rm pts.}$ for the CDF Run II inclusive jet data using the k_T jet algorithm No restriction is imposed on the shift in normalisation and the optimal value of "$-r_{\rm lumi.}$" is shown in brackets.

Comparisons to LHC data

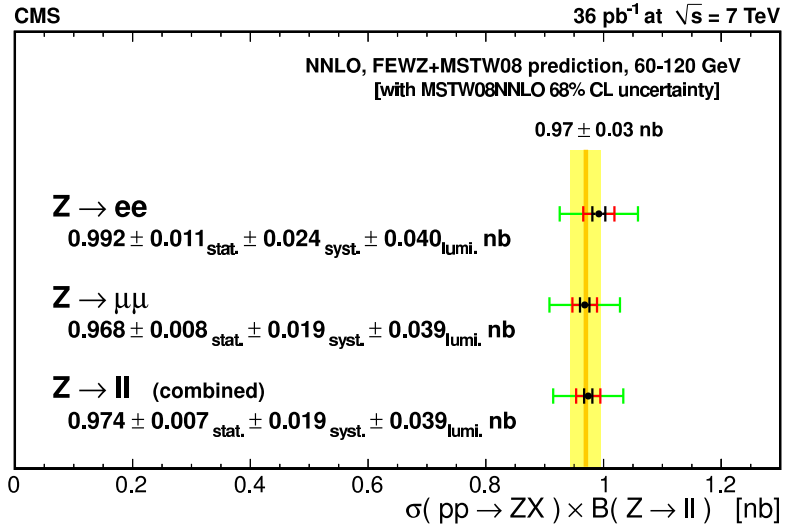

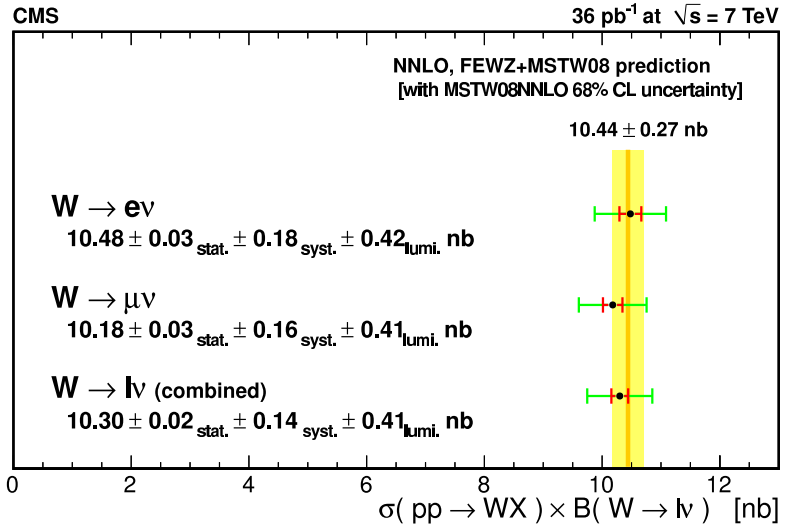

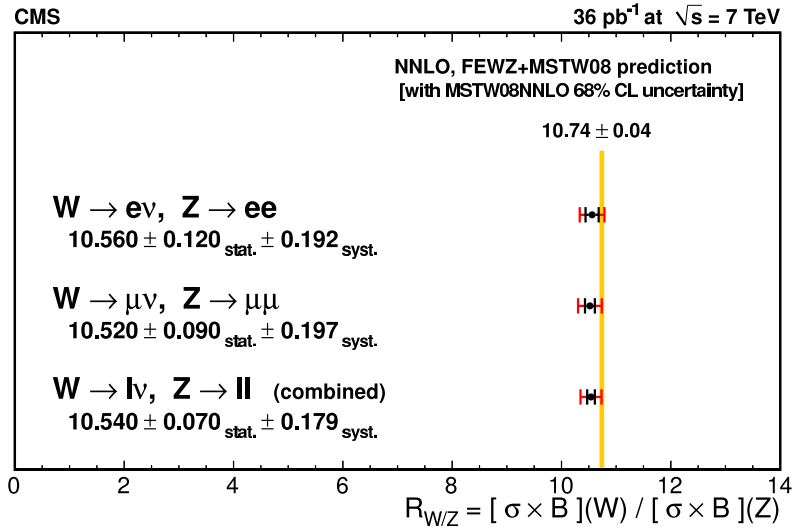

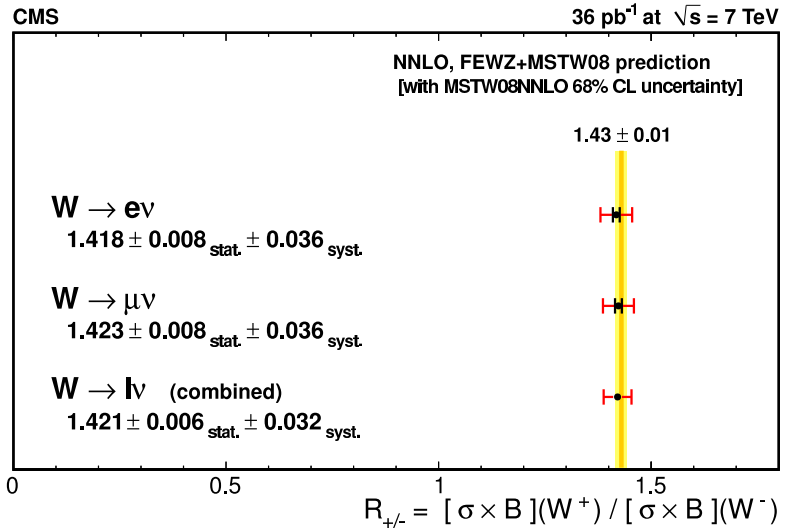

CMS results very similar.

Differences in predictions at NNLO compared to NLO (Watt).

Differences very much the same as they are comparing at NLO.

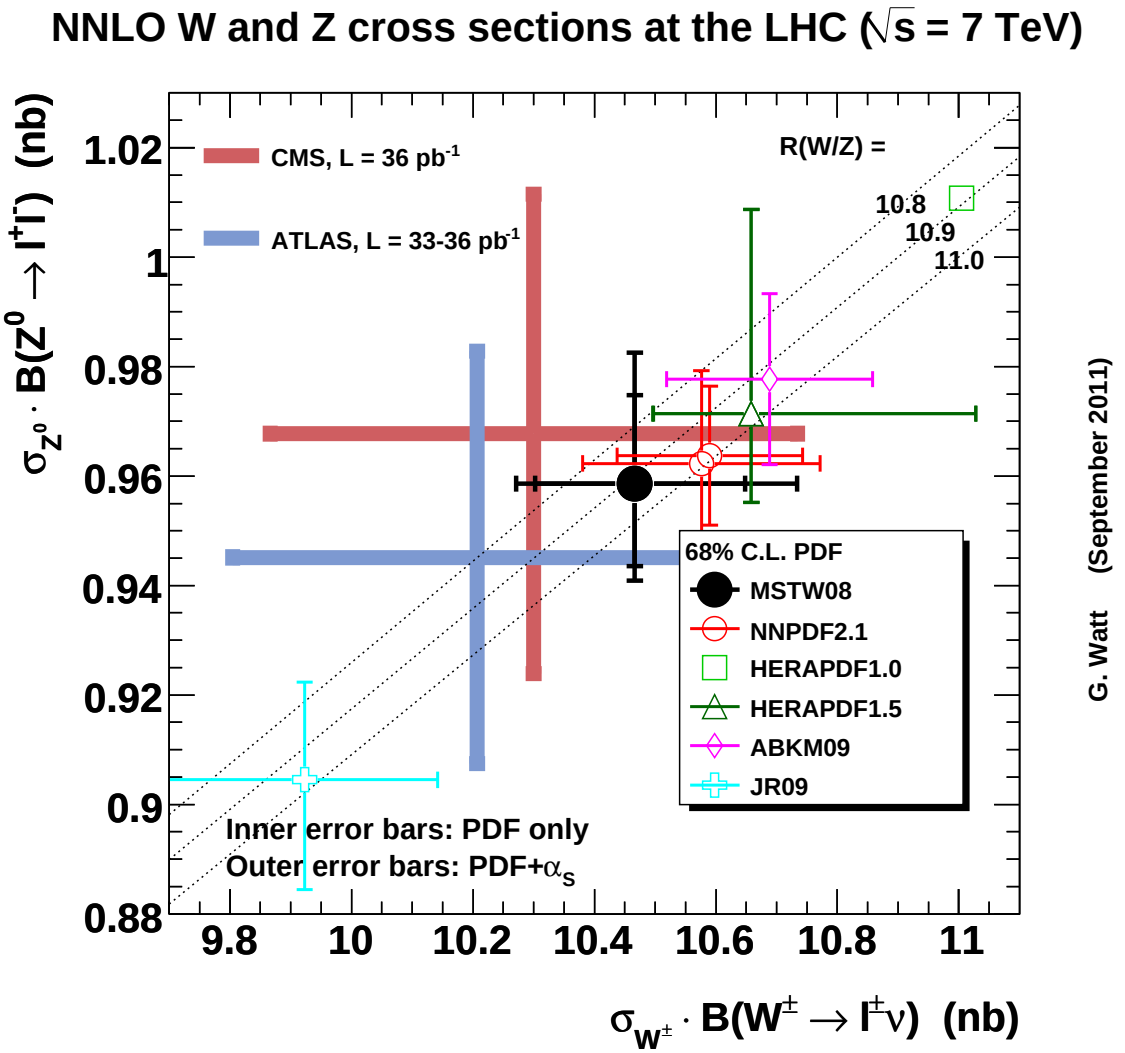

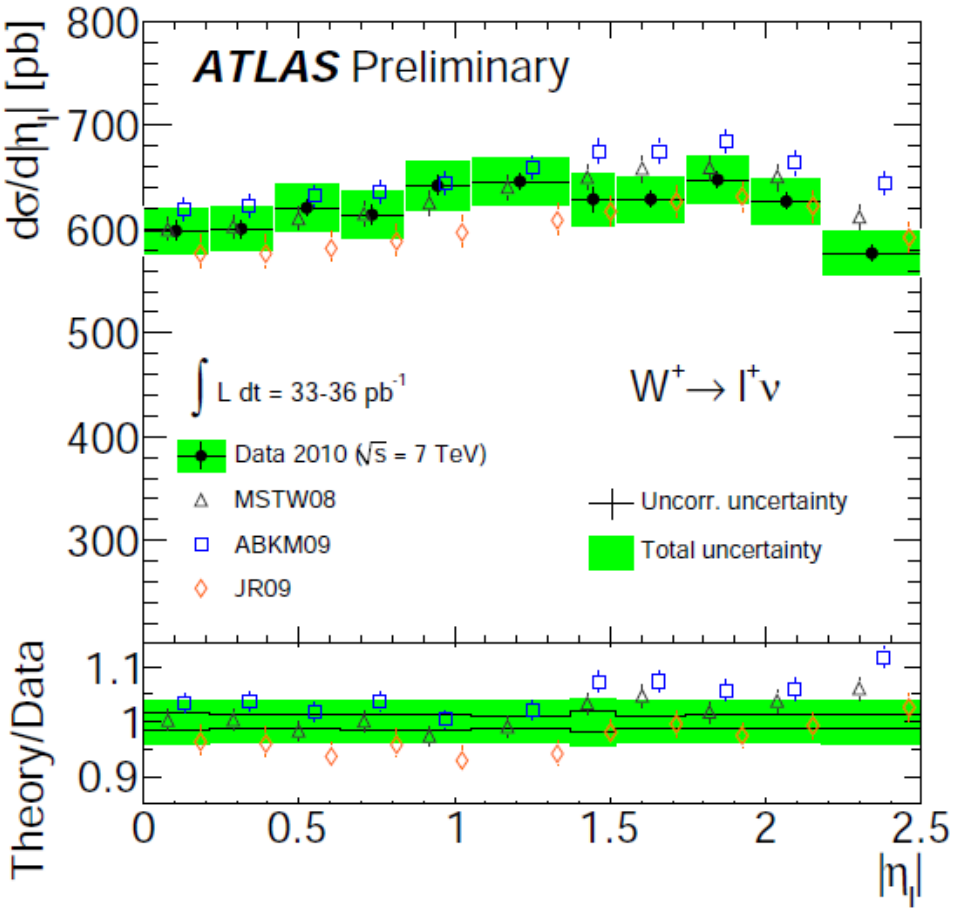

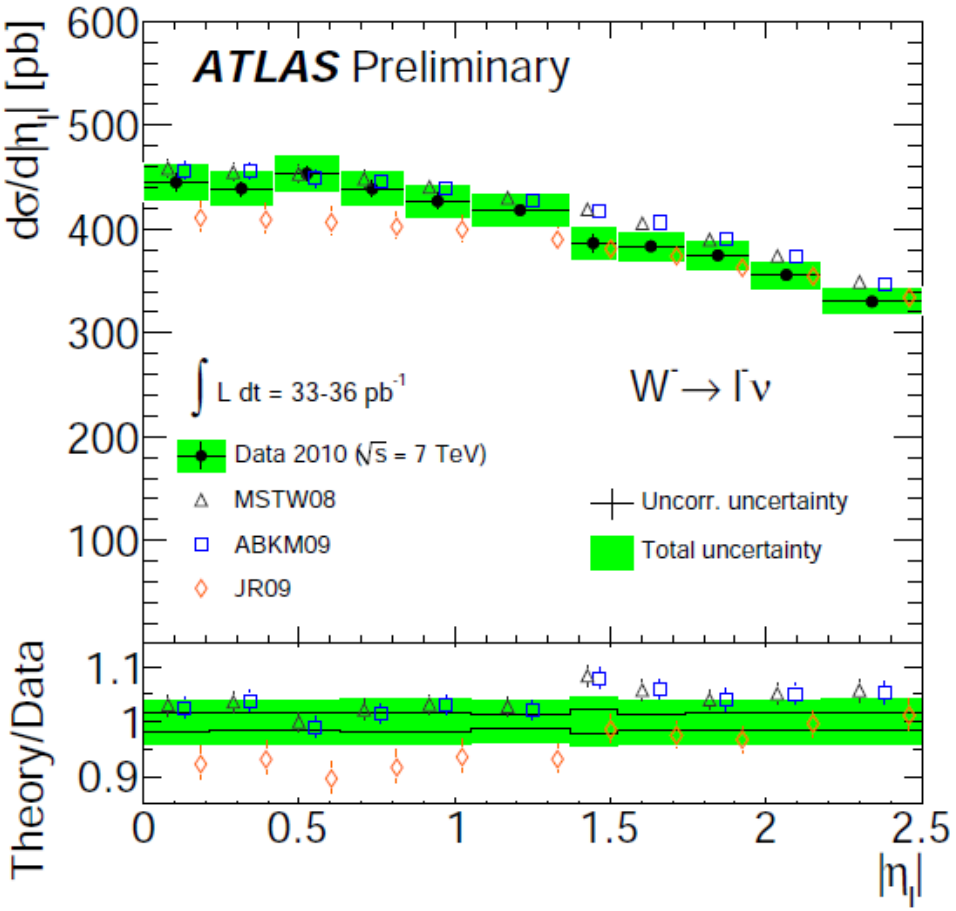

Differential data on rapidity is becoming very constraining – on both shapes and on normalisations of predictions.

Would be particularly interesting to see for $\gamma^\star$ at low masses (LHCb).

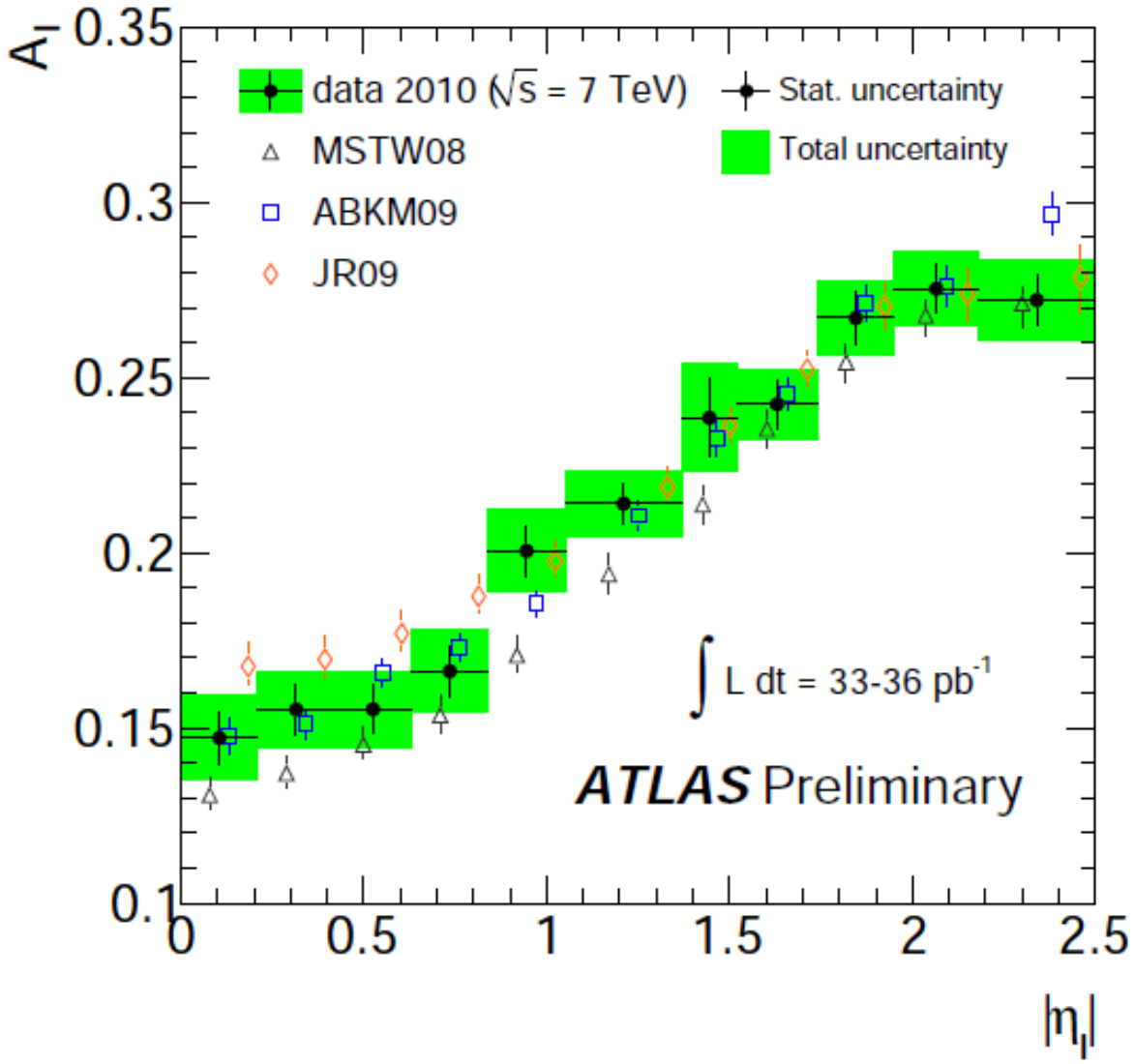

Clearly some of this information lost in ratios and asymmetries.

Ideally want individual distributions, with full correlations.

Details from single charged-lepton cross sections and asymmetries – Stirling

for low p_T main boost from W decay to leptons.

Dip towards -1 for lower p_T cuts from preferential forward production from $d_V(x_1)\bar{u}(x_2)$ due to axial vector nature of coupling.

Eventual turn-up when/if $u_V(x_1)\bar{d}(x_2) \gg d_V(x_1)\bar{u}(x_2)$

The larger the lepton p_T the earlier (in terms of increasing y_ℓ) this will happen, and for $p_T \to m_W/2$ there is no $V \pm A$ dominance at all.

So asymmetry at large y_ℓ in terms of p_T tells us about d/u at large x.

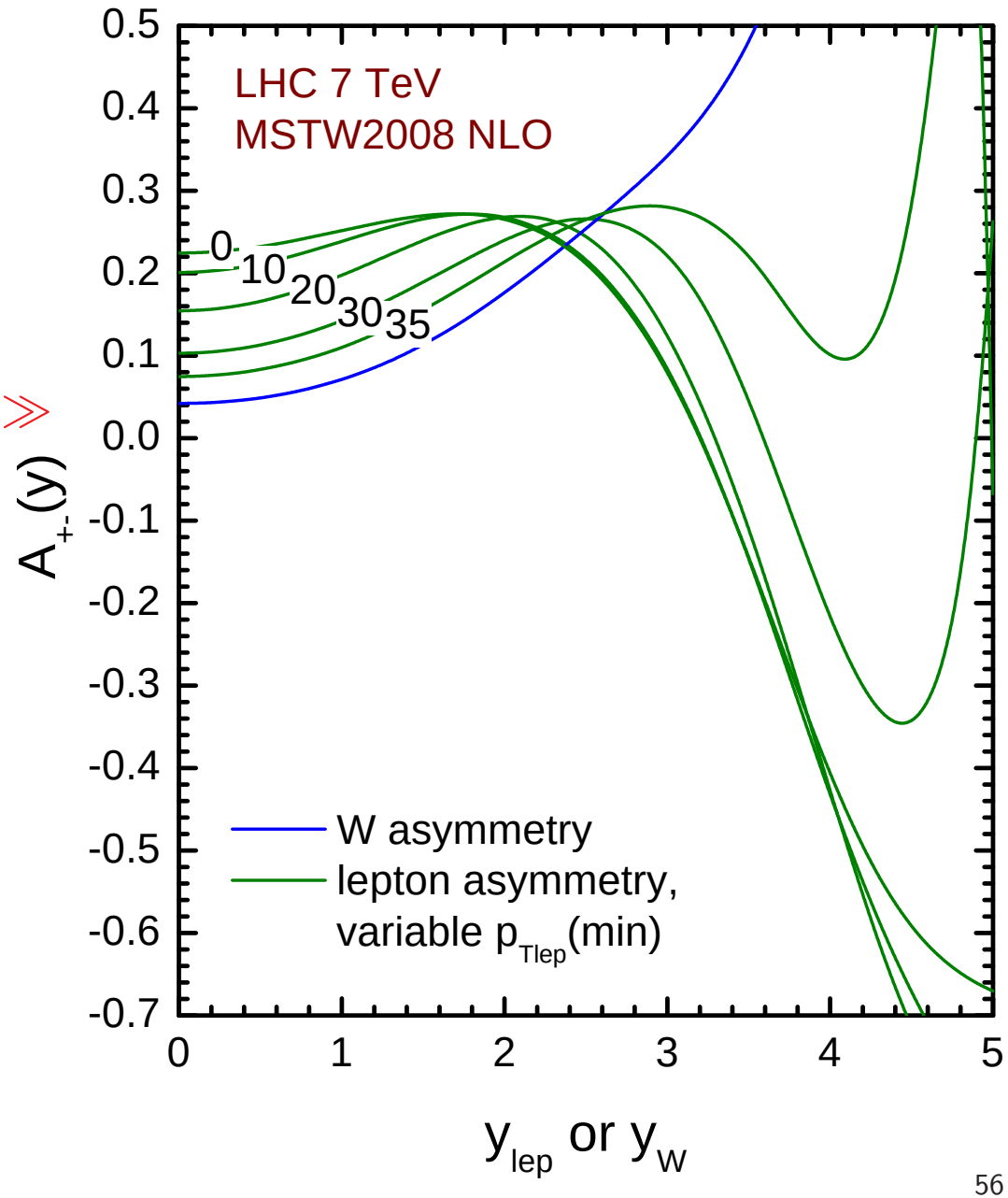

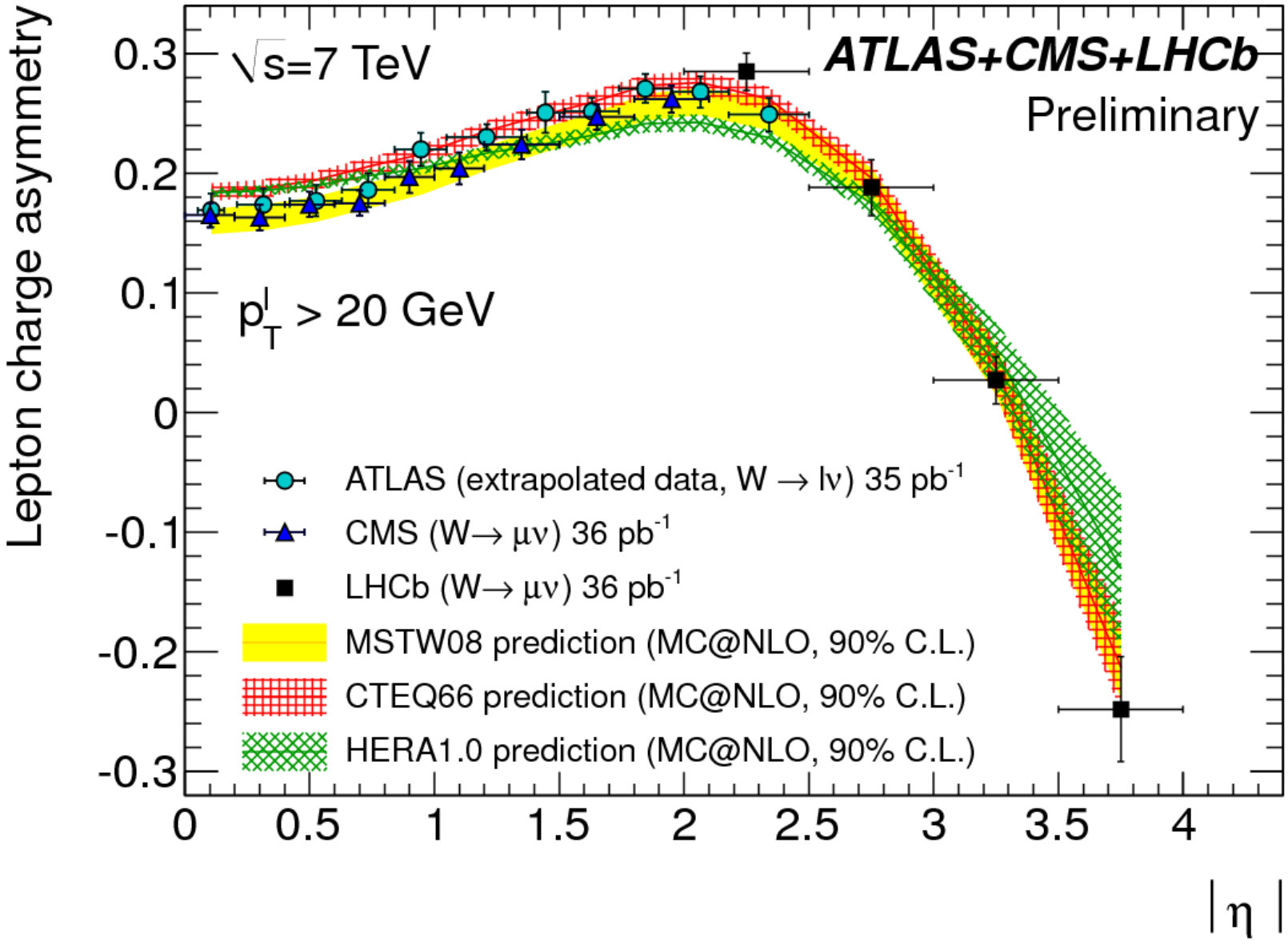

MSTW comparison better if p_T cut at $20\mathrm{GeV}^2$.

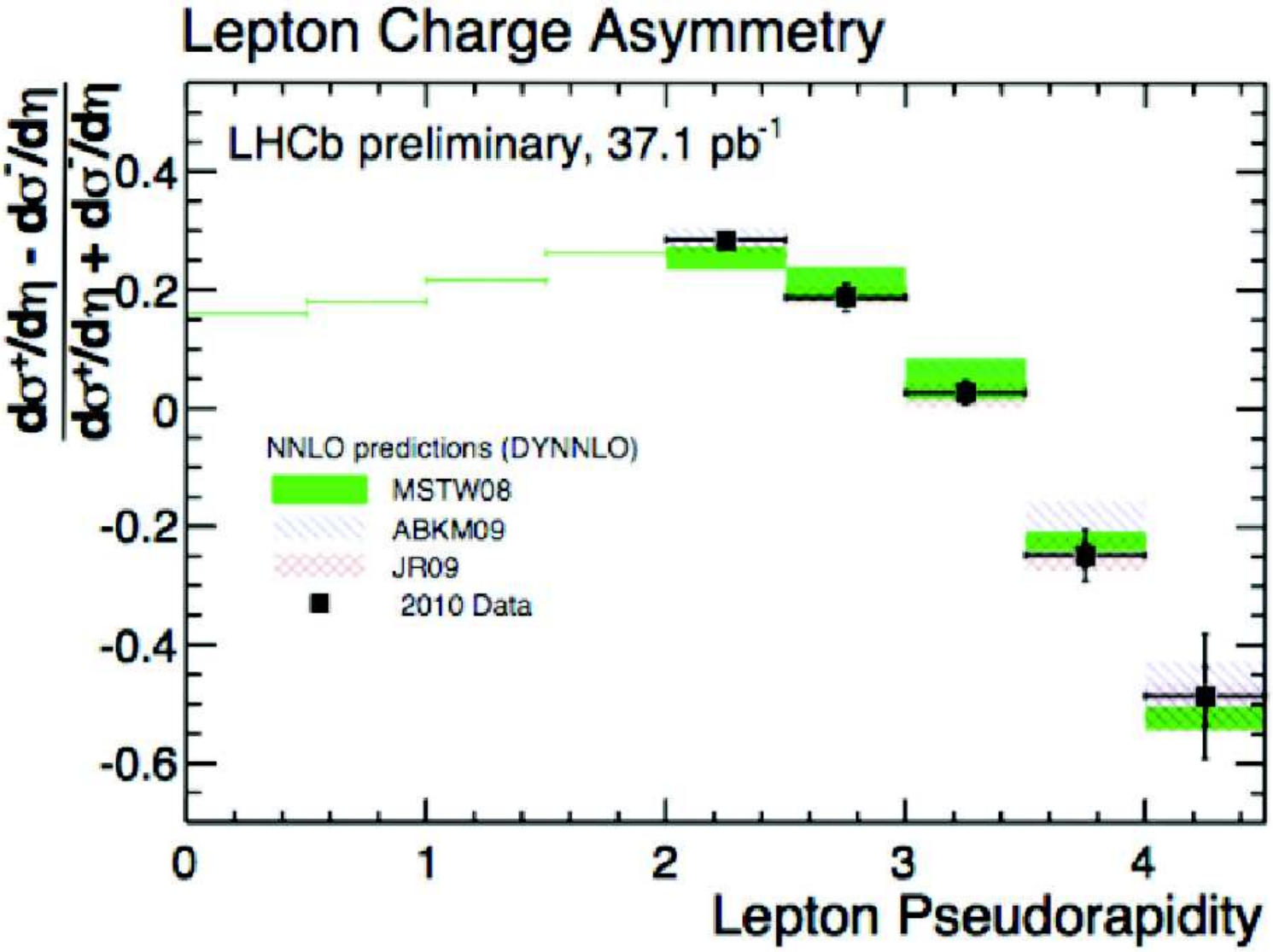

LHCb (with $p_T(\mathrm{min}) = 20\mathrm{GeV}$) already testing dip.

With higher $p_T(\mathrm{min})$ could potentially see upturn.

Inclusive Jets at the LHC

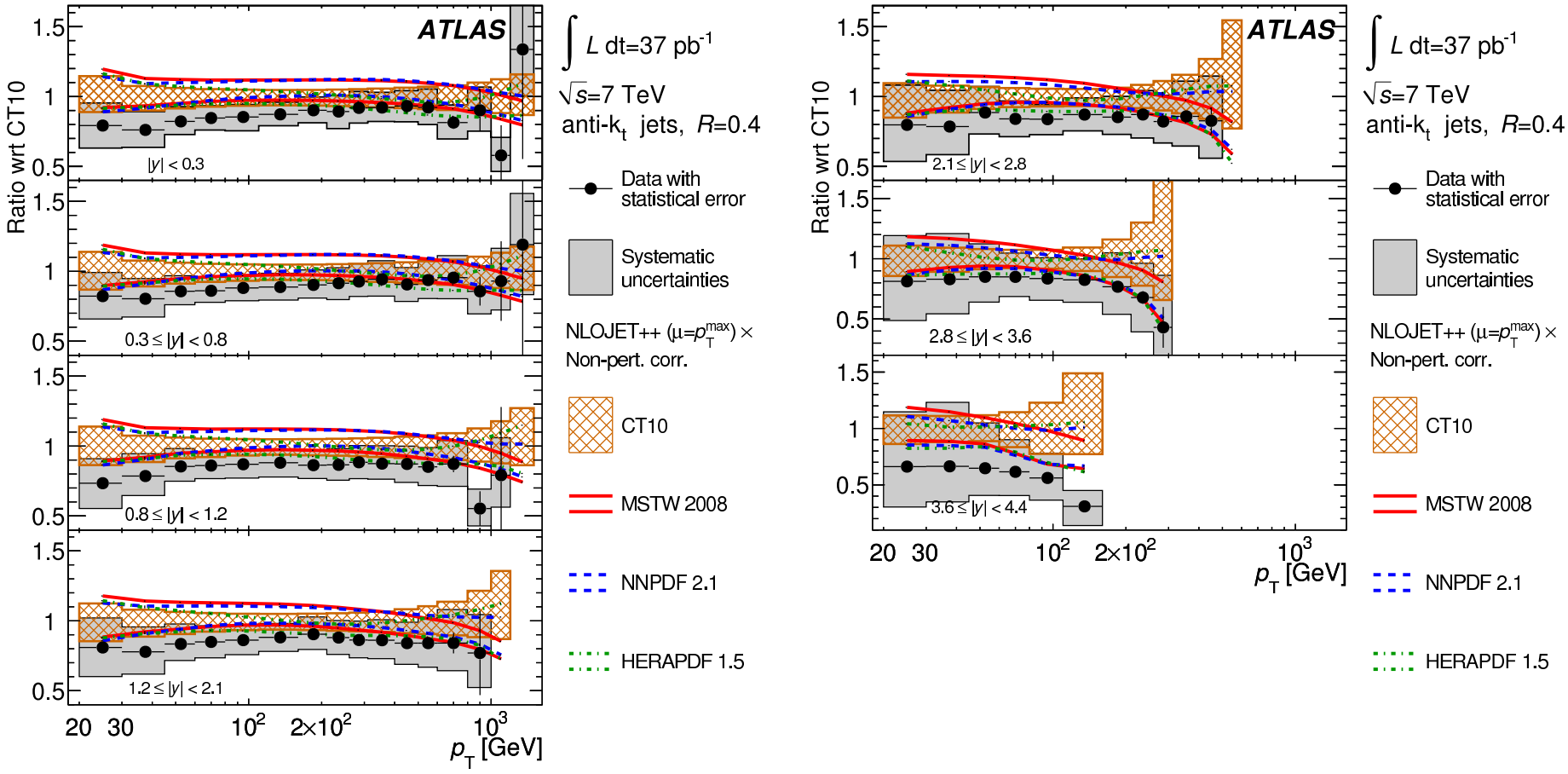

ATLAS data compared to various PDF set predictions. Each fit well so far with size of correlated uncertainties limiting discriminative power.

Interesting to see jets from LHCb as well.

Top-antitop Cross-section Inclusive cross-section known approximately to NNLO

Intrinsic theory uncertainty not very large – for example, recent NNLL calculation by Beneke et al.

Data getting precise. Main uncertainty in choice of PDFs, not in individual uncertainty but choice of set. Correlated to Higgs predictions.

		Tevatron	LHC ($\sqrt{s} = 7$ TeV)	LHC ($\sqrt{s} = 14$ TeV)
$\mathrm{NNLO}_{\mathrm{approx}}^{\mathrm{1PI}}$	(Ref. [41])	$7.08^{+0.20}_{-0.24}$	163^{+7}_{-5}	920^{+60}_{-39}
$\mathrm{NNLO}_{\mathrm{approx}}^{\mathrm{1PI_{SCET}}}$	(Ref. [42])	$6.63^{+0.00}_{-0.27}$	155^{+3}_{-2}	851^{+25}_{-5}
$\mathrm{NNLO}_{\mathrm{approx}}^{\mathrm{PIM_{SCET}}}$	(Ref. [38])	$6.62^{+0.05}_{-0.40}$	155^{+8}_{-8}	860^{+46}_{-43}
$\mathrm{NNLL}^{\mathrm{1PI_{SCET}}}$	(Ref. [42])	$6.55^{+0.16}_{-0.14}$	150^{+7}_{-7}	824^{+41}_{-44}
$\mathrm{NNLL}^{\mathrm{PIM_{SCET}}}$	(Ref. [38])	$6.46^{+0.18}_{-0.19}$	147^{+7}_{-6}	811^{+45}_{-42}
$\mathrm{NNLL}_{\mathrm{a}}$	this work	$7.22^{+0.31}_{-0.47}$	163^{+7}_{-8}	896^{+40}_{-37}

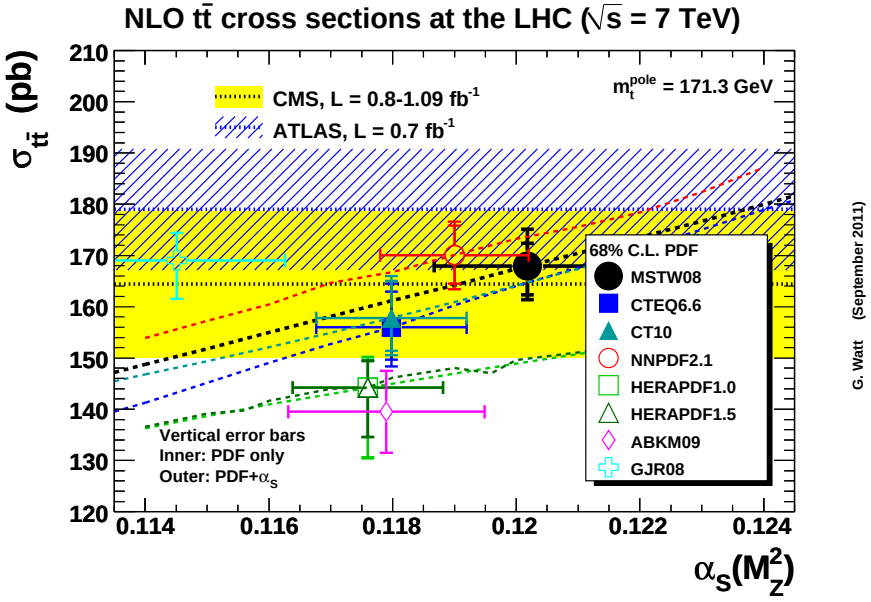

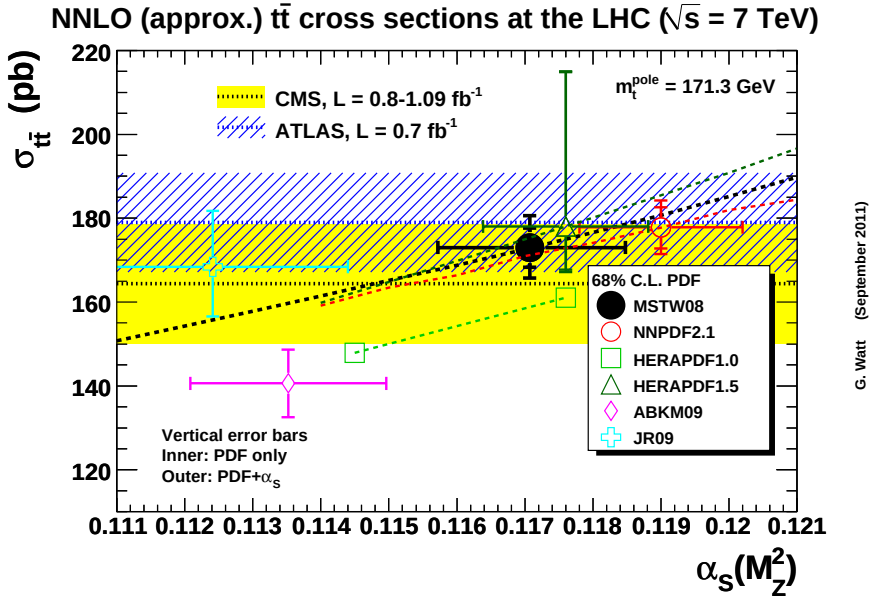

Plots by G. Watt. Differences between groups significant at NLO, and at NNLO.

Uncertainty in $t\bar{t}$, Higgs via gluon fusion and ratios. PDF only uncertainty, but α_S uncertainty cancels in ratios.

Very strong correlation of top with Higgs production for $m_H \sim 400\mathrm{GeV}$ at the LHC.

Similar correlation for $m_H \sim 400 \times 1.96/7 \sim 130\mathrm{GeV}$ at the Tevatron.

Particularly important at the moment.

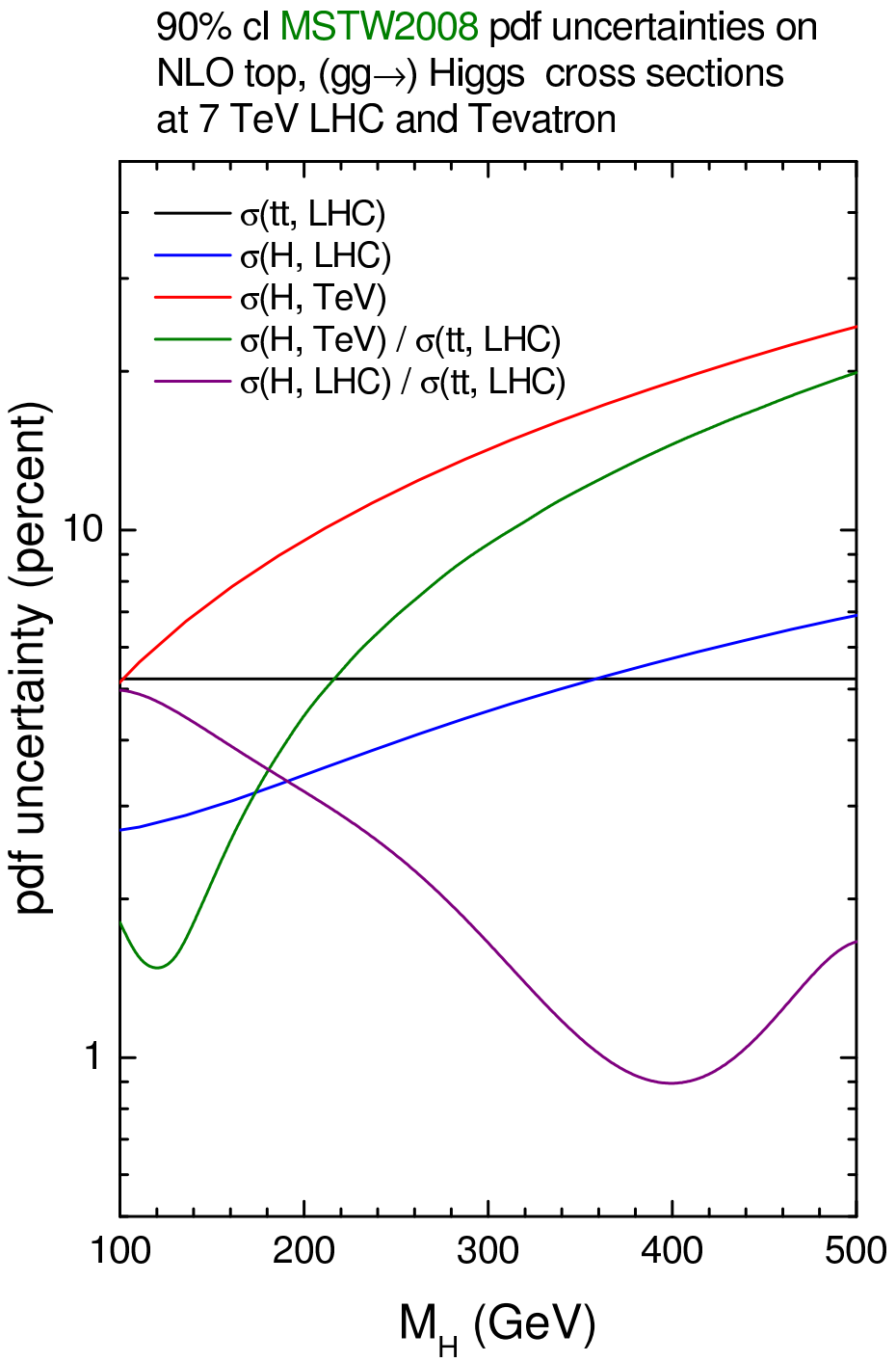

What will be the advantages of running at 8TeV?

Limited for quark dominated processes up to $m_X > 1\text{TeV}$, but more for gluon dominated processes for $M_X > 200 - 300\text{GeV}$.

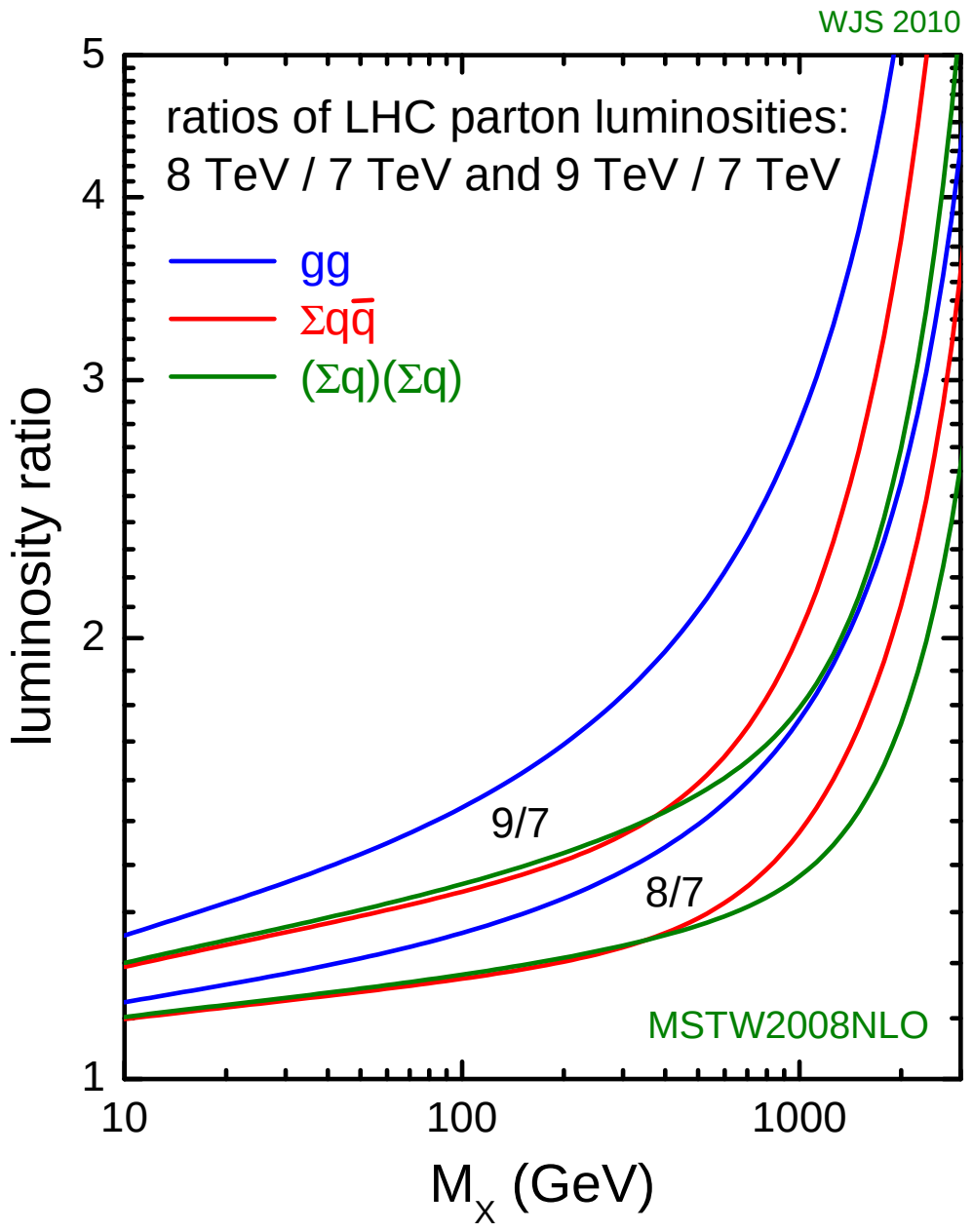

Conclusions

One can determine the parton distributions and predict cross-sections at the LHC, and the fit quality using NLO or NNLO QCD is fairly good. Nearly full range of NNLO PDFs now. Comparison between different PDF sets at NLO and NNLO very similar.

Various ways of looking at $experimental$ uncertainties. Uncertainties $\sim 1-5\%$ for most LHC quantities. Ratios, e.g. W^+/W^- tight constraint on partons, but don't want to lose information when taking ratios.

Effects from input assumptions e.g. selection of data fitted, cuts and input parameterisation can shift central values of predictions significantly. Also affect size of uncertainties. Want balance between freedom and sensible constraints.

Data from the LHC just starting to have some effect on improving the precision of PDFs. Might start to discriminate between PDFs first.

Extraction of PDFs from existing data and use for LHC far from a straightforward procedure. Lots of issues to consider for real precision. Relatively few cases where Standard Model discrepancies will not require some significant input from PDF physics to determine real significance.

Different PDF sets

- MSTW08 – fit all previous types of data. Most up-to-date Tevatron jet data. Not most recent HERA combination of data. PDFs at LO, NLO and NNLO.

- CT10 – very similar. PDFs at NLO. CT10 include HERA combination and more Tevatron data though also run I jet data. Not large changes from CTEQ6.6. CT10W gives higher weight to Tevatron asymmetry data.

- NNPDF2.1 – include all except HERA jet data (not strong constraint). NNPDF2.1 improves on NNPDF2.0 by better heavy flavour treatment. PDFs at NLO and very recently NNLO and LO .

- HERAPDF1.0 – based on HERA inclusive structure functions, neutral and charged current. Use combined data. PDFs at NLO and (without uncertainties) NNLO.

- ABKM09 – fit to DIS and fixed target Drell-Yan data. PDFs at NLO and NNLO. Less conservative cuts at low W^2 than other groups – fit for higher twist corrections rather than attempt to avoid them.

- GJR08 – fit to DIS, fixed target Drell-Yan and Tevatron jet data (not at NNLO. PDFs at NLO and NNLO.

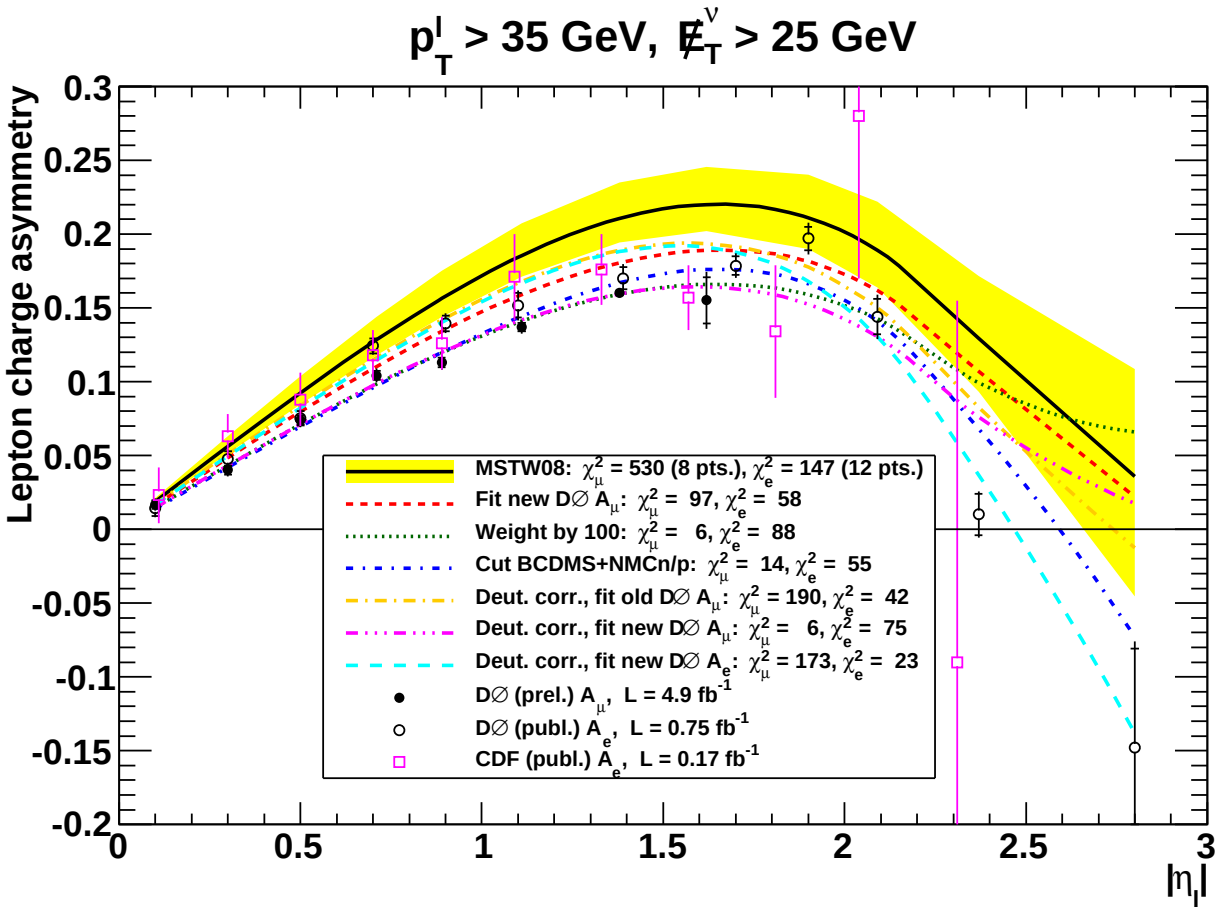

MSTW (and NNPDF and CTEQ) have difficulty fitting new D0 lepton asymmetry (particularly muon in different E_T bins) along with other data.

MSTW better when low number of data points sets given (slightly) more weight. Also improved using deuterium corrections.

The inappropriateness of using $\Delta\chi^2 = 1$ when including a large number of sometimes conflicting data sets is shown by examining the best value of σ_W and its uncertainty using $\Delta\chi^2 = 1$ for individual data sets as obtained by CTEQ using Lagrange Multiplier technique.

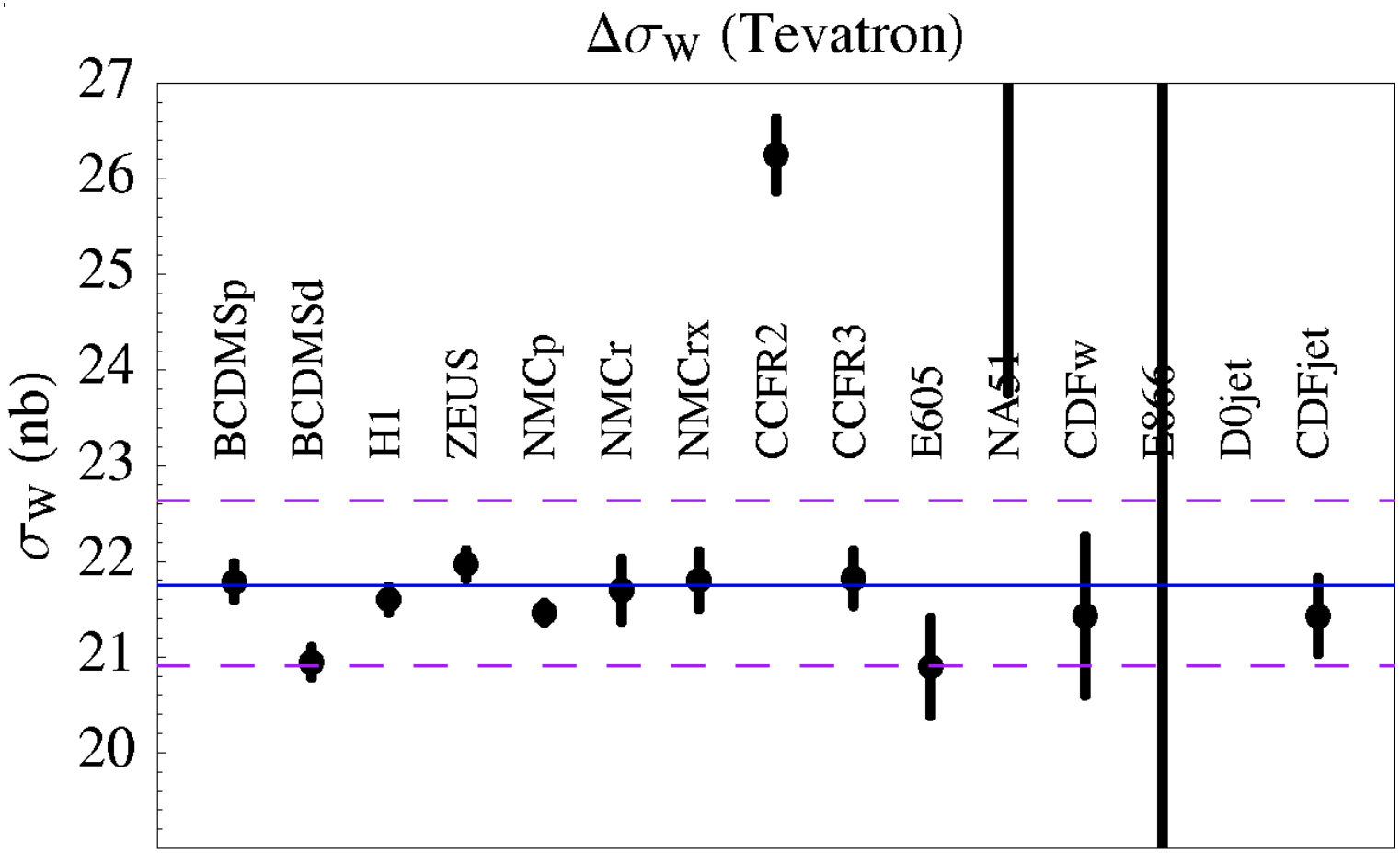

Predictions by various groups - parton luminosities – NLO. Plots by G. Watt.

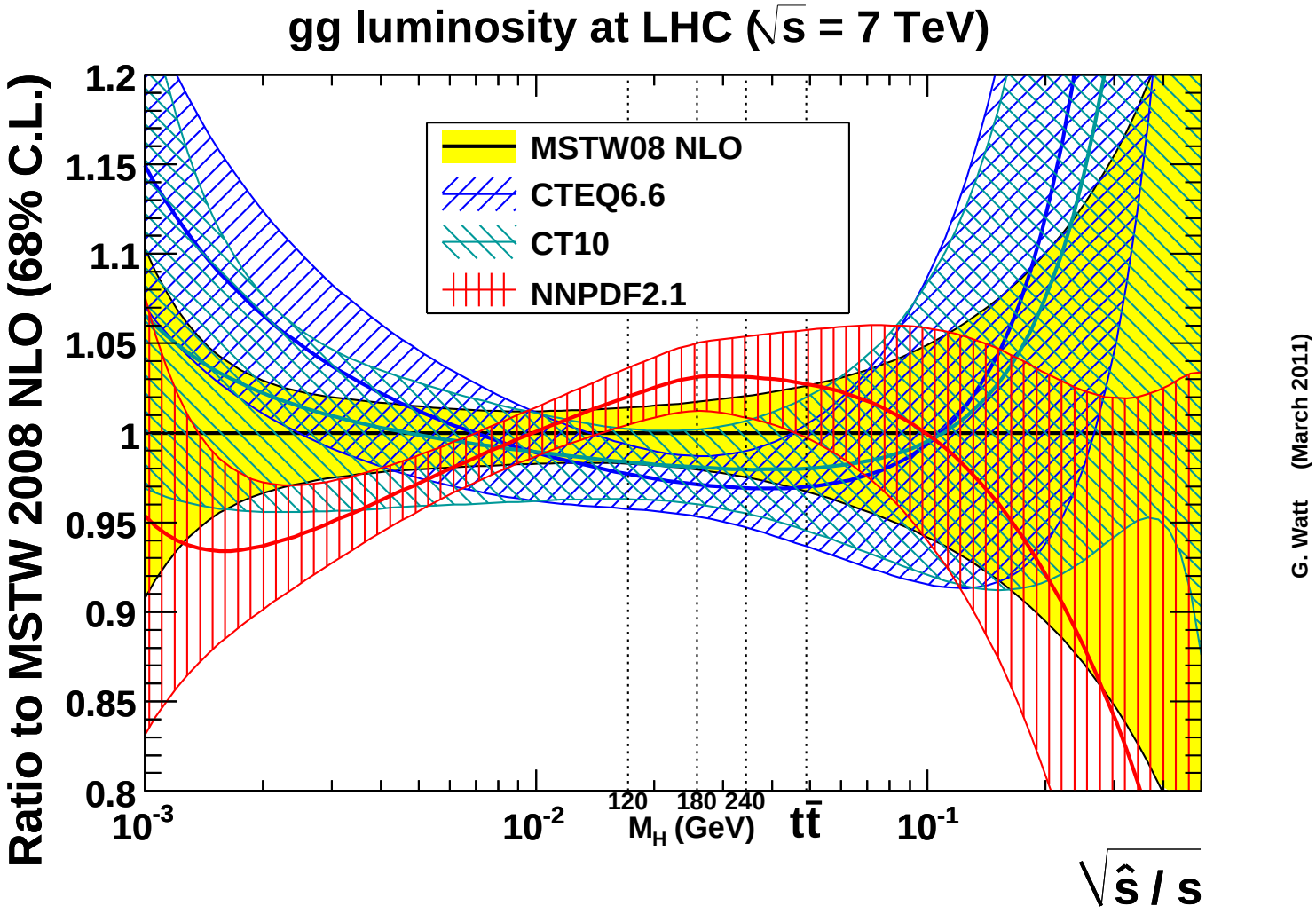

Cross-section for $t\bar{t}$ almost identical in PDF terms to 450GeV Higgs.

Also $H + t\bar{t}$ at $\sqrt{\hat{s}/s} \sim 0.1$.

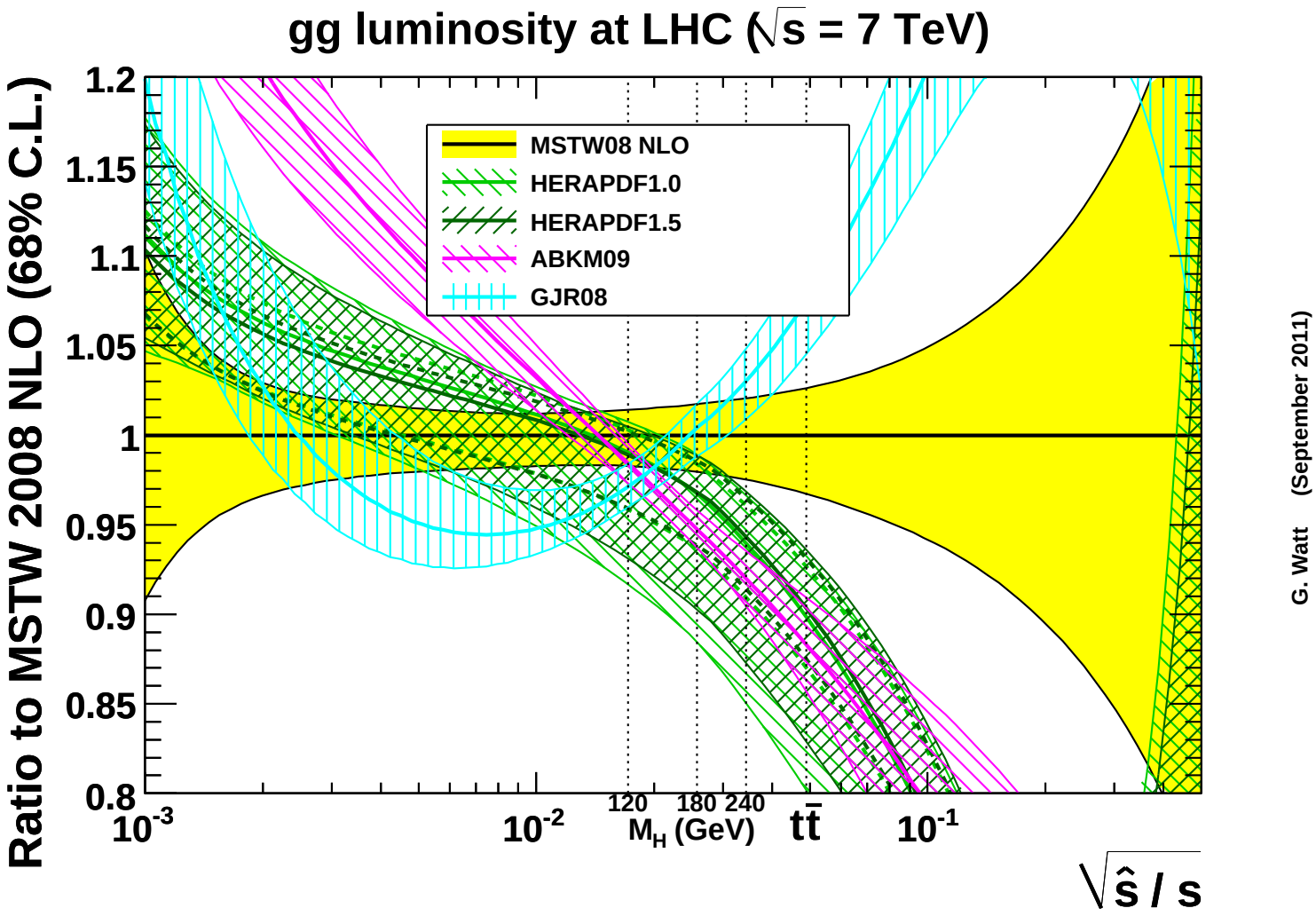

Clearly some distinct variation between groups. Much can be understood in terms of previous differences in approaches.

Uncertainties not completely comparable.

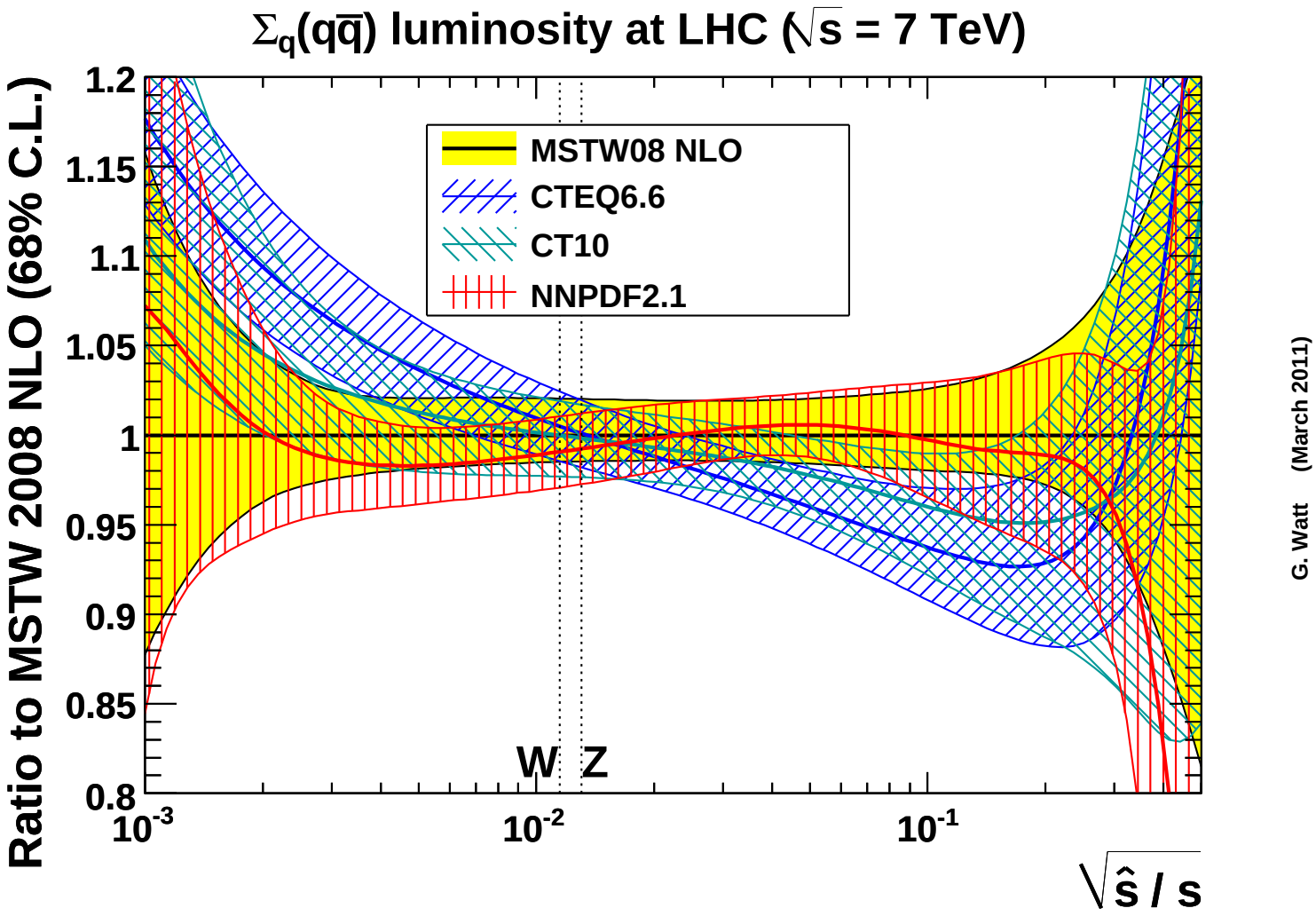

Many of the same general features for quark-antiquark luminosity. Some differences mainly at higher x.

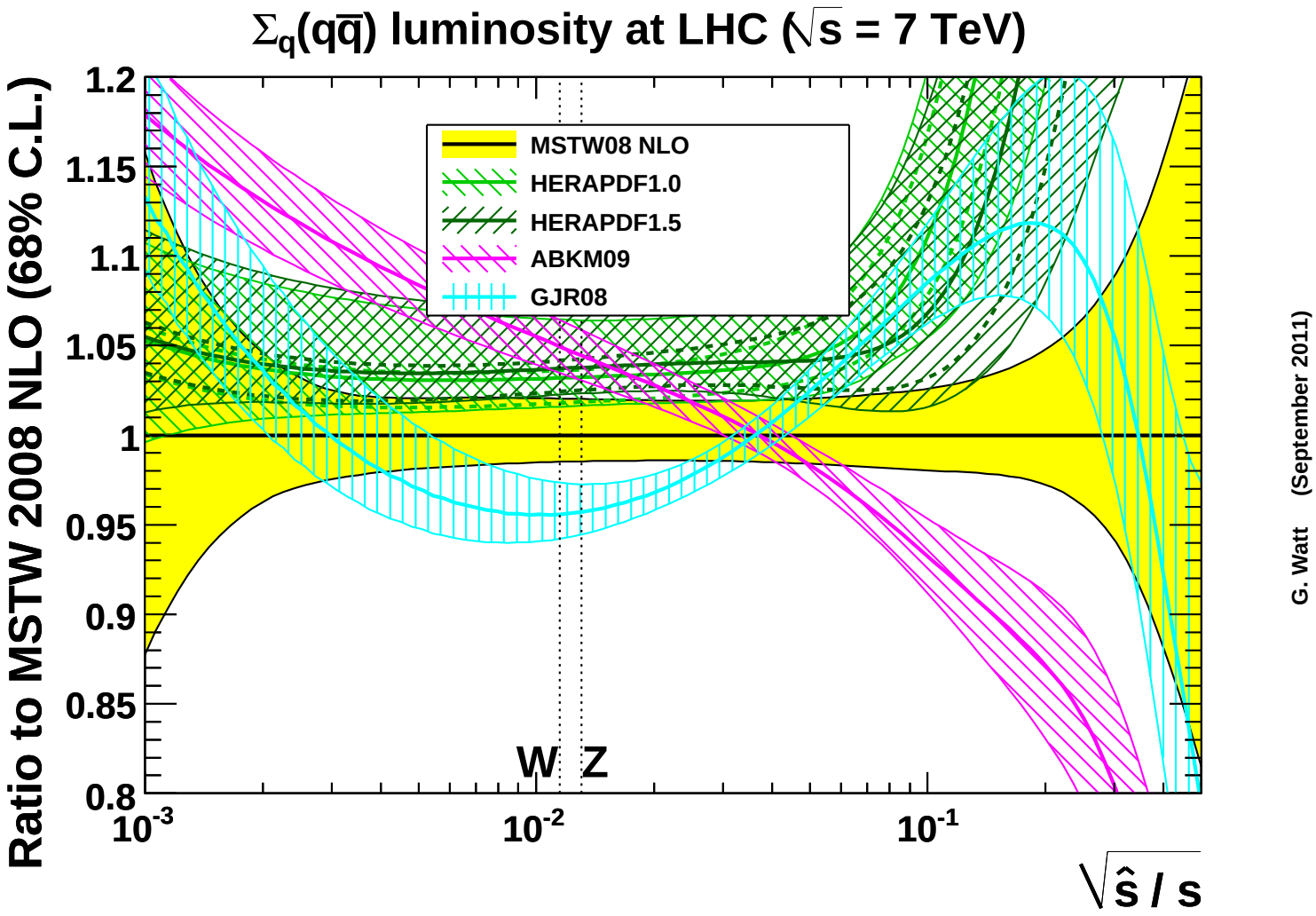

Canonical example W, Z production, but higher $\hat{s}/s$ relevant for WH or vector boson fusion.

All plots and more at http://projects.hepforge.org/mstwpdf/pdf4lhc

Variations in Cross-Section Predictions – NLO

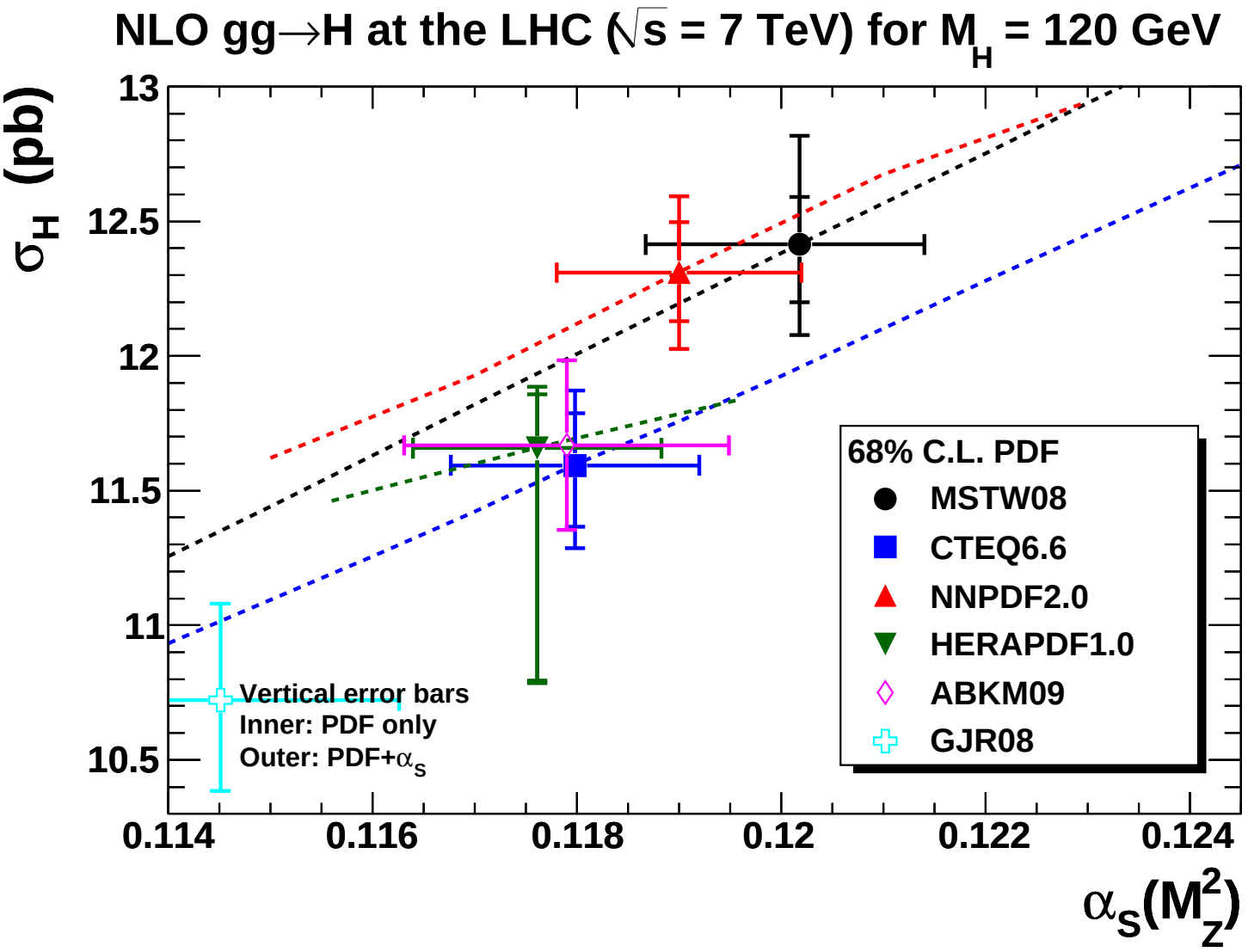

Dotted lines show how central PDF predictions vary with $\alpha_S(M_Z^2)$.

Again plots by G Watt using PDF4LHC benchmark criteria.

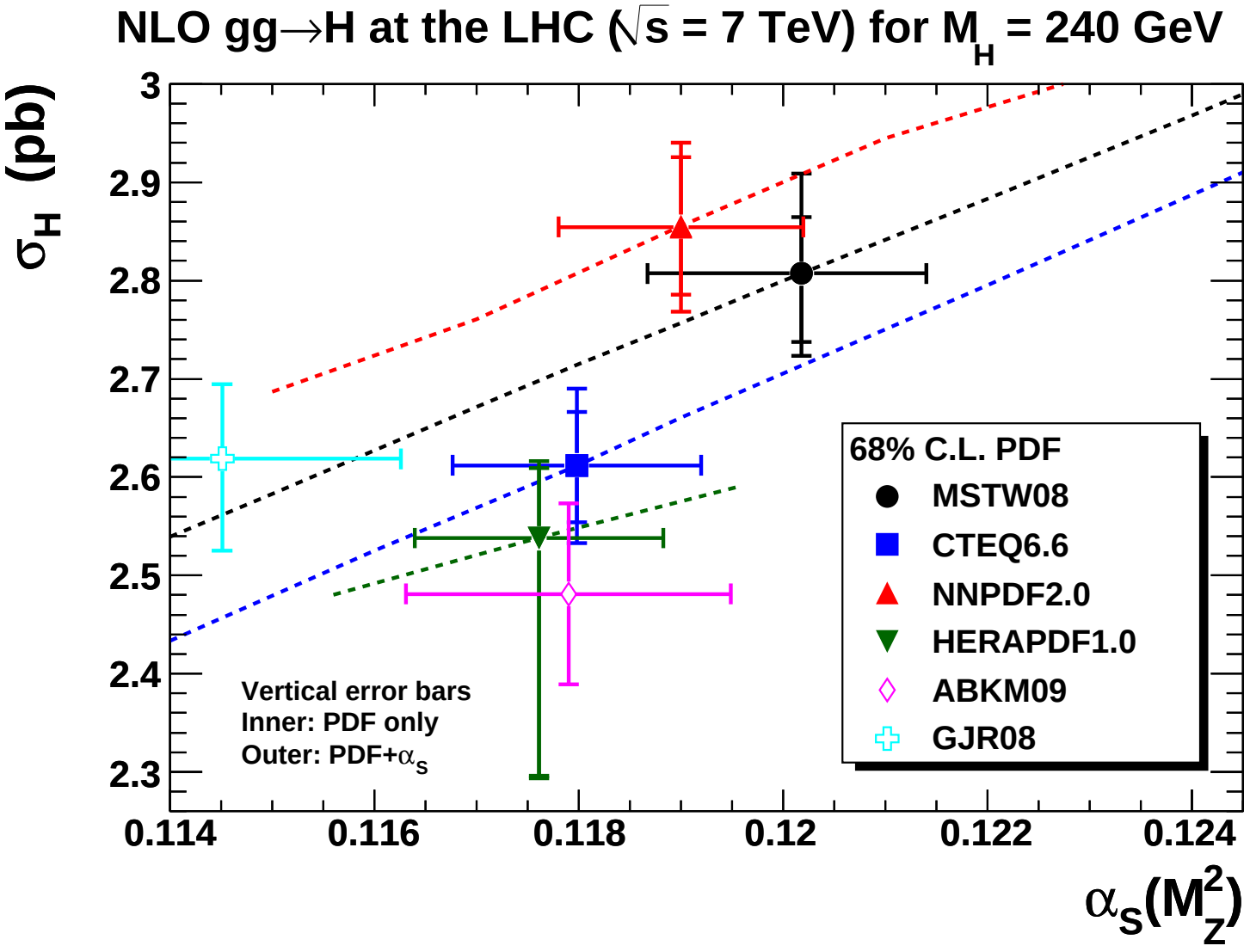

Excluding GJR08 amount of difference due to $\alpha_S(M_Z^2)$ variations $3-4\%$.

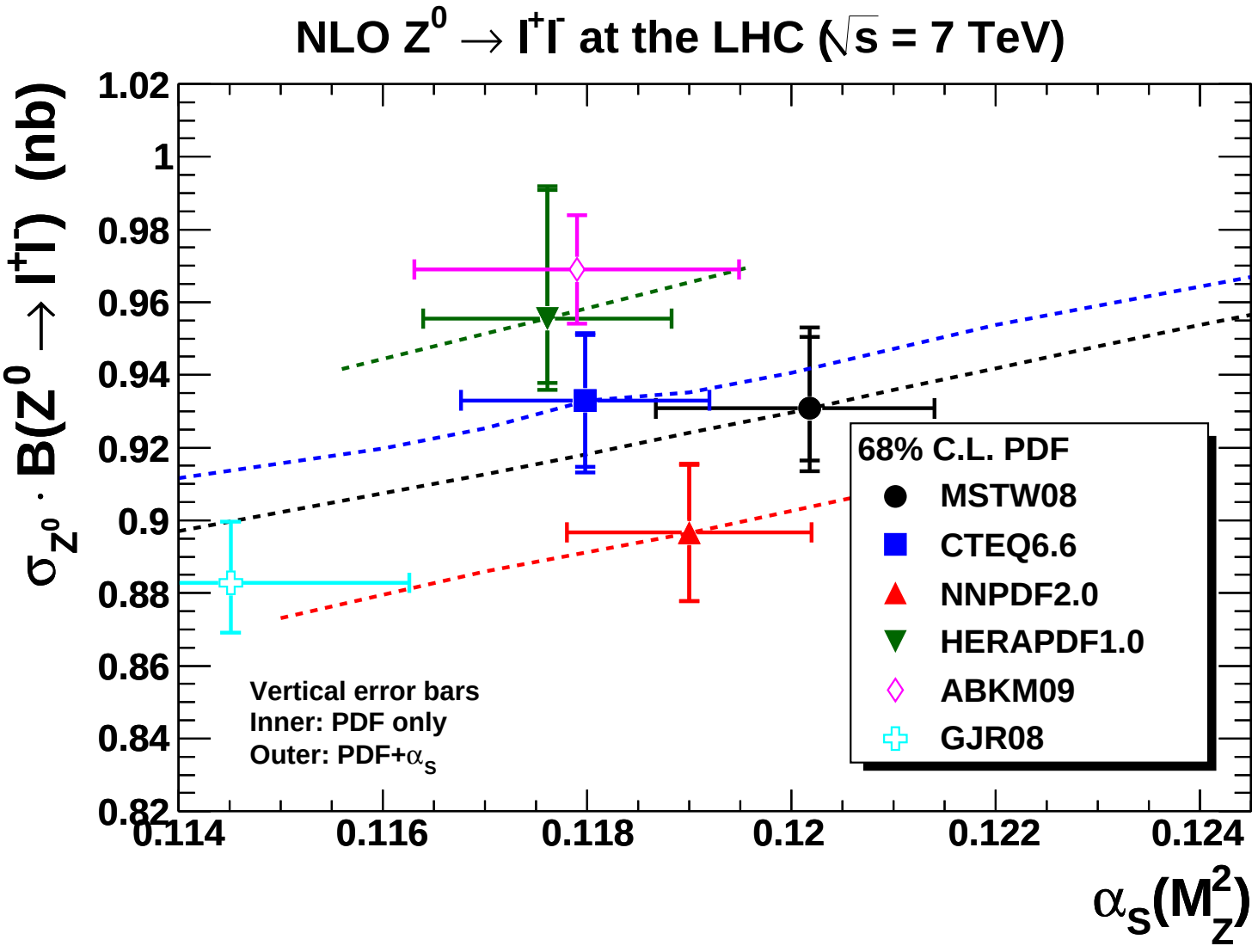

$\alpha_S(M_Z^2)$ dependence now more due to PDF variation with $\alpha_S(M_Z^2)$.

Again variations somewhat bigger than individual uncertainties.

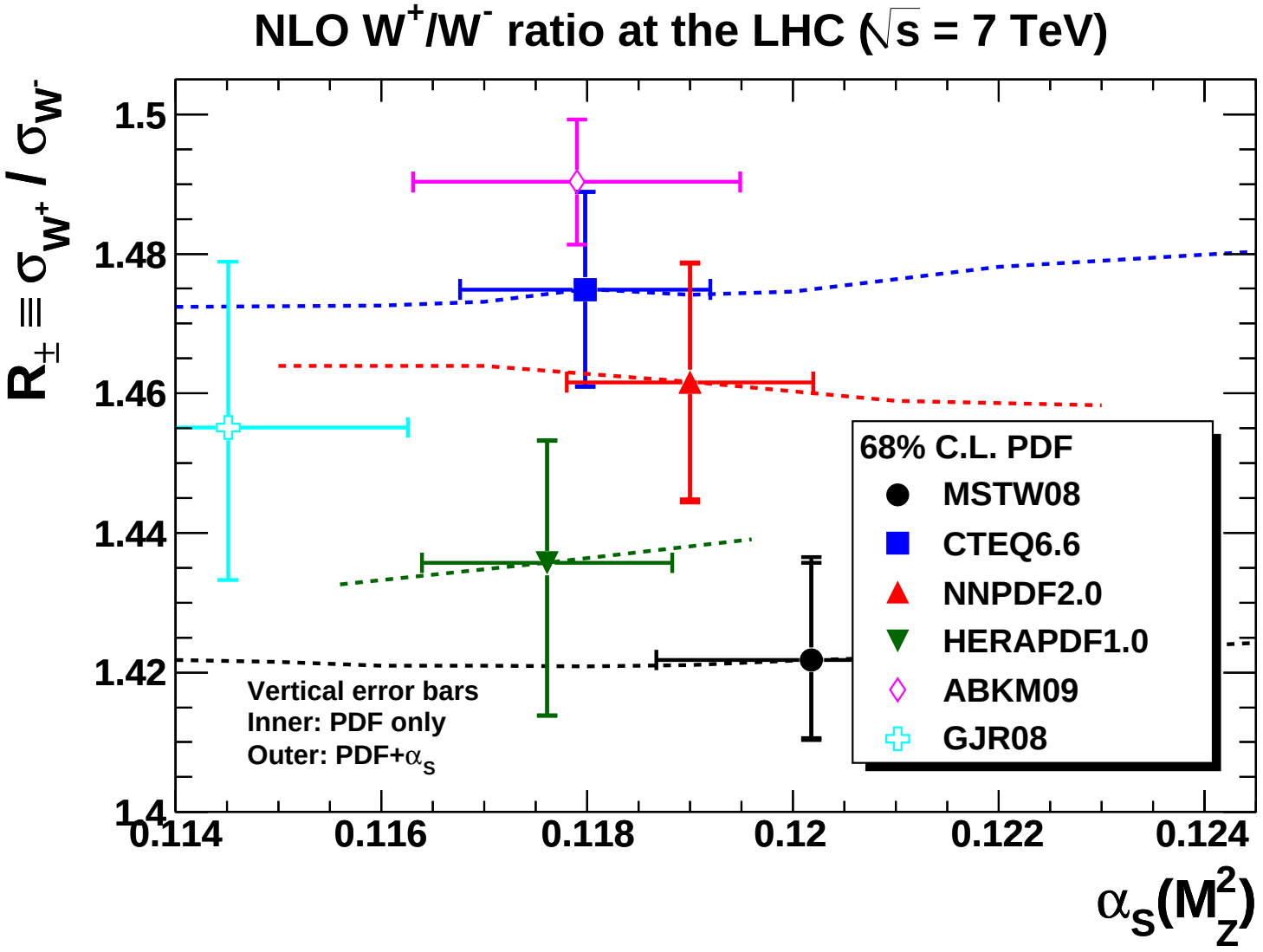

Quite a variation in ratio. Shows variations in flavour and quark-antiquark decompositions.

All plots and more at http://projects.hepforge.org/mstwpdf/pdf4lhc

Deviations In predictions clearly much more than uncertainty claimed by each.

In some cases clear reason why central values differ, e.g. lack of some constraining data, though uncertainties then do not reflect true uncertainty.

Sometimes no good understanding, or due to difference in procedure which is simply a matter of disagreement, e.g. gluon parameterisation at small x affects predicted Higgs cross-section.

What is true uncertainty for comparing to unknown production cross section. Task asked of PDF4LHC group.

Interim recommendation take envelope of $global$ sets, MSTW, CTEQ NNPDF (check other sets) and take central point as uncertainty.

Not very satisfactory, but not clear what would be an improvement, especially as a general rule.

Usually not a big disagreement, and factor of about 2 expansion of MSTW uncertainty.

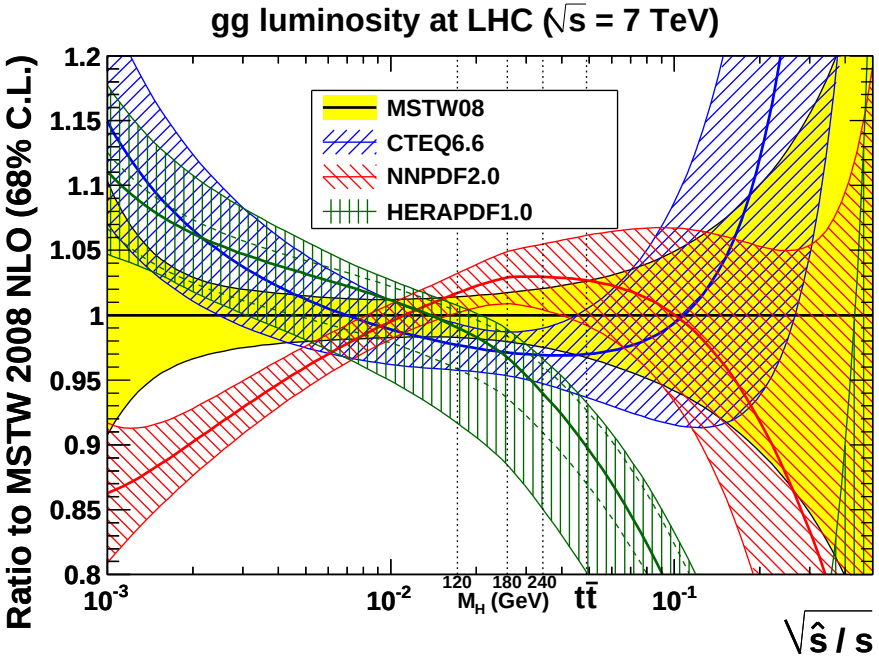

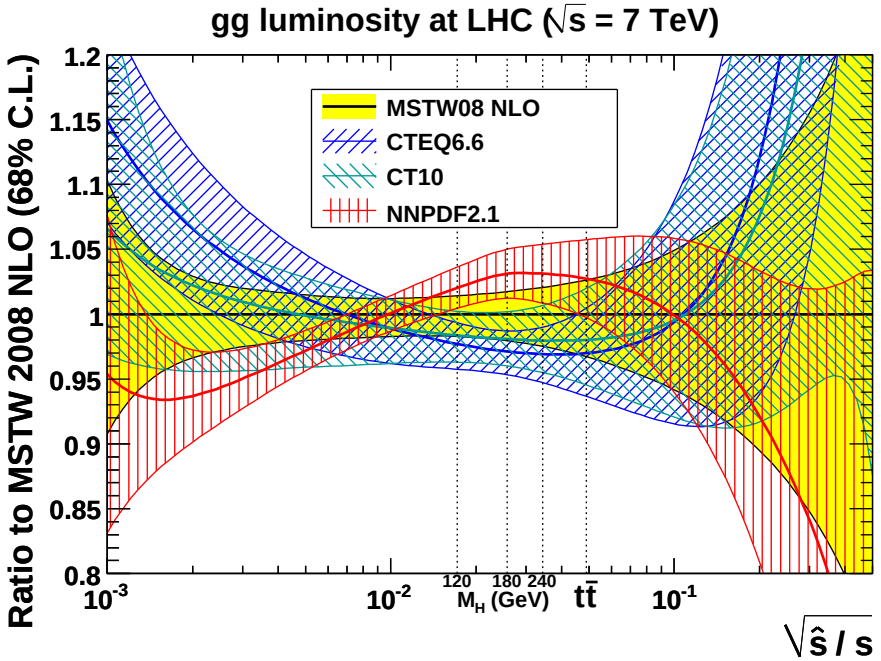

G. Watt (March 2011)

MSTW, NNPDF and CTEQ are converging somewhat.

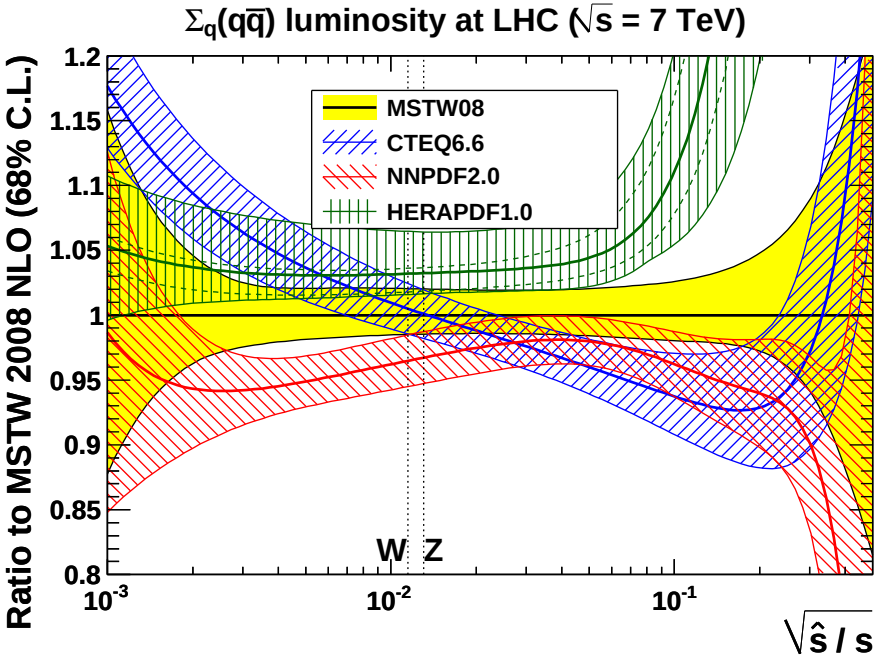

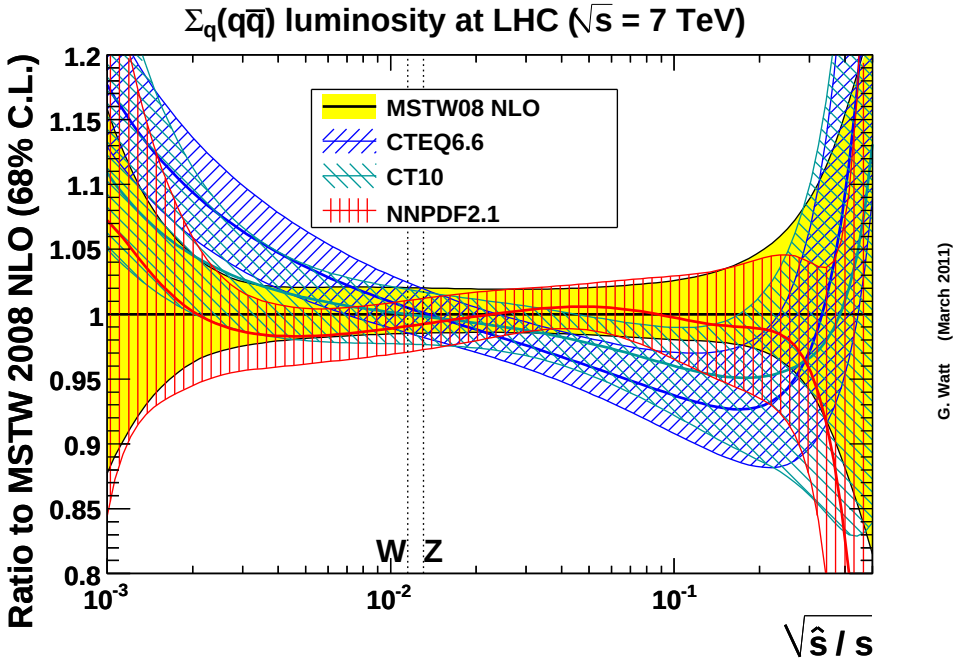

Same for quark-antiquark luminosities.

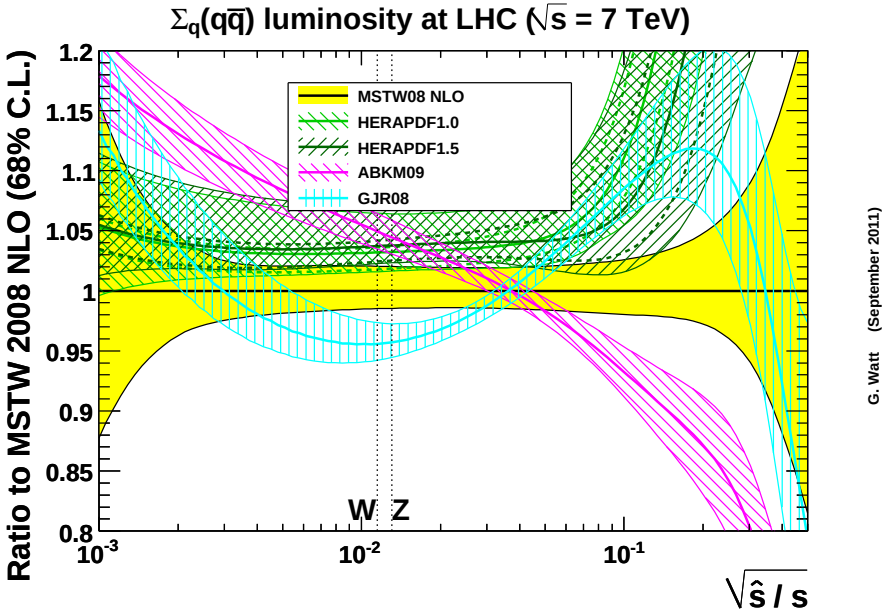

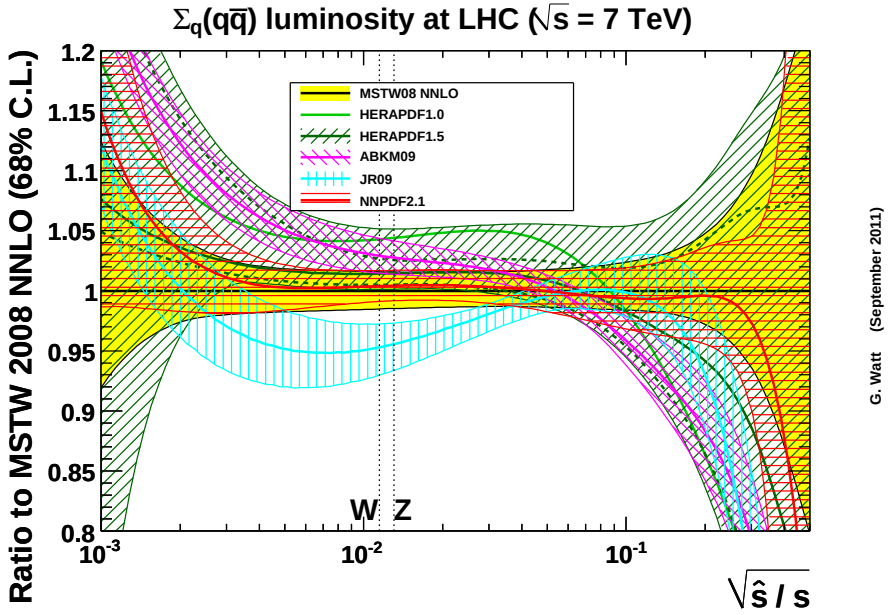

Not all luminosity differences the same at NLO as at NNLO, e.g. HERAPDF $q\bar{q}$.

The PDFs are related to the issue of the use and uncertainty of $\alpha_S(M_Z^2)$.

There is a significant systematic change in value from fit as one goes from NLO to NNLO. Seen in (most) other extractions. Also highlighted in stability of predictions.

Consider percentage change from NLO to NNLO in MSTW08 predictions for best fit α_S compared to fixed $\alpha_S(M_Z^2) = 0.119$.

	$\sigma_{W(Z)}$ 7TeV	$\sigma_{W(Z)}$ 14TeV	σ_H 7TeV	σ_H 7TeV
MSTW08 best fit α_S	3.0	2.6	25	24
MSTW08 $\alpha_S = 0.119$	5.3	5.0	32	30

$\alpha_S(M_Z^2)$ is not a physical quantity. In (nearly) all PDF related quantities (and many others) shows tendency to decrease from order to order. Noticeable if one has fit at NNLO. Any settling on, or near common $\alpha_S(M_Z^2)$ **has** to take this into account.

DØ Run II inclusive jet data (cone, R = 0.7)
(Ratio w.r.t. NLO $\hat{\sigma}$ with $\mu = p_T$ using MSTW08 NNLO PDFs)

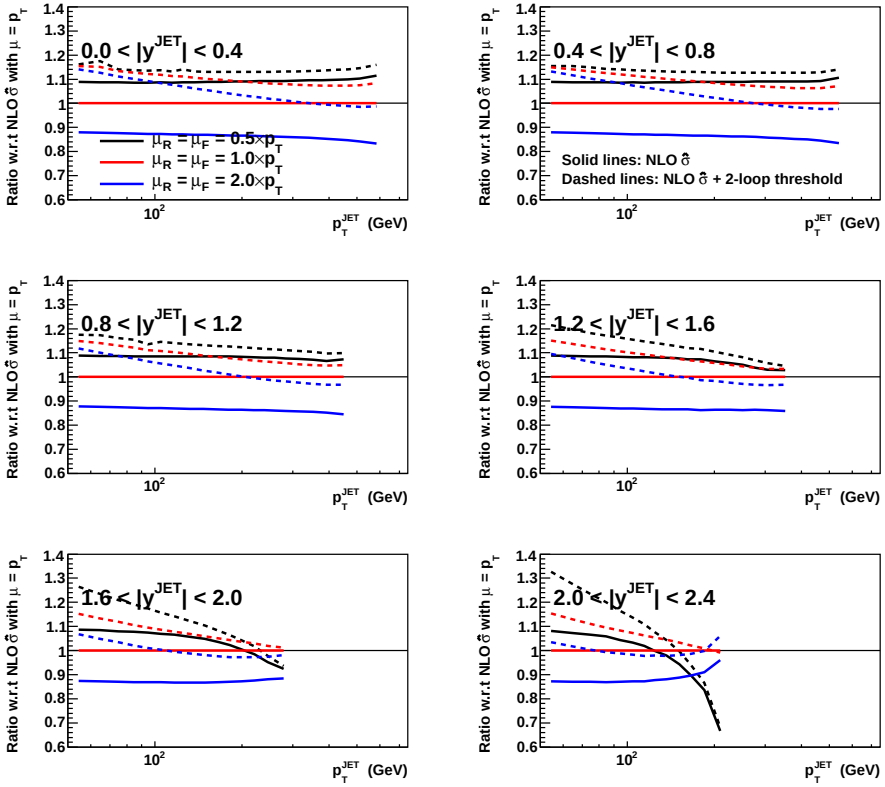

DØ Run II dijet data (cone, R = 0.7)
(Ratio w.r.t. NLO $\hat{\sigma}$ with $\mu = p_T$ using MSTW08 NNLO PDFs)

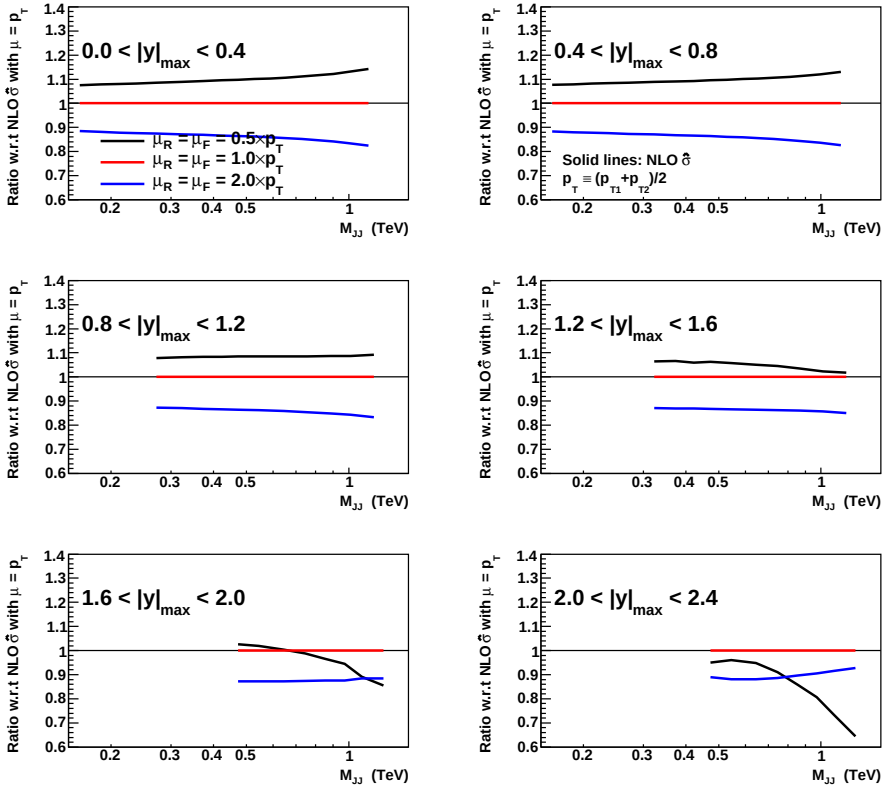

Shape of corrections as function of p_T at NLO and also at approx. NNLO in inclusive case. Problem at highest p_T and rapidity even for inclusive jets.

NLO PDF (with NLO $\hat{\sigma}$)	$\mu = p_T/2$	$\mu = p_T$	$\mu = 2p_T$
MSTW08	1.45 (0.89)	**1.08** (0.20)	**1.05** (1.22)
CTEQ6.6	1.62 (1.15)	1.56 (0.59)	1.61 (1.35)
CT10	1.39 (0.88)	1.26 (0.37)	1.32 (1.29)
NNPDF2.1	1.41 (0.87)	1.29 (0.20)	1.22 (0.96)
HERAPDF1.0	1.73 (0.27)	1.84 (0.74)	1.83 (2.79)
HERAPDF1.5	1.78 (0.29)	1.87 (0.75)	1.84 (2.81)
ABKM09	1.39 (0.35)	1.43 (1.07)	1.63 (3.66)
GJR08	1.90 (1.46)	1.34 (0.45)	**1.03** (0.51)

NNLO PDF (with NLO+2-loop $\hat{\sigma}$)	$\mu = p_T/2$	$\mu = p_T$	$\mu = 2p_T$
MRST06	3.19 (5.00)	1.77 (3.22)	1.25 (1.50)
MSTW08	1.95 (0.90)	1.23 (0.44)	**1.08** (0.35)
HERAPDF1.0, $\alpha_S(M_Z^2) = 0.1145$	2.11 (0.37)	1.68 (0.35)	1.41 (0.63)
HERAPDF1.0, $\alpha_S(M_Z^2) = 0.1176$	2.28 (0.95)	1.50 (0.40)	**1.17** (0.21)
ABKM09	1.68 (0.79)	1.55 (1.21)	1.63 (2.04)
JR09	1.84 (0.47)	1.61 (0.36)	1.58 (0.50)

Table 3: Values of $\chi^2/N_{\text{pts.}}$ for the DØ Run II inclusive jet data using a cone jet algorithm with $N_{\text{pts.}} = 110$ and $N_{\text{corr.}} = 23$, for different PDF sets and different scale choices. At most a 1-σ shift in normalisation is allowed.

NLO PDF (with NLO $\hat{\sigma}$)	$\mu = p_T/2$	$\mu = p_T$	$\mu = 2p_T$
MSTW08	1.40 (*+1.05*)	1.08 (−0.55)	0.85 (*−2.25*)
CTEQ6.6	1.52 (*−1.61*)	1.25 (*−2.88*)	1.01 (**−4.02**)
CT10	1.39 (−0.66)	1.11 (*−2.02*)	0.90 (**−3.35**)
NNPDF2.1	1.41 (+0.37)	1.23 (*−1.22*)	0.95 (*−2.67*)
HERAPDF1.0	1.55 (*−2.16*)	1.38 (**−3.51**)	1.07 (**−4.52**)
HERAPDF1.5	1.63 (*−1.98*)	1.45 (**−3.35**)	1.12 (**−4.40**)
ABKM09	1.25 (*−1.90*)	1.04 (**−3.20**)	0.89 (**−4.44**)
GJR08	1.72 (*+2.14*)	1.34 (+0.53)	0.98 (*−1.05*)

NNLO PDF (with NLO+2+loop $\hat{\sigma}$)	$\mu = p_T/2$	$\mu = p_T$	$\mu = 2p_T$
MRST06	2.92 (*+2.66*)	1.70 (*+1.31*)	1.25 (+0.44)
MSTW08	1.87 (*+1.34*)	1.23 (+0.09)	1.08 (−0.87)
HERAPDF1.0, $\alpha_S(M_Z^2) = 0.1145$	2.11 (−0.82)	1.52 (*−2.03*)	1.14 (*−2.61*)
HERAPDF1.0, $\alpha_S(M_Z^2) = 0.1176$	2.28 (+0.94)	1.50 (−0.49)	1.11 (*−1.23*)
ABKM09	1.48 (*−2.33*)	1.13 (**−3.35**)	1.02 (**−4.03**)
JR09	1.84 (+0.63)	1.61 (−0.60)	1.50 (*−1.35*)

Table 4: Values of $\chi^2/N_{\text{pts.}}$ for the DØ Run II inclusive jet data using a cone jet algorithm with $N_{\text{pts.}} = 110$ and $N_{\text{corr.}} = 23$, for different PDF sets and different scale choices. No restriction is imposed on the shift in normalisation and the optimal value of "$-r_{\text{lumi}}$" is shown in brackets.

Comparison of the raw comparison to CDF inclusive jet data using the k_T and cone algorithms.

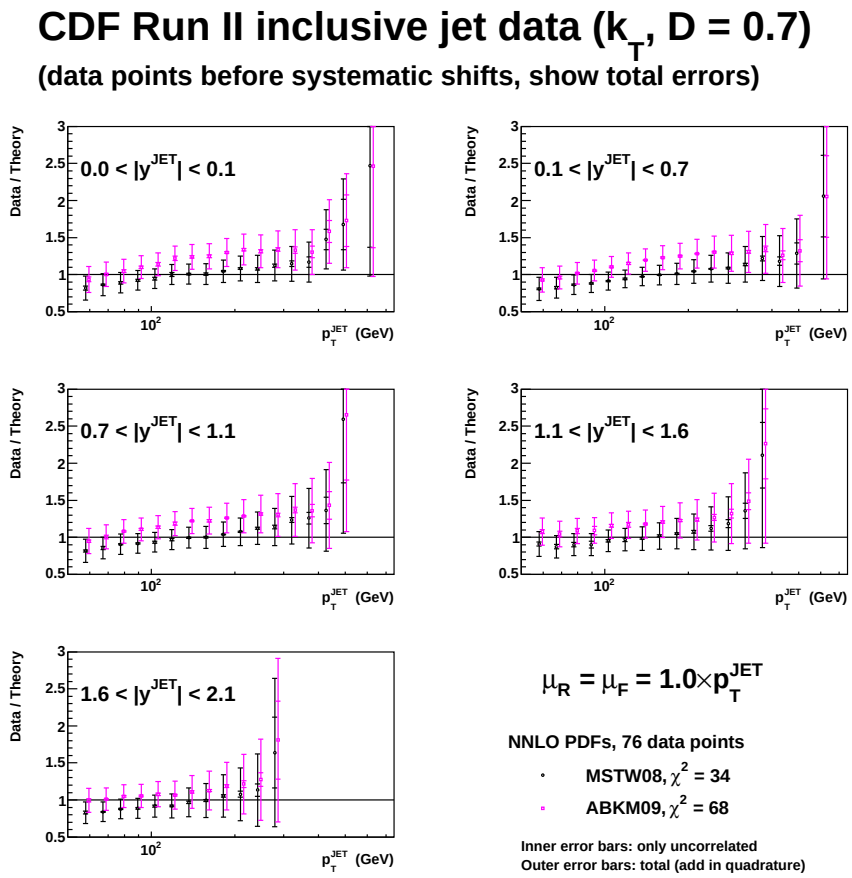

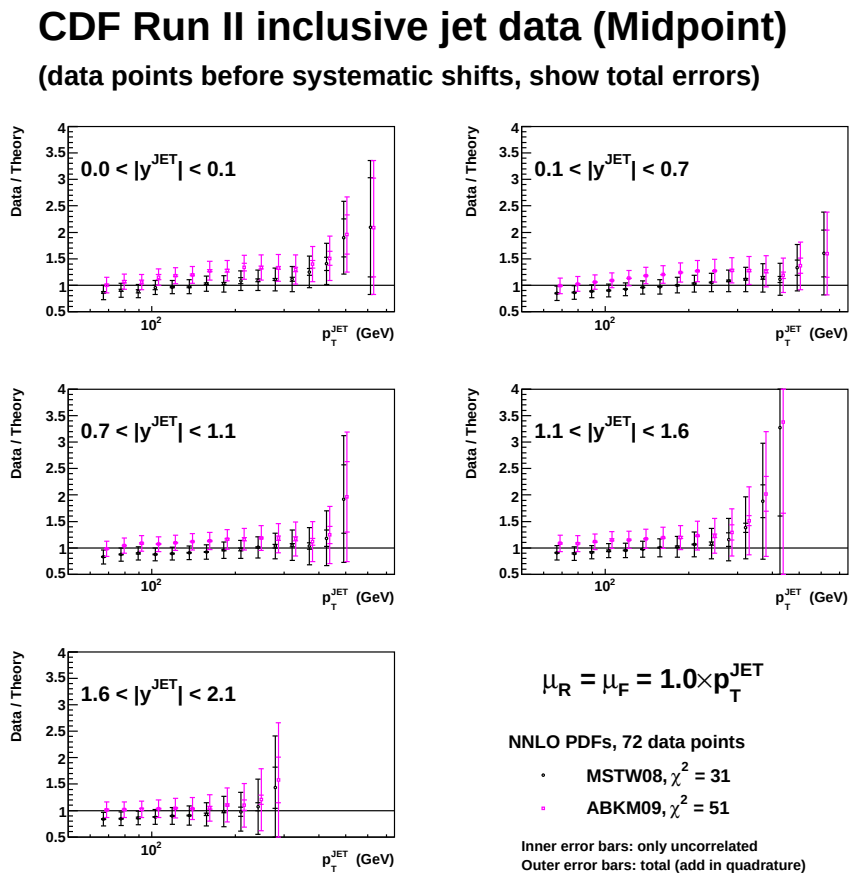

Data/theory the same shape for both. Good compatibility. Verified by fits.

Comparison of the raw comparison to D0 inclusive jet data using the cone algorithms and D0 dijet data.

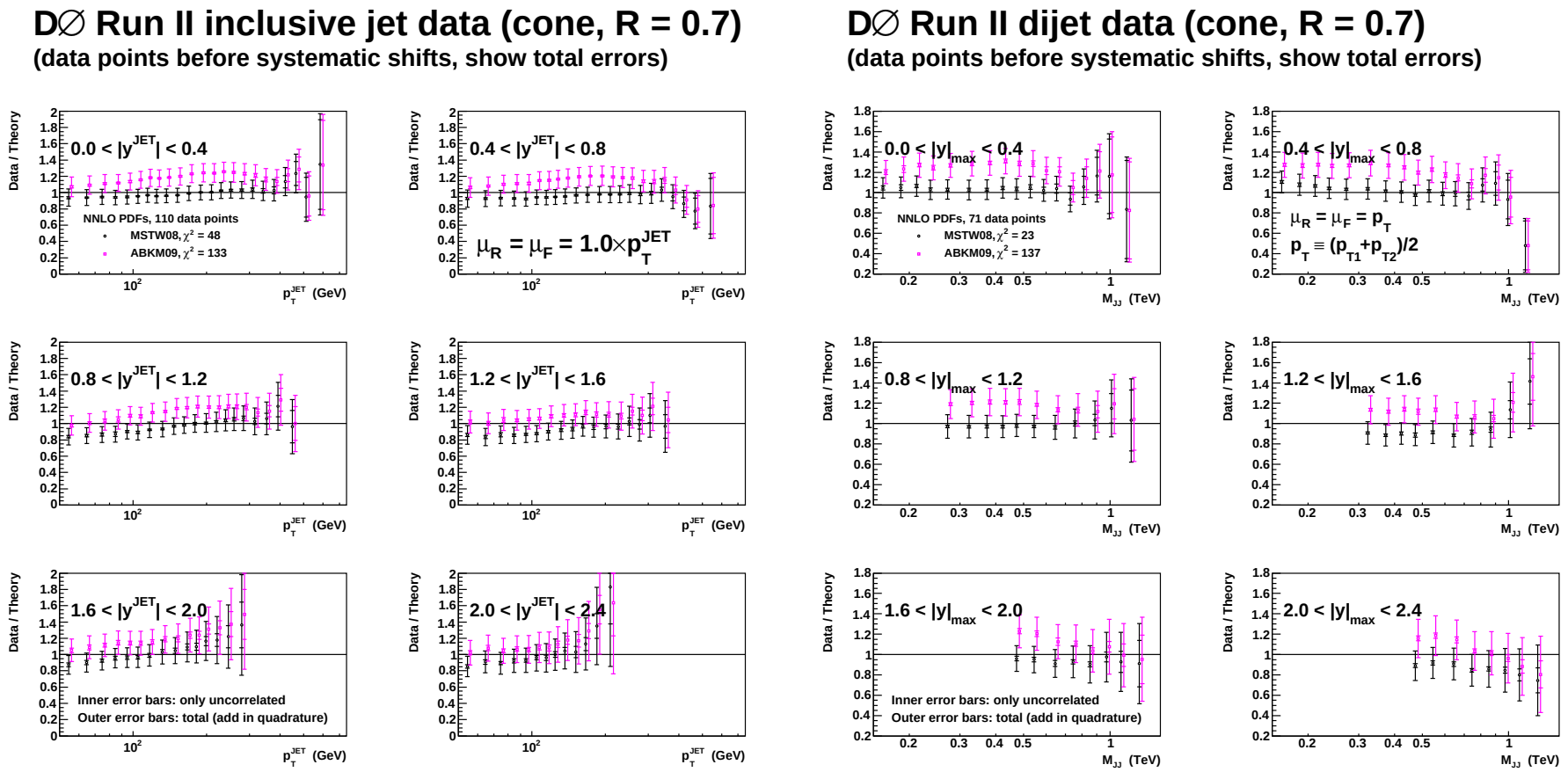

Not such good compatibility as for the two CDF sets.

Three-jet cross-sections

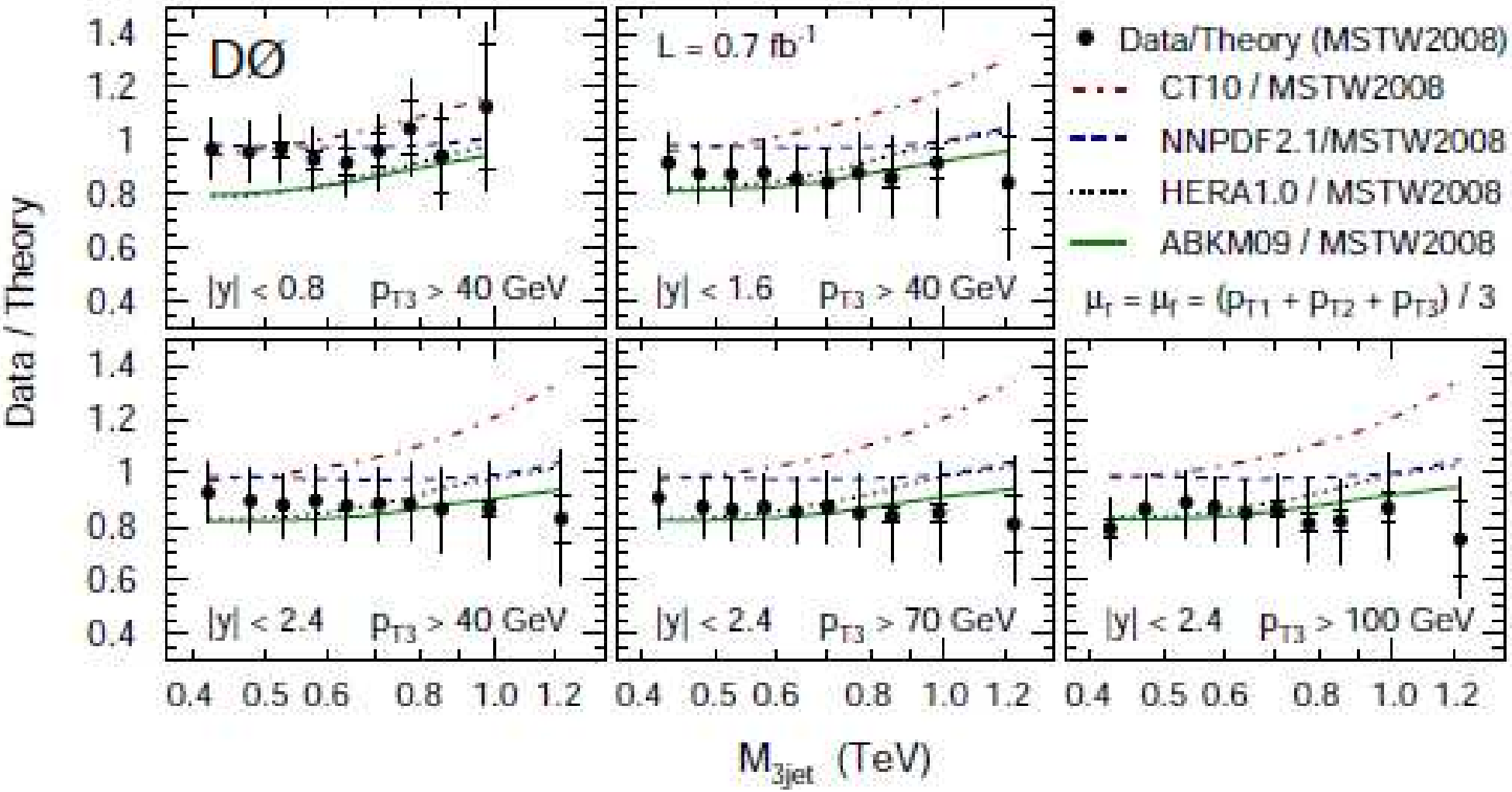

Recent results from D0 (`arXiv 1104.1986`) on three jets cross sections.

All the same work already done.

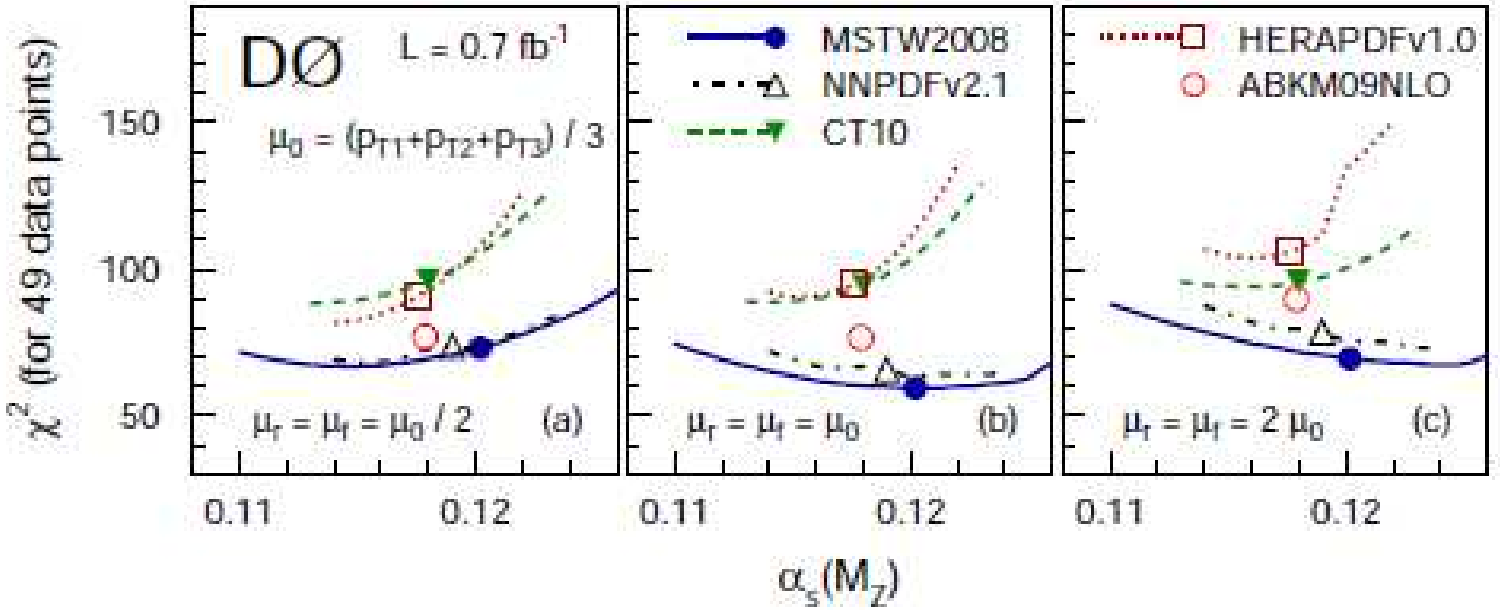

TABLE II: χ^2 values between data and theory for different PDF parametrizations in the order of decreasing χ^2, for all 49 data points.

PDF set	Default $\alpha_s(M_Z)$	χ^2 at $\mu_r = \mu_f = \mu_0$ for default $\alpha_s(M_Z)$	χ^2_{minimum}
HERAPDFv1.0	0.1176	95.1	81.7
CT10	0.1180	94.5	88.2
ABKM09NLO	0.1179	76.5	76.5
NNPDFv2.1	0.1190	65.9	63.3
MSTW2008NLO	0.1202	59.5	59.5

Broadly similar results.

Sometimes the reason for cross section differences is unexpected.

Warsinsky at recent Higgs-LHC working group meeting.

m_b values bring CTEQ and MSTW together but exaggerate NNPDF difference.

Couplings have assumed common mass value.

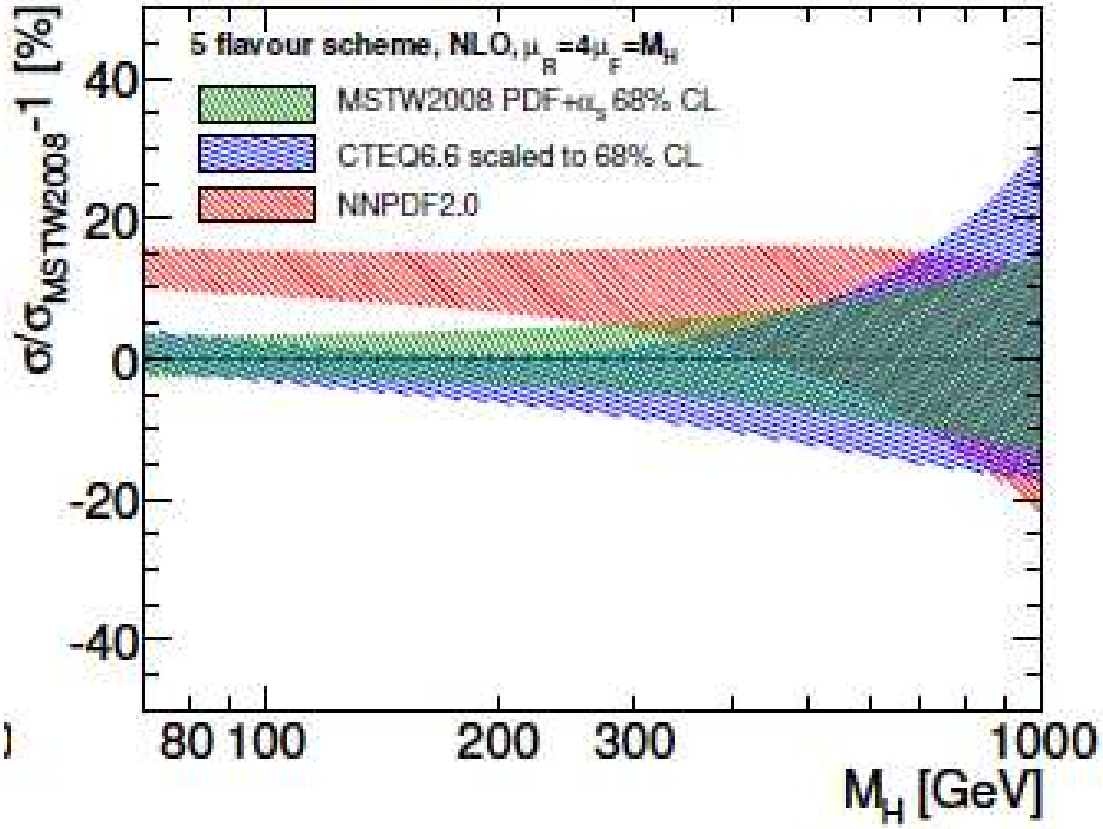

Small-x Theory

Reason for this instability – at each order in α_S each splitting function and coefficient function obtains an extra power of $\ln(1/x)$ (some accidental zeros in P_{gg}), i.e. $P_{ij}(x, \alpha_s(Q^2)), C_i^P(x, \alpha_s(Q^2)) \sim \alpha_s^m(Q^2) \ln^{m-1}(1/x)$.

BFKL equation for high-energy limit

$$f(k^2, x) = f_I(Q_0^2) + \int_x^1 \frac{dx'}{x'} \bar{\alpha}_S \int_0^\infty \frac{dq^2}{q^2} K(q^2, k^2) f(q^2, x),$$

where $f(k^2, x)$ is the unintegrated gluon distribution $g(x, Q^2) = \int_0^{Q^2} (dk^2/k^2) f(x, k^2)$, and $K(q^2, k^2)$ is a calculated kernel known to NLO.

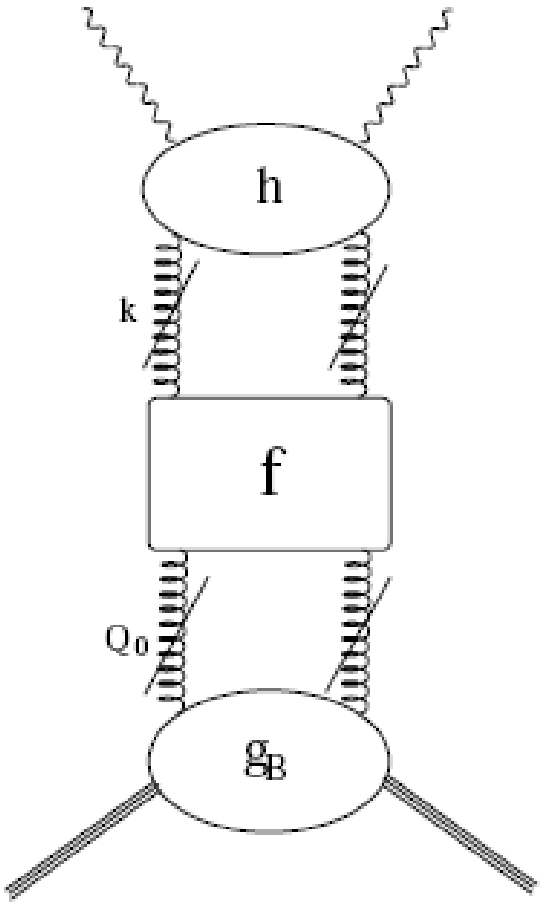

Physical structure functions obtained from

$$\sigma(Q^2, x) = \int (dk^2/k^2)\, h(k^2/Q^2) f(k^2, x)$$

where $h(k^2/Q^2)$ is a calculable impact factor.

The global fits usually assume that this is unimportant in practice, and proceed regardless.

Fits work well at small x, but could improve.

Good recent progress in incorporating $\ln(1/x)$ resummation Altarelli-Ball-Forte, Ciafaloni-Colferai-Salam-Stasto and White-RT.

Include running coupling effects and variety (depending on group) of other corrections

By 2008 very similar results coming from the competing procedures, despite some differences in technique.

Full set of coefficient functions still to come in some cases, but splitting functions comparable.

Note, in all cases NLO corrections lead to dip in functions below fixed order values until slower growth (running coupling effect) at very small x.

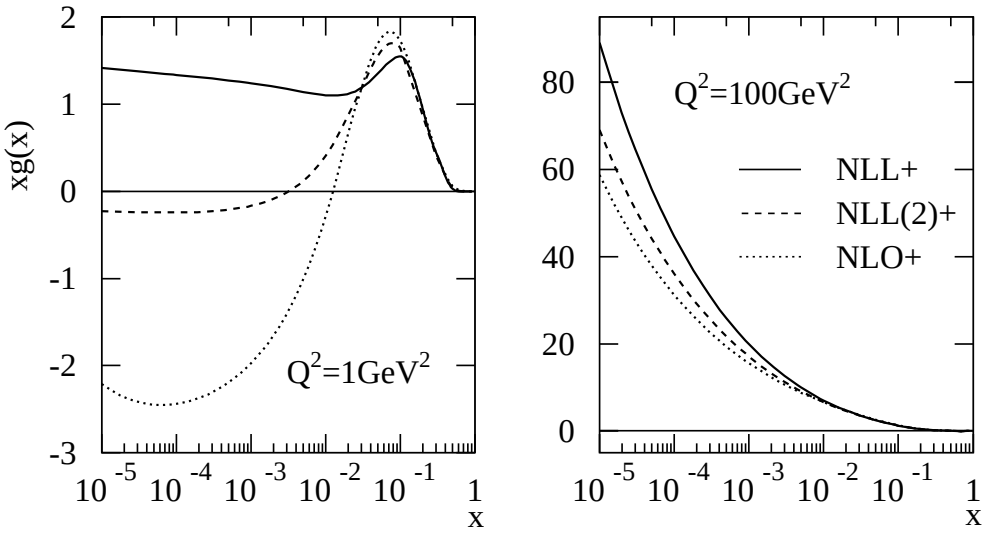

A fit to data with NLO plus NLO resummation, with heavy quarks included (White,RT) performed.

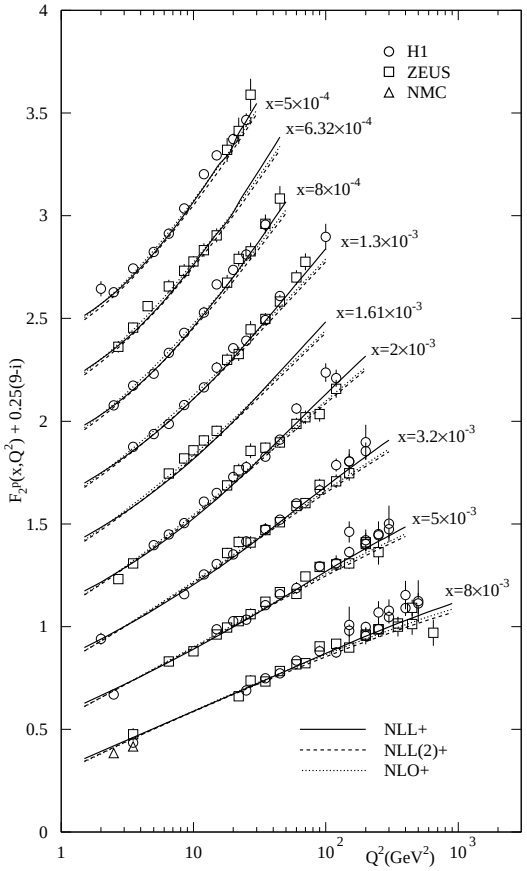

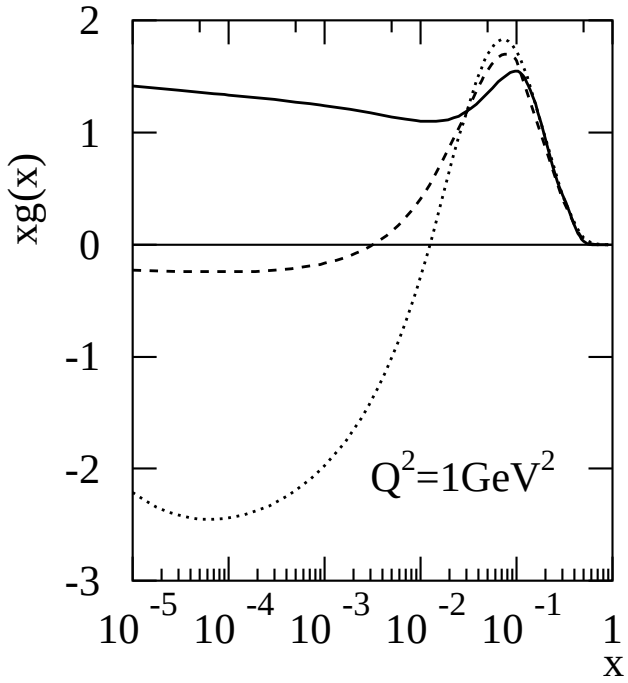

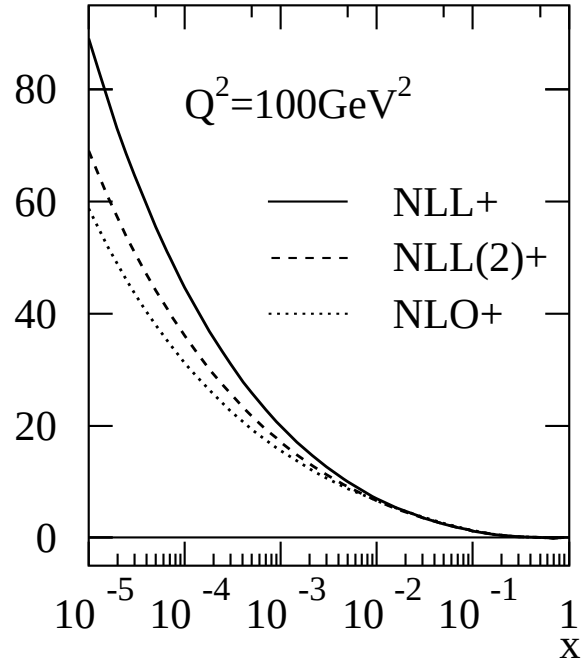

→ moderate improvement in fit to HERA data within global fit, and change in extracted gluon (more like quarks at low Q^2).

Together with indications from Drell Yan resummation calculations (Marzani, Ball) few percent effect quite possible.

PDF Correlations

The PDF uncertainty analysis may be extended to define a *correlation* between the uncertainties of two variables, say $X(\vec{a})$ and $Y(\vec{a})$.

The correlations were calculated using the MCFM NLO program (versions 5.8 and 6.0) with a common set of input files for all groups. Each group did their own calculations.

For the groups using a Hessian approach the correlations were calculated using

$$\cos\varphi = \frac{\vec{\Delta}X \cdot \vec{\Delta}Y}{\Delta X \Delta Y} = \frac{1}{4\Delta X \Delta Y} \sum_{i=1}^{N} \left(X_i^{(+)} - X_i^{(-)}\right)\left(Y_i^{(+)} - Y_i^{(-)}\right)$$

$$\Delta X = \left|\vec{\Delta}X\right| = \frac{1}{2}\sqrt{\sum_{i=1}^{N}\left(X_i^{(+)} - X_i^{(-)}\right)^2}$$

or some similar variation. This included the most up-to-date published sets for each group, i.e. , ABKM09, CT10, GJR 08, MSTW08. The basic results for CT10 and MSTW08 are PDF only, whereas ABKM09 and GJR08 include α_S as a parameter in the error matrix.

Due to the specific error calculation prescription for HERAPDF1.5 which includes parameterization and model errors, the correlations can not be calculated in exactly the same way. An alternative way is to use a formula for uncertainty propagation in which correlations can be expressed via relative errors of compounds and their combination:

$$\sigma^2\left(\frac{X}{\sigma(X)}+\frac{Y}{\sigma(Y)}\right)=2+2\cos\varphi,$$

where $\sigma(O)$ is the PDF error of observable O calculated using the HERAPDF prescription.

The correlations for the NNPDF prescription are calculated using

$$\rho\left(X,Y\right)=\frac{\left\langle XY\right\rangle_{\mathrm{rep}}-\left\langle X\right\rangle_{\mathrm{rep}}\left\langle Y\right\rangle_{\mathrm{rep}}}{\sigma_X\sigma_Y}$$

where the averages are performed over the $N_{\mathrm{rep}}=100$ replicas of the NNPDF2.1 set.

The averaging was done and diagrams made by J. Rojo.

Backgrounds

	Z	W	ZZ	WW	WZ	Wγ	WQQ	ZQQ	ggWW	ggZZ	ttbar	tW	tb	tbq
Z	1	0.95	0.67	0.70	0.95	0.9	0.43/0.53	0.08	-0.67	-0.75	-0.74	-0.81	0.59	-0.29
W	0.95	1	0.52/0.69	0.60/0.71	0.88/1.0	0.90/0.80	0.39/0.50	0.08	-0.67	-0.74	-0.73	-0.8	0.57	-0.29
ZZ	0.67	0.52/0.69	1	0.97	0.54/0.73	0.62	0.78/0.87	-0.09	-0.36	-0.34	-0.17	-0.81	0.9	-0.23
WW	0.70	0.60/0.71	0.97	1	0.63/0.75	0.69	0.80/0.86	-0.02	-0.34	-0.33	-0.20	-0.33	0.94	-0.08
WZ	0.95	0.88/1.0	0.54/0.73	0.63/0.75	1	0.9	0.55	0.1	-0.64	-0.71	-0.71	-0.73	0.61	-0.34
Wγ	0.9	0.90/0.80	0.62	0.69	0.9	1	0.63/0.53	0.32	-0.44	-0.54	-0.68	0.61	0.61	0
WQQ	0.43/0.53	0.39/0.50	0.78/0.87	0.80/0.86	0.55	0.63/0.53	1	0.08	-0.12	-0.12	-0.05	-0.15	0.64	-0.32
ZQQ	0.08	0.08	-0.09	-0.02	0.1	0.32	0.08	1	0.54	0.36	-0.26	-0.05	-0.03	0.59
ggWW	-0.67	-0.67	-0.36	-0.34	-0.64	-0.44	-0.12	0.54	1	0.98	0.65	0.81	-0.28	0.63
ggZZ	-0.75	-0.74	-0.34	-0.33	-0.71	-0.54	-0.12	0.36	0.98	1	0.79	0.91	-0.27	0.55
ttbar	-0.74	-0.73	-0.17	-0.20	-0.71	-0.68	-0.05	-0.26	0.65	0.79	1	0.97	-0.12	0.17
tW	-0.81	-0.8	-0.81	-0.33	-0.73	0.61	-0.15	-0.05	0.65	0.91	0.97	1	-0.25	0.31
tb	0.59	0.57	0.9	0.94	0.61	0.61	0.64	-0.03	-0.28	-0.27	-0.12	-0.25	1	0.04
tbq	-0.29	-0.29	-0.23	-0.08	-0.34	0	-0.32	0.59	0.63	0.55	0.17	0.31	0.04	1

Full study involves range of backgrounds shown by Huston at PDF4LHC- July 2011. Will be found at

https://twiki.cern.ch/twiki/bin/view/LHCPhysics/PDFCorrelations

m_H=120

	ggH	VBF	WH	ZH	ttH	Z	W+/W-	ZZ	WW	WZ	Wγ	WQQ	ZQQ	ggWW	ggZZ	ttbar	tW	tb	tbq
ggH	1	-0.57	-0.23	-0.14	-0.6	0.01	0.03	0.02	-0.20	0.04	0.23	-0.14	0.95	0.47	0.28	-0.35	-0.12	-0.24	0.52
VBF	-0.57	1	0.63/0.73	0.76	0.09	0.43	0.26/0.41	0.79	0.72	0.28/0.43	0.28/0.37	0.52/0.71	-0.41	-0.47	-0.4	-0.10	-0.28	0.65	-0.25
WH	-0.23	0.63/0.73	1	0.93	0	0.62	0.52/0.64	0.92	0.93	0.65/058	0.65/0.56	0.79/0.95	-0.02	-0.29	-0.28	-0.15	-0.28	0.99/0.77	0.05/-0.30
ZH	-0.14	0.76	0.93	1	0.03	0.64	0.53/0.66	0.99	0.99	0.55/0.71	0.63	0.83	-0.07	-0.31	-0.3	-0.14	-0.28	0.93	-0.14
ttH	-0.6	0.09	0	0.03	1	-0.61	-0.6	0	-0.05	-0.58	-0.64	0.04	-0.5	0.03	0.56	0.94	0.84	0.02	-0.07

m_H=160

	ggH	VBF	WH	ZH	ttH	Z	W+/W-	ZZ	WW	WZ	Wγ	WQQ	ZQQ	ggWW	ggZZ	ttbar	tW	tb	tbq
ggH	1	-0.61	-0.29	-0.35	-0.24	-0.32	-0.32	-0.35	-0.29	-0.29	-0.06	-0.12	0.9	0.82	0.68	0.1	0.33	-0.27	0.67
VBF	-0.61	1	0.62	0.74	0.2	0.35	0.19/0.34	0.75	0.66	0.20/0.36	0.19/0.28	0.46/0.70	-0.47	-0.46	-0.37	-0.03	-0.22	0.6	-0.29
WH	-0.29	0.62	1	0.93	0.1	0.55	0.52	0.9	0.93	0.56	0.56	0.93	-0.07	-0.26	-0.23	-0.07	-0.21	1	0.03
ZH	-0.35	0.74	0.93	1	0.16	0.54	0.43/0.58	0.98	0.97	0.45/0.63	0.52	0.93	-0.14	-0.29	-0.25	-0.04	-0.2	0.91	-0.16
ttH	-0.24	0.2	0.1	0.16	1	-0.59	-0.58	0.03	-0.03	-0.56	-0.62	-0.05	-0.54	0.33	0.51	0.92	0.8	0.04	-0.12

m_H=200

	ggH	VBF	WH	ZH	ttH	Z	W+/W-	ZZ	WW	WZ	Wγ	WQQ	ZQQ	ggWW	ggZZ	ttbar	tW	tb	tbq
ggH	1	-0.5	-0.26	-0.3	0.13	-0.59	-0.59	-0.36	-0.32	-0.55	-0.33	-0.11	0.68	0.98	0.93	0.5	0.69	-0.27	0.67
VBF	-0.5	1	0.60/0.73	0.72	0.26	0.28	0.13/0.28	0.7	0.62	0.15/0.30	0.12/0.20	0.40/0.69	-0.52	-0.44	-0.34	0.02	-0.17	0.55	-0.32
WH	-0.26	0.60/0.73	1	0.92	0.2	0.44	0.44/0.38	0.89	0.86	0.48/0.41	0.47/0.36	0.78/0.74	-0.15	-0.24	-0.2	0	0.15	0.98/0.69	0
ZH	-0.3	0.72	0.92	1	0.24	0.46	0.34/0.51	0.95	0.93	0.37/0.56	0.43	0.74/0.85	-0.19	-0.3	-0.22	0.02	-0.14	0.88	-0.2
ttH	0.13	0.26	0.2	0.24	1	-0.57	-0.57	0.03	-0.03	-0.55	-0.63	0.03	-0.56	0.29	0.48	0.9	0.78	0.03	-0.15

And similar for signals. However, too detailed for concise presentation when averaging/comparing, and precision much higher than spread between groups.

Full list also not vital since W production is very similar to Z production, both depending on partons (quarks in this case) at very similar hard scales and x values. Similarly for WW and ZZ, and the subprocesses $\mathrm{gg} \to \mathrm{WW(ZZ)}$ and $\mathrm{gg} \to \mathrm{H}$ for $M_H = 200$ GeV.

The up-to-date PDF4LHC average (CT10, MSTW08, NNPDF2.1) for the correlations between all signal processes with other signal and background processes for Higgs production considered here. The processes have been classified in correlation classes of width 0.2.

120 GeV				
	ggH	VBF	WH	$t\bar{t}H$
ggH	1	-0.6	-0.2	-0.2
VBF	-0.6	1	0.6	-0.4
WH	-0.2	0.6	1	-0.2
$t\bar{t}H$	-0.2	-0.4	-0.2	1
W	-0.2	0.6	0.8	-0.6
WW	-0.4	0.8	1	-0.2
WZ	-0.2	0.4	0.8	-0.4
$W\gamma$	0	0.6	0.8	-0.6
$Wb\bar{b}$	-0.2	0.6	1	-0.2
$t\bar{t}$	0.2	-0.4	-0.4	1
$t\bar{b}$	-0.4	0.6	1	-0.2
$t(\rightarrow \bar{b})q$	0.4	0	0	0

160 GeV				
	ggH	VBF	WH	$t\bar{t}H$
ggH	1	-0.6	-0.4	0.2
VBF	-0.6	1	0.6	-0.2
WH	-0.4	0.6	1	0
$t\bar{t}H$	0.2	-0.2	0	1
W	-0.4	0.4	0.6	-0.4
WW	-0.4	0.6	0.8	-0.2
WZ	-0.4	0.4	0.8	-0.2
$W\gamma$	-0.4	0.6	0.6	-0.6
$Wb\bar{b}$	-0.2	0.6	0.8	-0.2
$t\bar{t}$	0.4	-0.4	-0.2	0.8
$t\bar{b}$	-0.4	0.6	1	0
$t(\rightarrow \bar{b})q$	0.6	0	0	0

200 GeV				
	ggH	VBF	WH	$t\bar{t}H$
ggH	1	-0.6	-0.4	0.4
VBF	-0.6	1	0.6	-0.2
WH	-0.4	0.6	1	0
$t\bar{t}H$	0.4	-0.2	0	1
W	-0.6	0.4	0.6	-0.4
WW	-0.4	0.6	0.8	-0.2
WZ	-0.4	0.4	0.8	-0.2
$W\gamma$	-0.4	0.4	0.6	-0.6
$Wb\bar{b}$	-0.2	0.6	0.8	-0.2
$t\bar{t}$	0.6	-0.4	-0.2	0.8
$t\bar{b}$	-0.4	0.6	0.8	0
$t(\rightarrow \bar{b})q$	0.6	-0.2	0	0

300 GeV				
	ggH	VBF	WH	$t\bar{t}H$
ggH	1	-0.4	-0.2	0.6
VBF	-0.4	1	0.4	-0.2
WH	-0.2	0.4	1	0.2
$t\bar{t}H$	0.6	-0.2	0.2	1
W	-0.6	0.4	0.4	-0.6
WW	-0.4	0.6	0.8	-0.2
WZ	-0.6	0.4	0.6	-0.4
$W\gamma$	-0.6	0.4	0.4	-0.6
$Wb\bar{b}$	-0.2	0.4	0.8	-0.2
$t\bar{t}$	1	-0.4	0	0.8
$t\bar{b}$	-0.4	0.4	0.8	-0.2
$t(\rightarrow \bar{b})q$	0.4	-0.2	0	-0.2

500 GeV	ggH	VBF	WH	$t\bar{t}H$
ggH	1	-0.4	0	0.8
VBF	-0.4	1	0.4	-0.2
WH	0	0.4	1	0
$t\bar{t}H$	0.8	-0.2	0	1
W	-0.6	0.4	0.2	-0.6
WW	-0.4	0.6	0.6	-0.4
WZ	-0.6	0.4	0.6	-0.4
$W\gamma$	-0.6	0.4	0.2	-0.6
$Wb\bar{b}$	-0.4	0.4	0.6	-0.4
$t\bar{t}$	1	-0.4	0	0.8
$t\bar{b}$	-0.4	0.4	0.8	-0.2
$t(\rightarrow \bar{b})q$	0.2	-0.2	0	-0.2

Generally the results expected, i.e. gluon dominated processes correlated with each other as are quark dominated processes. Little correlation between the two.

However, see that breakdown of correlation between gluon probed at different x values, e.g $gg \rightarrow H$ for $M_H = 120$ GeV and $t\bar{t}$ since from momentum conservation gluon changes in one place (high x) are compensated by those in another (low x), and the crossing point is between 0.01 and 0.1 but varies slightly between groups.

The same for the correlations between background processes.

	W	WW	WZ	Wγ	W$b\bar{b}$	$t\bar{t}$	$t\bar{b}$	$t(\rightarrow \bar{b})q$
W	1	0.8	0.8	1	0.6	-0.6	0.6	-0.2
WW	0.8	1	0.8	0.8	0.8	-0.4	0.8	0
WZ	0.8	0.8	1	0.8	0.8	-0.4	0.8	0
Wγ	1	0.8	0.8	1	0.6	-0.6	0.8	0
W$b\bar{b}$	0.6	0.8	0.8	0.6	1	-0.2	0.6	0
$t\bar{t}$	-0.6	-0.4	-0.4	-0.6	-0.2	1	-0.4	0.2
$t\bar{b}$	0.6	0.8	0.8	0.8	0.6	-0.4	1	0.2
$t(\rightarrow \bar{b})q$	-0.2	0	0	0	0	0.2	0.2	1

Similar conclusions as for signals.

What about variations between groups?

Correlation between the gluon fusion $gg \to H$ process and the other signal and background processes as a function of M_H.

The class width of 0.2 is typical of the scatter of most deviations between groups.

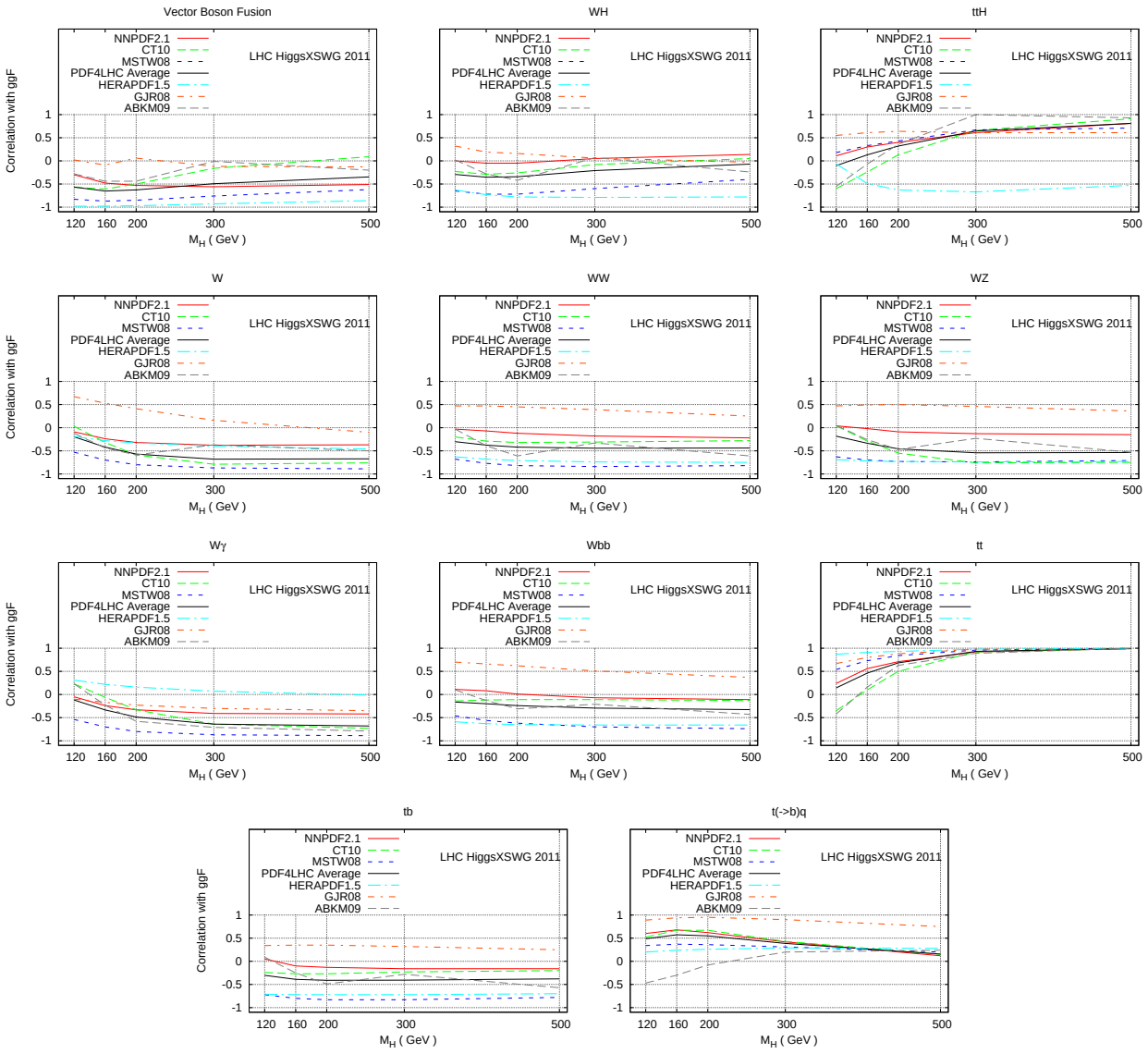

Correlation between the vector boson fusion process and the other signal and background processes as a function of M_H.

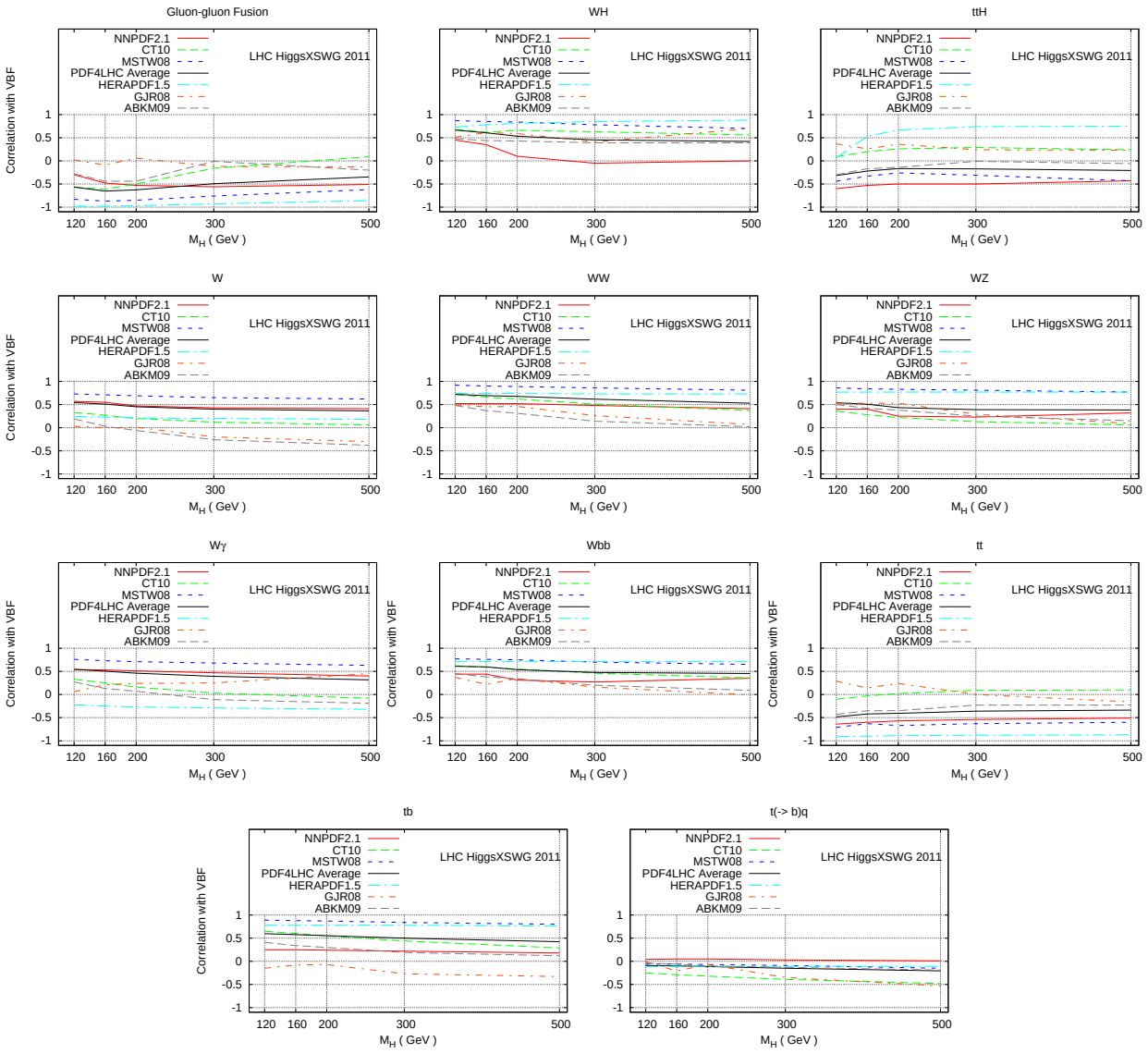

Correlation between the WH process and the other signal and background processes as a function of M_H.

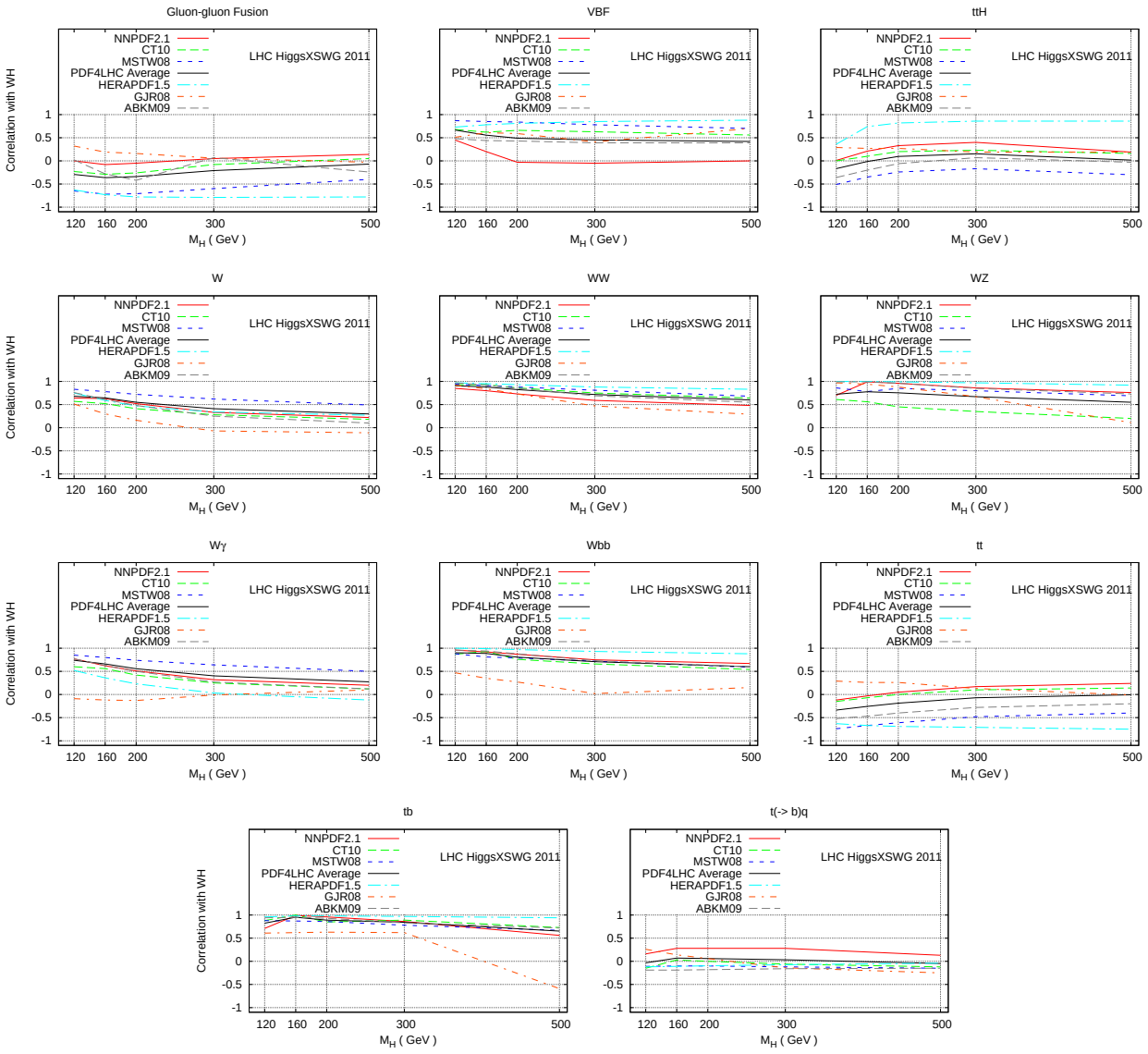

Correlation between the $t\bar{t}H$ process and the other signal and background processes as a function of M_H.

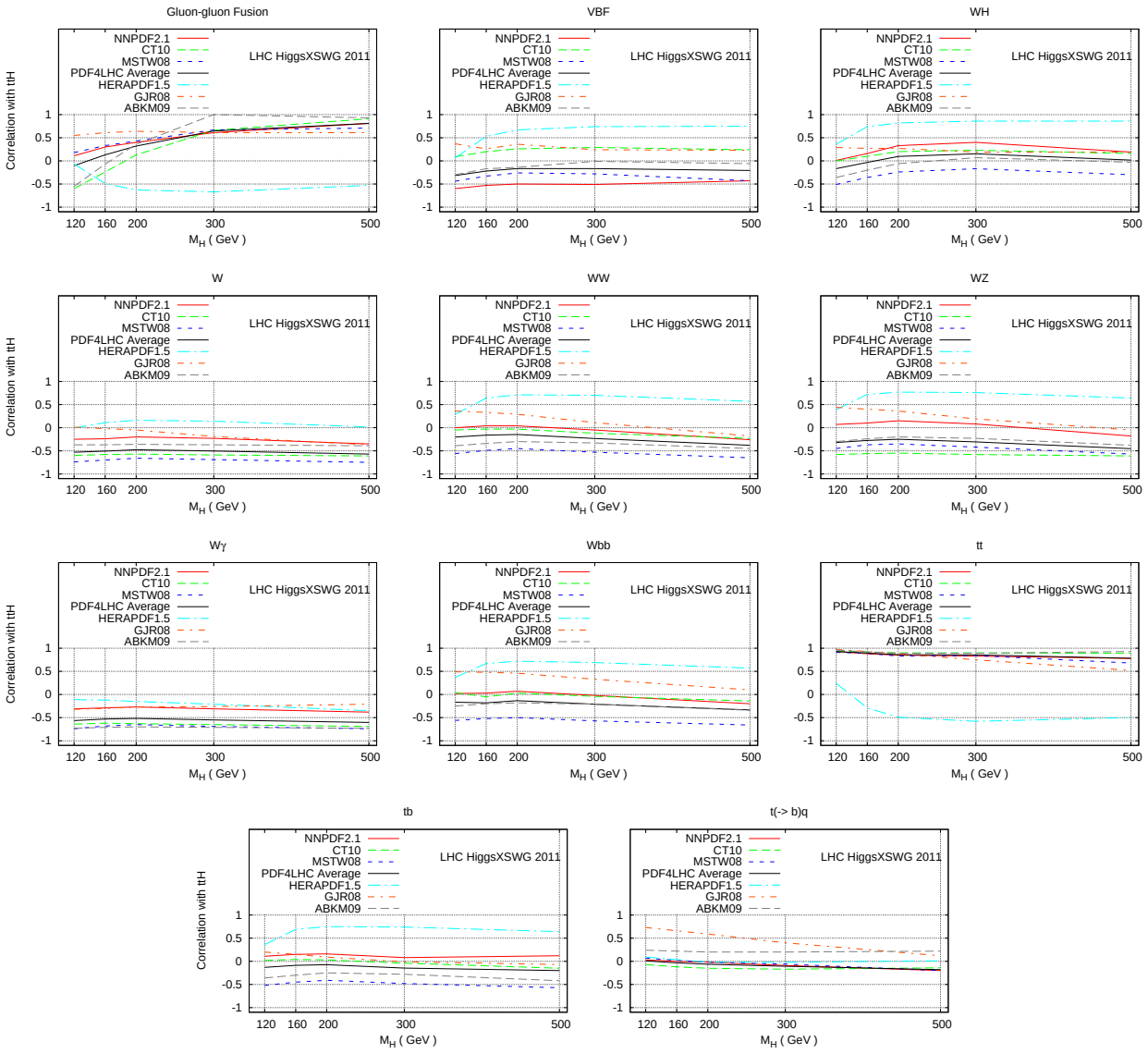

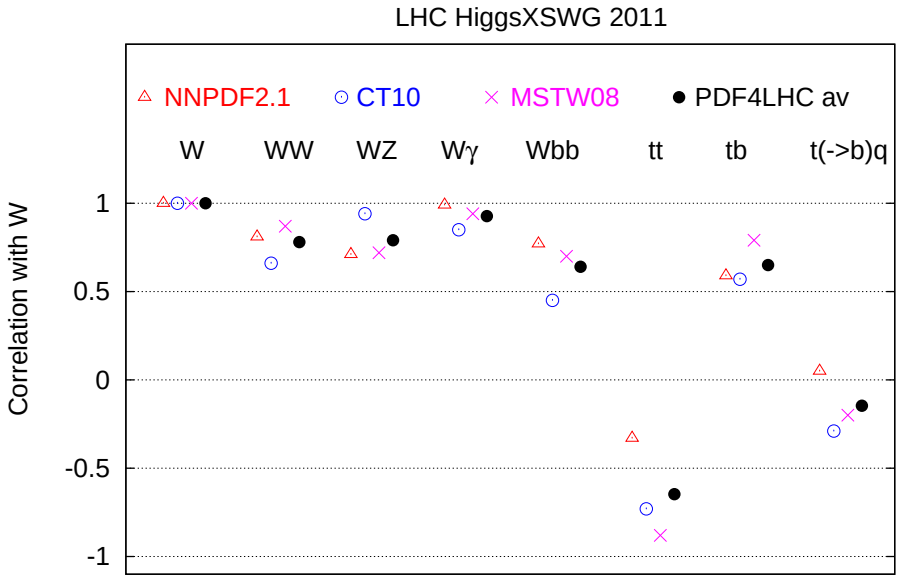

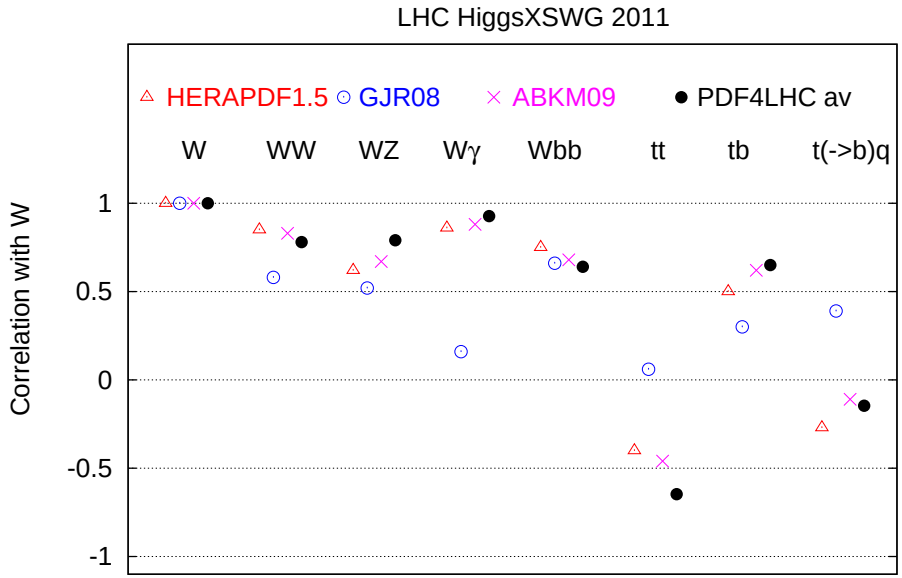

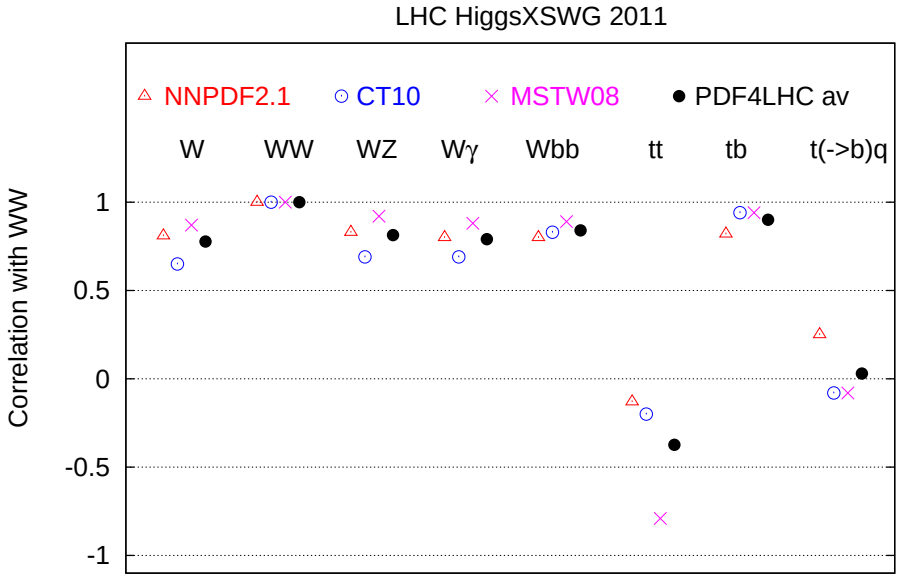

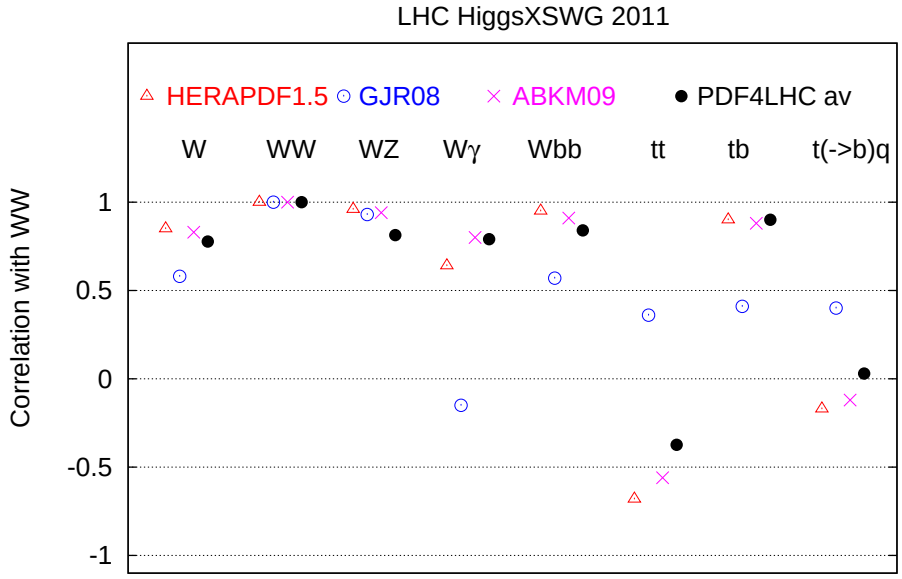

The correlations between W production and WW production and the other background processes considered.

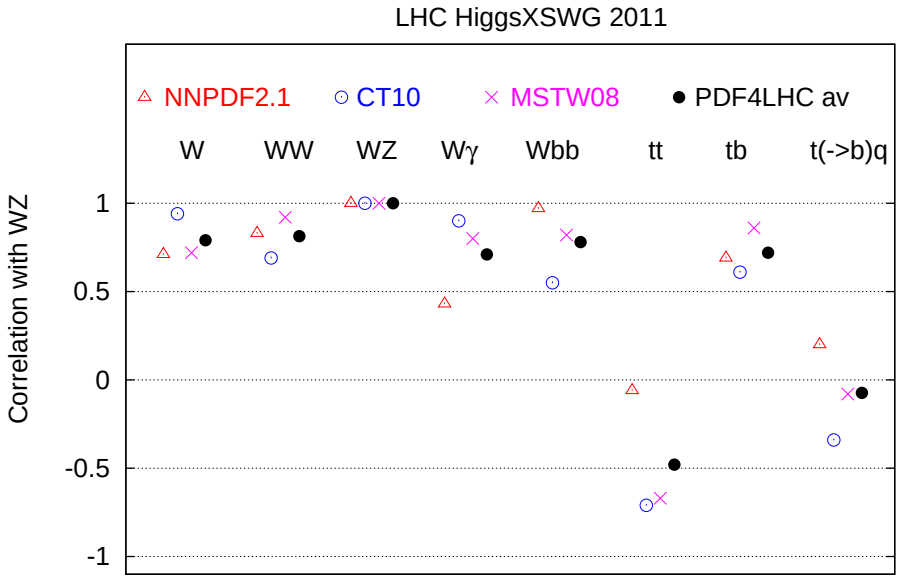

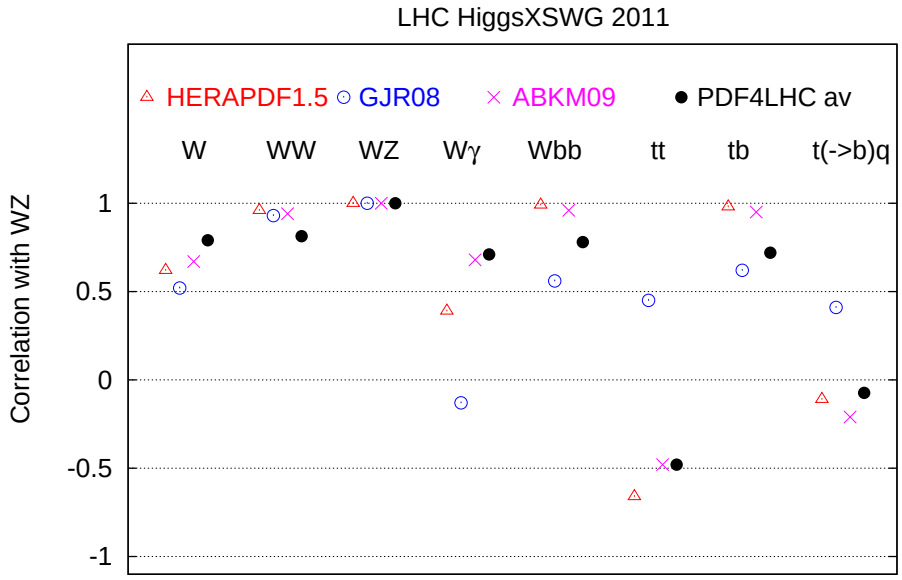

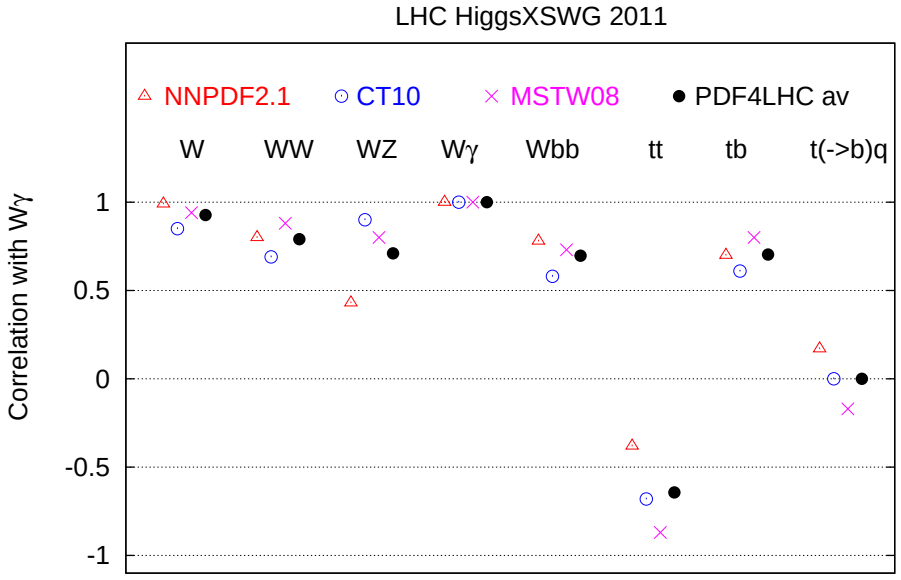

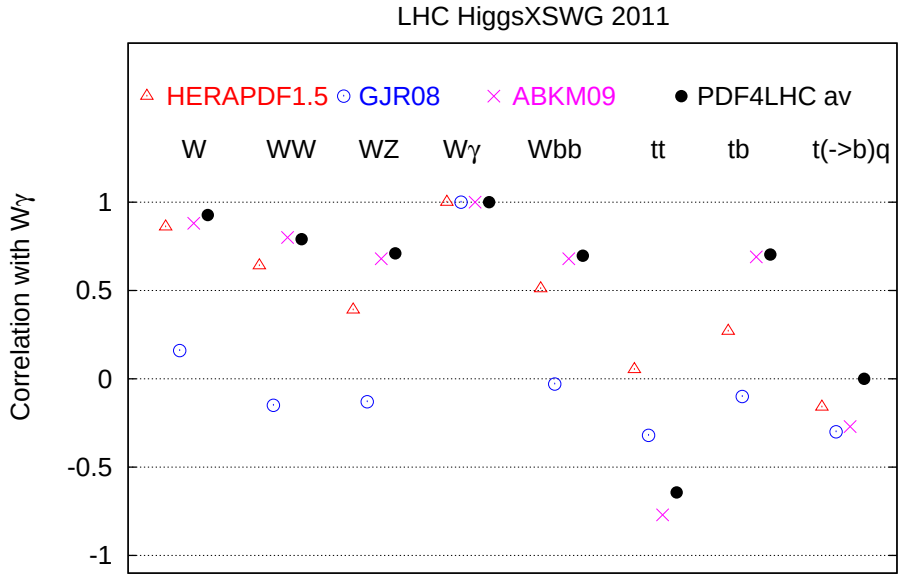

The correlations between WZ production and $W\gamma$ production and the other background processes considered.

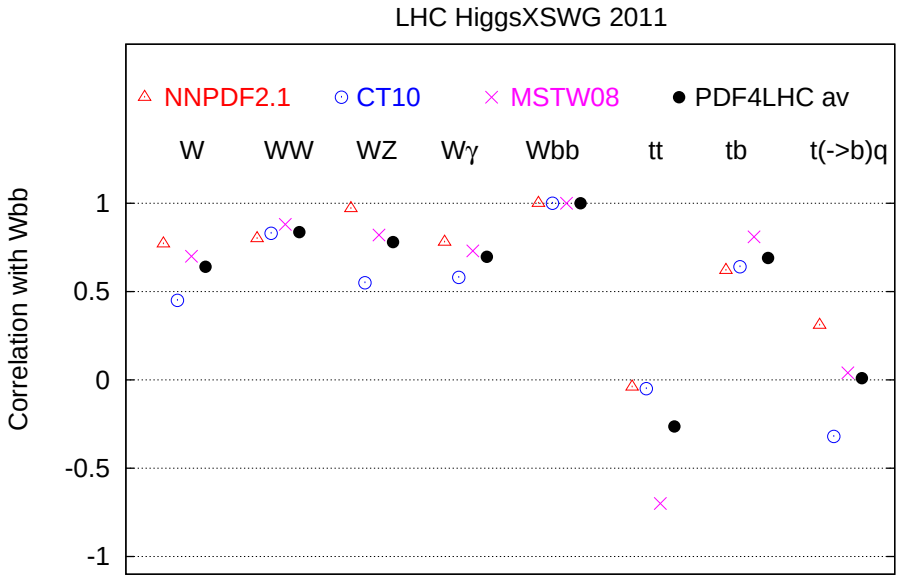

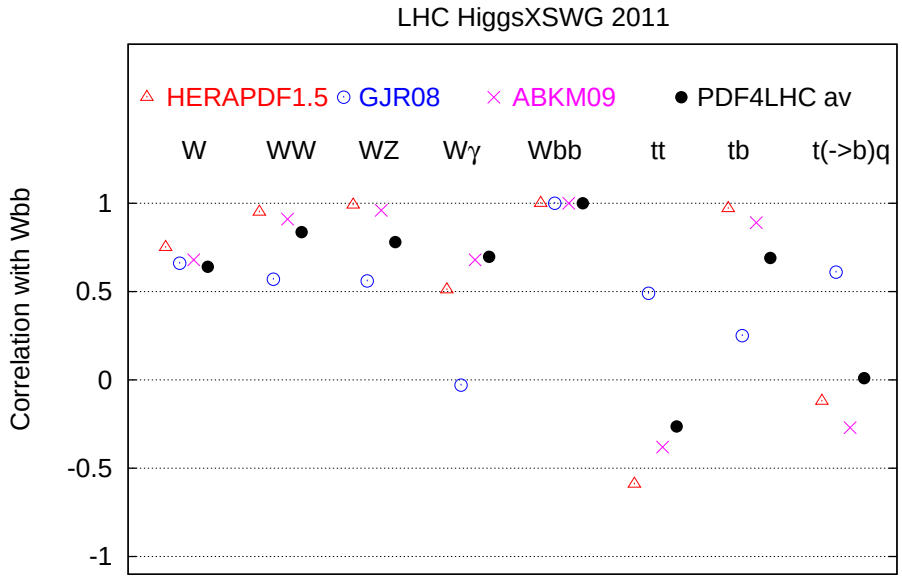

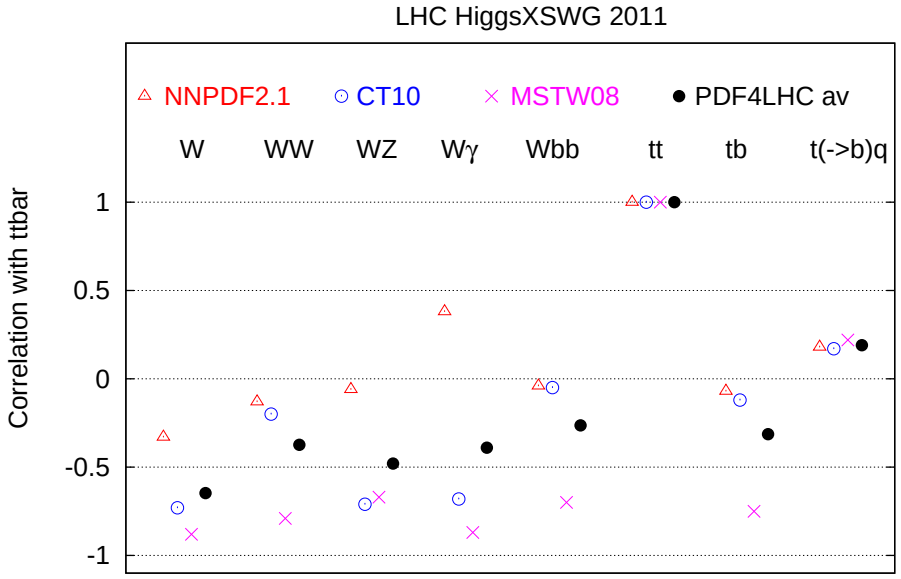

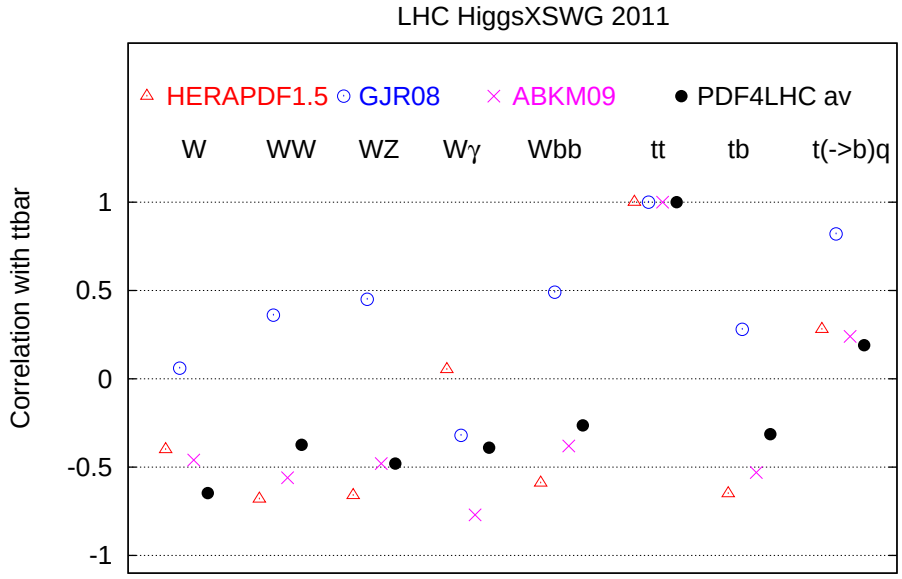

The correlations between $\mathrm{W}\mathrm{b}\bar{\mathrm{b}}$ production and $\mathrm{t}\bar{\mathrm{t}}$ production and the other background processes considered.

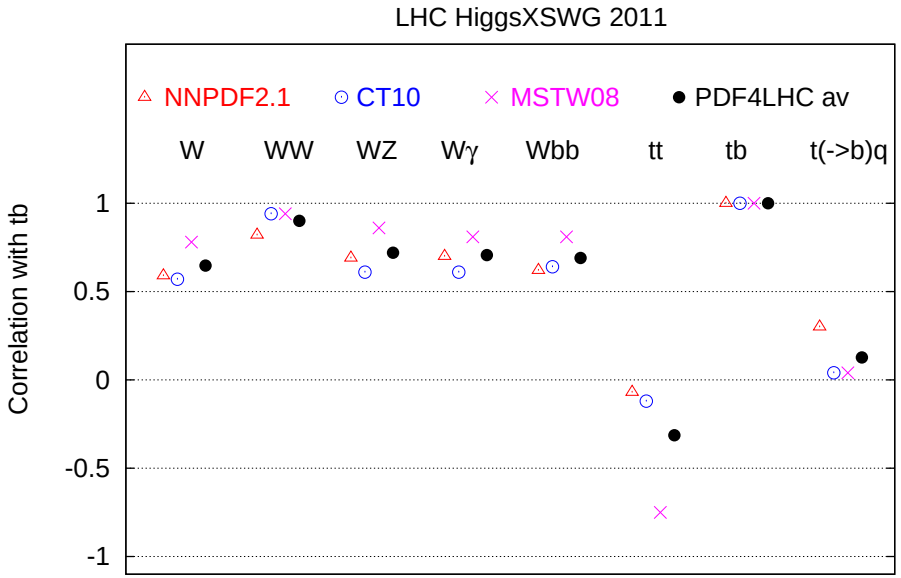

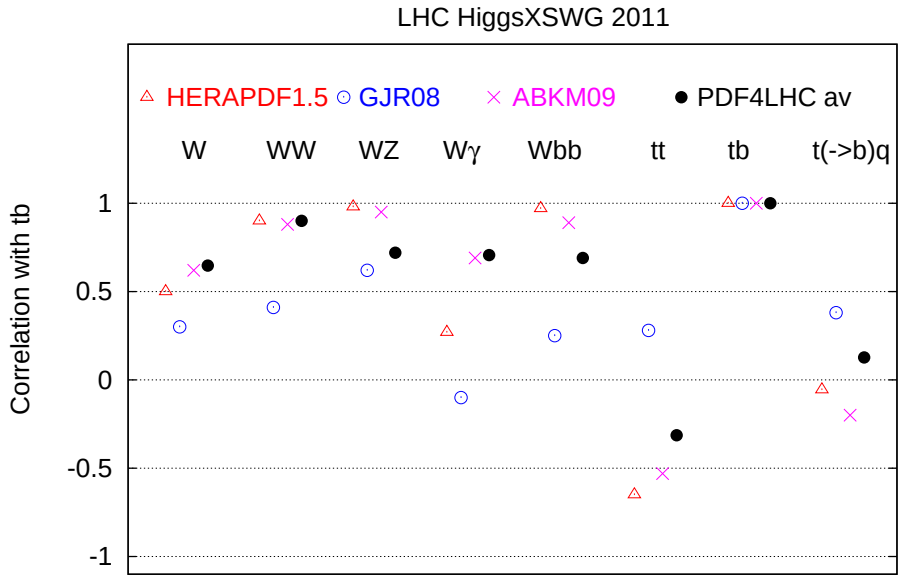

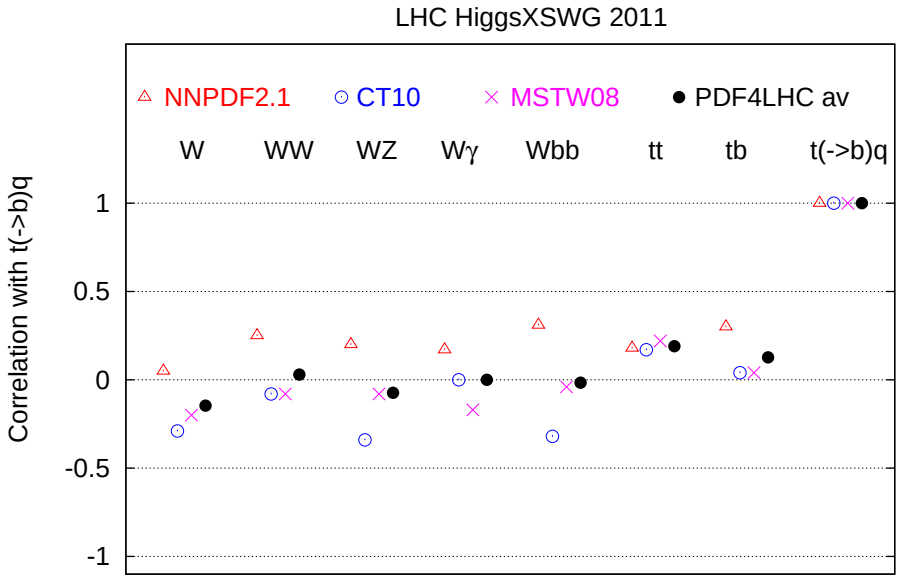

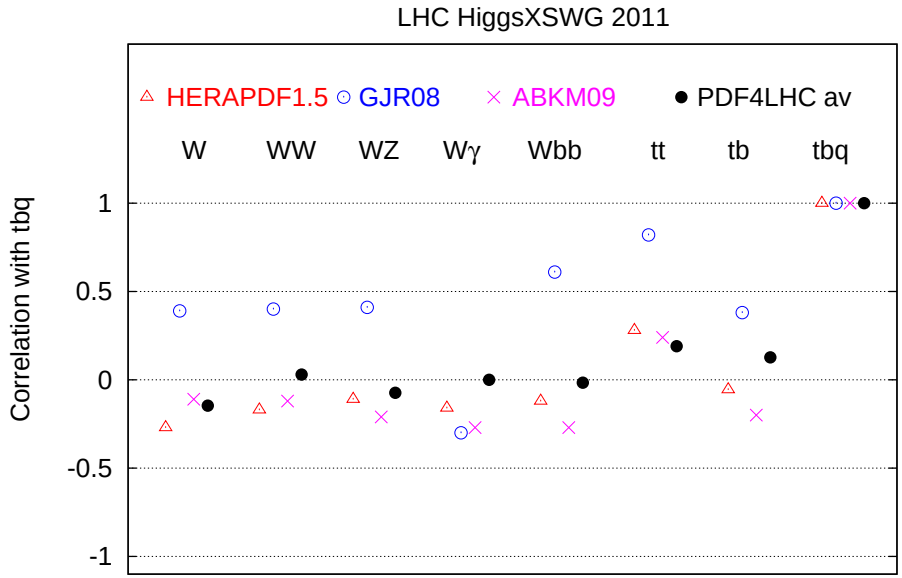

The correlations between $\mathrm{t\bar{b}}$ production and $\mathrm{t}(\rightarrow \mathrm{\bar{b}}) + \mathrm{q}$ production and the other background processes considered.

There is usually a fairly narrow clustering of the individual results about the average, with a small number of cases where there is one, or perhaps two outliers. The averages using all 6 sets are nearly always within one class of the PDF4LHC average.

The sets with the largest parameterisations for the PDFs generally tend to give smaller magnitude correlations or anticorrelations, but this is not always the case, e.g. NNPDF2.1 gives the largest anti-correlation for VBF-$\mathrm{t\bar{t}H}$.

There are some unusual features, e.g. for HERAPDF1.5 and high values of M_H the $\mathrm{t\bar{t}H}$ correlations with quantities depending on the high-x gluon, e.g. $\mathrm{gg} \to \mathrm{H}$ and $\mathrm{t\bar{t}}$ is opposite to the other sets and the correlations with quantities depending on high-x quarks and antiquarks, e.g. VBF and WW is stronger. This is possibly related to the large high-x antiquark distribution in HERAPDF1.5 (at NLO) which contributes to $\mathrm{t\bar{t}H}$ but not $\mathrm{gg} \to \mathrm{H}$ or very much to $\mathrm{t\bar{t}}$.

GJR08 has a tendency to obtain more correlation between some gluon dominated processes, e.g. $\mathrm{gg} \to \mathrm{H}$ and $\mathrm{t\bar{t}}$ and quark dominated processes, e.g. W and WZ, perhaps because the dynamical generation of PDFs couples the gluon and quark more strongly.